

KU Leuven
Biomedical Sciences Group
Faculty of Pharmaceutical Sciences
Department of Pharmaceutical and Pharmacological Sciences



STUDY OF PHARMACEUTICALLY RELEVANT CONTAMINANTS IN WASTE AND SURFACE WATER USING ADVANCED TECHNIQUES IN LIQUID CHROMATOGRAPHY

Glenn Loos

Jury:

Promoter: Prof. Dr. Deirdre Cabooter
Co-promoter: Prof. Dr. Ann Van Schepdael
Chair: Prof. Dr. Arthur Van Aerschot
Secretary: Prof. Dr. Guy Van den Mooter
Jury members: Prof. Dr. Ken Broeckhoven
Prof. Dr. Eva Tyteca
Prof. Dr. Kristof Demeestere

Dissertation presented in
partial fulfillment of the
requirements for the
degree of Doctor in
Pharmaceutical Sciences

December 2017

Curriculum vitae

Glenn Loos was born on February 11, 1988 in Neerpelt, Belgium. His secondary school diploma was obtained in 2006 at Instituut Agnetendal Peer. In 2010 he completed his bachelor studies in Chemistry at Hasselt University and started a master in Biochemistry and Biotechnology at the University of Antwerp. This degree was obtained in 2012 after which he started as a physics teacher for one year. To gain industrial acquaintance he joined Noliko NV in 2013 after which he started his PhD research at the Pharmaceutical Analysis laboratory of KU Leuven in 2014. Under supervision of Prof. Dr. ir. Deirdre Cabooter as promoter and Prof. Dr. Ann Van Schepdael as co-promoter innovative UHPLC approaches were developed to analyze pharmaceutically relevant contaminants in waste and surface water. He was enrolled in the doctoral school of Biomedical Sciences where he completed the Drug Design and Development training in 2017.

Personal acknowledgements

Since this thesis would never have been established without the support of other people, I would like to express my grateful appreciation for all the time and care I received.

First, I want to thank my promoter Prof. Dr. Deirdre Cabooter and co-promoter Prof. Dr. Ann Van Schepdael for giving me the opportunity to perform a PhD in the Pharmaceutical Analysis lab. Besides the many scientific discussions, there was also time for jokes and small talk. The permanent support and availability are absolutely appreciated.

Further, I want to thank Prof. Dr. Arthur Van Aerschot, Prof. Dr. Guy Van den Mooter, Prof. Dr. Ken Broeckhoven, Prof. Dr. Kristof Demeestere and Prof. Dr. Eva Tyteca to be my jury members. The critical comments and suggestions have definitely improved this manuscript.

I also want to thank Prof. Dr. Erwin Adams, Prof. Dr. Jos Hoogmartens and Kris Wolfs for sharing their knowledge and help me surmount some difficult issues during my PhD. Besides, I want to thank my students Stijn, Lien, Timothy and Kaat for their enthusiasm and contribution to my project.

I started my thesis with an IWT-TETRA project that occupied an even larger than expected part of my stay. This, however, gave me the opportunity to cooperate fruitfully with experts in environmental water treatment. Thank you Raf, Thomas, Bart and Kwinten.

Every year I also spend some time in the student lab. Although these periods were short, they were very demanding. Fortunately, the didactical staff and my fellow assistants made these weeks worth while. Thank you Steffi, Lieven, Monica, Walter, Suzy, Katia, Nicolas, Sanne, Lien, Daniëlle, Chloë, Linde, Ivana and Koen.

Working in the Pharmaceutical Analysis lab also means working with a large diversity of people and cultures. I enjoyed tasting the exotic dishes during our Christmas/New Year's parties and liked the occasional evening drinks. Therefore, I want to thank all my (ex) colleagues, Manama, Erasmus, post-graduate, exchange, bachelor and master students for creating a pleasant atmosphere in the lab. A special attention for Bart, Stijn, Niels, Getu, Stanislav and Pranov. I really enjoyed our time together and our paths will definitely cross again.

A special attention definitely goes to my family. Mom, Dad, little sisters, without your support, good advice and credits I would never have been able to start my studies and PhD. Many thanks go also to my parents-in-law who supported me by showing their interest.

And last but not least, I want to thank my lovely wife Jasmine. You were, are and will always be my motivation to continue and succeed. Your daily support, understanding and encouragement helped me through the difficult moments. We have already experienced a lot, both sad and wonderful moments and I am really looking forward to our beautiful future together.

List of publications

- 1.a Loos G, Dittmann M, Choikhet K, Desmet G, Cabooter D. 2016 Generic UHPLC methodology for the simultaneous analysis of compounds with a large variety in polarity. *LC-GC Eur.* 29, 240-247.
- 1.b Loos G, Dittmann M, Choikhet K, Desmet G, Cabooter D. 2016 Generic UHPLC methodology for the simultaneous analysis of compounds with a large variety in polarity. *LC-GC North America.* 35 (2), 123-131.
- 1.c Loos G, Dittmann M, Choikhet K, Desmet G, Cabooter D. 2016 Generic UHPLC methodology for the simultaneous analysis of compounds with a large variety in polarity. *LC-GC Asia Pacific.* 19 (2), 6-15.
- 2 Loos G, Van Schepdael A, Cabooter D. 2016 Quantitative mass spectrometry methods for pharmaceutical analysis. *Philosophical Transactions of the Royal Society A* 374, issue 2079, 1-25.
- 3 Loos G, Shoykhet K, Dittmann M, Cabooter D. 2016 Restriction capillaries as an innovative mixing principle for intermediate solvent exchange in multidimensional analysis. *Journal of Chromatography A*, 1497, 70-80.
- 4 Van Eyck K, Scheers T, Loos G, Van Schepdael A, Adams E, Van der Bruggen B, Cabooter D, Dewil R., 2016 Removal of pharmaceutical products from hospital wastewater via ozonation and UV photodegradation: a pilot scale assessment of process efficiency, kinetics and ecotoxicity. Submitted
- 5 Loos G, Scheers T, Van Eyck K, Van Schepdael A, Adams E, Van der Bruggen B, Cabooter D, Dewil R., Electrochemical oxidation of key pharmaceuticals using a Boron-Doped Diamond electrode. Submitted
- 6 Scheers T, Loos G, Van Eyck K, Van Schepdael A, Adams E, Van der Bruggen B, Cabooter D, Dewil R., Chemical oxidation of key pharmaceuticals through the addition of ozone, UV-radiation and/or H₂O₂. In preparation
- 7 Loos G, Nelis M, Dumont E, Sandra K, Sandra P, Cabooter D., Validation of a generic offline SPE-LC-MS/MS methodology for the simultaneous analysis of polar and non-polar pharmaceuticals in environmental water samples. In preparation

Table of contents

| | |
|--|-----|
| Curriculum vitae | i |
| Personal acknowledgements | iii |
| List of publications..... | v |
| Table of contents..... | vii |
| List of abbreviations | xi |
| List of symbols | xv |
| CHAPTER 1 | |
| General introduction | 1 |
| 1.1 The indispensability of pharmaceuticals in the pursuit of optimum living standards | 2 |
| 1.1.1 Increased availability and consumption of drugs..... | 2 |
| 1.1.2 Drug use in Belgium..... | 2 |
| 1.1.3 Global drug market expansion | 3 |
| 1.2 Drug appearance and persistence in the environment..... | 5 |
| 1.2.1 Potential entrance pathways of pharmaceuticals into the environment | 5 |
| 1.2.2 Global occurrence of pharmaceuticals in water | 8 |
| 1.2.3 Persistence of pharmaceutically relevant contaminants | 9 |
| 1.3 Adverse biological effects..... | 9 |
| 1.3.1 Prediction models to define ecological risk..... | 10 |
| 1.3.2 Ecological effects of pharmaceuticals | 11 |
| 1.4 European regulations | 12 |
| 1.4.1 History of the European water policy..... | 12 |
| 1.4.2 Composition of the first watch list | 12 |
| 1.5 Analytical methodologies for pharmaceuticals in water..... | 15 |
| 1.5.1 Mass spectrometry..... | 15 |
| 1.5.1.1 Mass analyzer | 15 |
| 1.5.1.2 Ionization source | 18 |
| 1.5.2 Separation of complex samples | 19 |
| 1.5.2.1 Gas chromatography | 19 |
| 1.5.2.2 Liquid chromatography | 19 |
| 1.5.2.2.1 Basic principles of chromatography..... | 19 |
| 1.5.2.2.2 Reversed phase and hydrophilic interaction liquid chromatography | 23 |

| | | |
|------------------|--|----|
| 1.5.2.3 | Sample preparation | 24 |
| 1.6 | References | 26 |
| CHAPTER 2 | | |
| | Objectives | 31 |
| CHAPTER 3 | | |
| | Electrochemical oxidation of key pharmaceuticals using a Boron Doped Diamond electrode | 33 |
| 3.1 | Introduction | 34 |
| 3.2 | Materials and methods | 36 |
| 3.2.1 | Chemicals | 36 |
| 3.2.2 | Electrochemical setup and experiments | 36 |
| 3.2.3 | LC-MS experiments | 37 |
| 3.2.4 | Kinetic evaluation | 38 |
| 3.3 | Results and discussion | 39 |
| 3.3.1 | Degradation kinetics in simulated wastewater | 39 |
| 3.3.2 | Influence of flow rate | 41 |
| 3.3.3 | Temperature dependency | 43 |
| 3.3.4 | Degradation in real effluent wastewater | 45 |
| 3.3.5 | Fate of the degradation products | 47 |
| 3.4 | Conclusions | 50 |
| 3.5 | References | 51 |
| CHAPTER 4 | | |
| | Generic UHPLC methodology for the simultaneous analysis of compounds with a wide range of polarities | 53 |
| 4.1 | Introduction | 54 |
| 4.2 | Experimental | 57 |
| 4.2.1 | Chemicals and columns | 57 |
| 4.2.2 | Apparatus | 58 |
| 4.2.3 | Methodology | 58 |
| 4.2.3.1 | Subdivision of the sample | 58 |
| 4.2.3.2 | Method development for the polar and non-polar compounds | 59 |
| 4.2.3.3 | Hyphenation of the final obtained methods | 59 |
| 4.3 | Results and discussion | 60 |
| 4.3.1 | Subdivision of the sample | 60 |
| 4.3.2 | Method development for the polar and non-polar compounds | 60 |

| | | |
|------------------|--|-----|
| 4.3.3 | Hyphenation of the final obtained methods..... | 63 |
| 4.4 | Conclusions..... | 68 |
| 4.5 | References..... | 69 |
| CHAPTER 5 | | |
| | Restriction capillaries as an innovative mixing unit for intermediate mobile phase exchange in multidimensional analysis | 71 |
| 5.1 | Introduction..... | 72 |
| 5.2 | Experimental | 74 |
| 5.2.1 | Chemicals..... | 74 |
| 5.2.2 | Columns and materials..... | 75 |
| 5.2.3 | Apparatus | 75 |
| 5.2.4 | Stock and working solutions..... | 77 |
| 5.2.5 | General methodology..... | 77 |
| 5.2.6 | Mixing unit consisting of restriction capillaries..... | 79 |
| 5.2.7 | Recovery | 79 |
| 5.3 | Results | 81 |
| 5.3.1 | Restriction capillaries | 82 |
| 5.3.1.1 | Proof-of-concept | 82 |
| 5.3.1.2 | Changing the dilution factor..... | 84 |
| 5.3.2 | HILIC x RP (1.0 x 3.0 mm)..... | 85 |
| 5.3.3 | HILIC x RP (1.0 x 2.1 mm)..... | 89 |
| 5.3.4 | HILIC x RP (2.1 x 3.0 mm)..... | 93 |
| 5.3.5 | HILIC x RP (2.1 x 2.1 mm)..... | 94 |
| 5.4 | Conclusion | 96 |
| 5.5 | References..... | 98 |
| CHAPTER 6 | | |
| | Development of a generic SPE methodology for the simultaneous analysis of polar and non-polar pharmaceuticals in environmental water samples | 101 |
| 6.1 | Introduction..... | 102 |
| 6.2 | Experimental | 104 |
| 6.2.1 | Chemicals and solvents | 104 |
| 6.2.2 | Solid-phase extraction..... | 107 |
| 6.2.3 | Instrumentation and analytical conditions | 107 |
| 6.2.4 | Recovery | 108 |
| 6.3 | Results and discussion..... | 108 |

| | | |
|------------------|---|-----|
| 6.3.1 | Optimization of SPE procedure | 108 |
| 6.4 | Conclusion | 113 |
| 6.5 | References..... | 114 |
| CHAPTER 7 | | |
| | General discussion and conclusions..... | 115 |
| 7.1 | Improving wastewater treatment strategies | 116 |
| 7.2 | Development of a generic UHPLC methodology..... | 117 |
| 7.3 | Strive for highest possible flexibility..... | 117 |
| 7.4 | Optimization of the sample preparation procedure | 120 |
| 7.5 | Method validation for real water samples..... | 121 |
| 7.6 | Mapping of pharmaceutically relevant contaminants | 123 |
| 7.7 | References | 124 |
| CHAPTER 8 | | |
| | Summary – samenvatting..... | 125 |
| 8.1 | Summary..... | 126 |
| 8.2 | Samenvatting..... | 128 |
| | Scientific acknowledgements and conflict of interest statement..... | 131 |

List of abbreviations

| | |
|-----------------|---|
| 2D-LC | two-dimensional liquid chromatography |
| ACN | acetonitrile |
| AF | ammonium formate |
| AOP | advanced oxidation processes |
| APCI | atmospheric pressure chemical ionization |
| API | active pharmaceutical ingredient |
| APPI | atmospheric pressure photo-ionization |
| ATC | anatomical therapeutic chemical |
| AUC | area under the curve of the chromatographic peak |
| BCF | bioaccumulation factor |
| BEH | ethylene bridged hybrid |
| CAGR | compound annual growth rate |
| CALUX | chemical assisted luciferase gene expression |
| CF | compression factor |
| COD | chemical oxygen demand |
| CS | core-shell |
| DCF | diclofenac |
| dw | drinking water |
| ECHA | European Chemical Agency |
| EE ₂ | 17 α -ethinylestradiol |
| EFSA | European Food Safety Authority |
| EMA | European Medicines Agency |
| EPA | Environmental Protection Agency |
| ERA | environmental risk assessment |
| ESI | electrospray ionization |
| EtOH | ethanol |
| EU | European Union |
| FA | formic acid |
| FP | fully porous |
| fw | freshwater |
| GC | gas chromatography |
| hh | human health |
| HILIC | hydrophilic interaction liquid chromatography |
| HLB | hydrophilic lipophilic balanced |
| HPLC | high performance liquid chromatography |
| HR | high flow resistance |
| HRMS | high-resolution mass spectrometry |
| I.D. | internal diameter |
| IOP | iopromide |
| IPA | isopropanol |
| IT | ion trap |
| IUCLID | international uniform chemical information database |

| | |
|----------|---|
| IWT | Flanders Innovation and Entrepreneurship |
| LC | liquid chromatography |
| LLE | liquid/liquid extraction |
| LOD | limits of detection |
| LOEC | lowest observed effect concentration |
| LOQ | limit of quantification |
| LR | low flow resistance |
| MCX | strong cation exchange |
| ME | matrix effects |
| MEC | measured environmental concentrations |
| MeOH | methanol |
| MEPS | microextraction by packed sorbent |
| (d)MRM | (dynamic) multiple reaction monitoring |
| MS | mass spectrometry |
| NOEC | no observed effect concentration |
| NRB | not readily biodegradable |
| PCI | post-column infusion |
| PEC | predicted environmental concentration |
| PNEC | predicted no effect concentration |
| PPP | plant protection product |
| PTFE | polytetrafluoroethylene/teflon |
| QIT | quadrupole ion trap |
| QLIT | quadrupole linear ion trap |
| QQQ | triple quadrupole |
| QTOF | quadrupole time-of-flight |
| QSARs | quantitative structure-activity relationships |
| RB | readily biodegradable |
| REACH | Registration, Evaluation and Authorization of Chemicals |
| RIVM | Dutch National Institute for Health and Environment |
| RP(LC) | reversed-phase (liquid chromatography) |
| RQ | risk quotient |
| RSD | relative standard deviation |
| RWW | real effluent wastewater |
| SBSE | stir-bar sorptive extraction |
| SCX | strong cation exchange |
| sed | sediment |
| sec pois | secondary poisoning |
| SIL-IS | isotopically labeled standards |
| SIM | selected ion monitoring |
| SMX | sulfamethoxazole |
| SPE | solid-phase extraction |
| SRM | selected reaction monitoring |
| stdev | standard deviation |
| SWW | simulated wastewater |
| TOF | time-of-flight |
| TP | transformation product |

| | |
|-------|--|
| UHPLC | ultra-high performance liquid chromatography |
| UPLC | ultra-performance liquid chromatography |
| v/v% | volume/volume % |
| w/w% | weight/weight % |
| WFD | Water Framework Directive |
| WWTP | wastewater treatment plant |

List of symbols

| | |
|-----------------------|---|
| Δp | pressure drop |
| A | observed area under the curve of the chromatographic peak |
| A_{\max} | maximum observed area under the curve of the chromatographic peak |
| d | diameter |
| d_p | particle size |
| E_a | activation energy |
| F | flow rate |
| F_{HR} | flow through high resistance restriction capillary |
| F_{LR} | flow through low resistance restriction capillary |
| F_{total} | total flow |
| H | height equivalent of a theoretical plate |
| I | electric current |
| k | retention factor |
| k | reaction rate constant |
| K_{oc} | organic carbon adsorption coefficient |
| L | column length |
| L | tubing length |
| $\log K_{ow}$ | octanol-water partition coefficient |
| $\log D$ | octanol-water distribution coefficient |
| N | column efficiency |
| n_p | peak capacity |
| R | universal gas constant |
| R^2 | correlation coefficient |
| Re | Reynolds number |
| R_s | resolution |
| T | temperature |
| t_0 | dead time |
| t_R | retention time |
| u | linear velocity |
| V1 | switching valve 1 |
| V2 | switching valve 2 |
| V3 | switching valve 3 |
| V_{inj}^2 | injection volume |
| V_{σ} | flow cell volume |
| w_t | peak width |
| α | selectivity factor |
| δ | dilution factor |
| δ_{tot} | total dilution factor |
| ϵ_e | bed porosity |
| η | mobile phase viscosity |
| σ^2 | peak variance |

CHAPTER 1

General introduction

1.1 The indispensability of pharmaceuticals in the pursuit of optimum living standards

1.1.1 Increased availability and consumption of drugs

In the last decades, the flourishing pharmaceutical industry has led to improved living standards. The consequently aging population and enhanced animal healthcare have resulted in an increased drug use. With the availability of 9590 small molecule and biotech drugs, drugs exist that target all possible receptors in the human body. Thereof, only 2278 are currently approved by different regional authorities worldwide [1]. For example, in the European Union, there are more than 1200 legally registered active pharmaceutical ingredients (APIs) [2]. Although risk assessments have led to the withdrawal of some drugs, new drugs will continue to reach the market thanks to the copious clinical trials that are performed to test novel drug formulations. Some severe diseases are nowadays largely overcome thanks to the multiple treatment options patients have. In particular, cancer therapy and management of rare diseases have progressed significantly. The growing global population and economic prosperity have also led to modified eating habits with an increased demand for meat, fish and dairy products. To meet these nutritional needs, cattle breeders and aquaculture farmers use more and more drugs to prevent and treat animal diseases. In Europe, there are more than 3000 different pharmaceutical products on the veterinary market to maintain an optimal food production [3].

1.1.2 Drug use in Belgium

Although the consumption of antibiotics in general, but mainly in animal husbandry is stabilizing due to recent governmental sensitization campaigns [4], the Belgian population is a large consumer of prescribed drugs (see Table 1.1). The most recent national health survey of 2013 indicated that 51% of the respondents took prescribed medicines and 17% took non-prescribed drugs two weeks prior to the survey. The consumption of prescribed drugs, however, increases with age going from 21% for young people (< 15 years) to 95% for elderly (> 75 years) [5]. According to the Belgian National Institute for Sickness and Disability Insurance, almost 80% of all prescribed drugs were allotted to people older than 60 years [6]. This is mainly caused by increasing chronic health issues such as hypertension and diabetes [5]. In addition, the status of medicines is gradually changing to consumables due to an excess of easily accessible products. The societal pressure to perform optimally and the delusion of medicines and supplements being panaceas that keep you going, enhance drug intake. Many

people are prone to appealing advertisements and buy antidepressants, painkillers, nose sprays, hypnotics and tranquilizers more frequently to obtain an enhanced sentiment and a better quality of life.

Table 1.1: Number of prescribed drugs in Belgium: distribution according to the major anatomical therapeutic chemical (ATC) groups in 2014 [6].

| ATC code | Anatomical main group | Prescribed DDD in 2014 | % |
|----------|---|------------------------|------|
| A | Alimentary tract and metabolism | 695280 | 13.5 |
| B | Blood and blood forming organs | 445444 | 8.6 |
| C | Cardiovascular system | 1984805 | 38.5 |
| D | Dermatologicals | 27101 | 0.5 |
| G | Genito urinary system and sex hormones | 253715 | 4.9 |
| H | Systemic hormonal preparations | 183546 | 3.6 |
| J | Anti-infectives for systemic use | 129078 | 2.5 |
| L | Antineoplastic and immunomodulating agents | 54115 | 1.0 |
| M | Musculo-skeletal system | 258579 | 5.0 |
| N | Nervous system | 590952 | 11.5 |
| P | Antiparasitic products, insecticides and repellents | 2468 | 0.0 |
| R | Respiratory system | 446686 | 8.7 |
| S | Sensory organs | 83645 | 1.6 |
| V | Various | 849 | 0.0 |

1.1.3 Global drug market expansion

According to a survey of the major market research company Evaluate, the worldwide sales of prescribed drugs is expected to have a Compound Annual Growth Rate (CAGR) of 6.3 percent between 2016 and 2022 (Figure 1.1). No declining sales trend is forecasted for any therapy area while certain areas such as oncology and macular degeneration which causes loss of vision acuity, are increasing rapidly due to the aging population (Figure 1.2) [7]. Senior people are also more susceptible to polypharmacy, a phenomenon wherein minimum 5 different drugs are consumed in 1 day. In Belgium, polypharmacy occurs in more than 30% of people above 75 years [5].

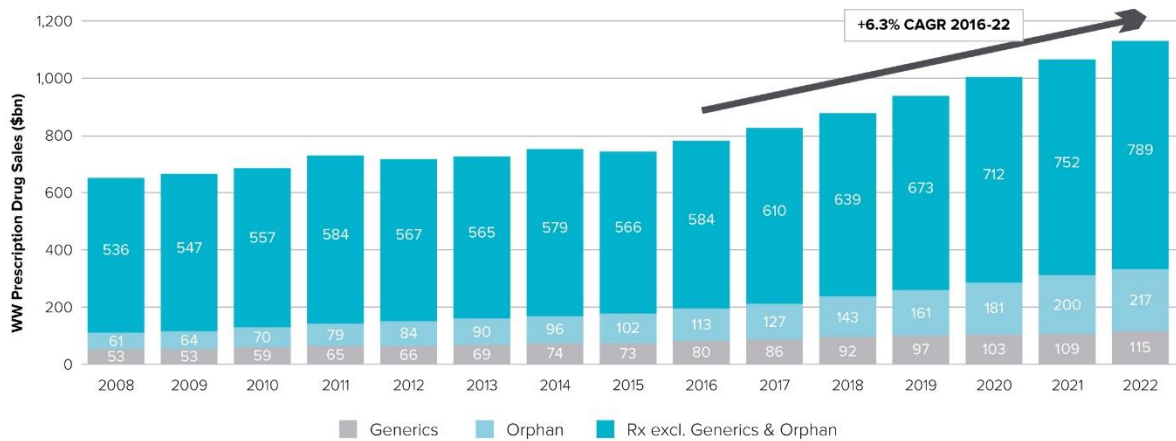


Figure 1.1: Industry sales prediction of prescribed drugs based on the top 500 pharmaceutical and biotech companies worldwide. Forecasted numbers are represented in billion US dollars [7].

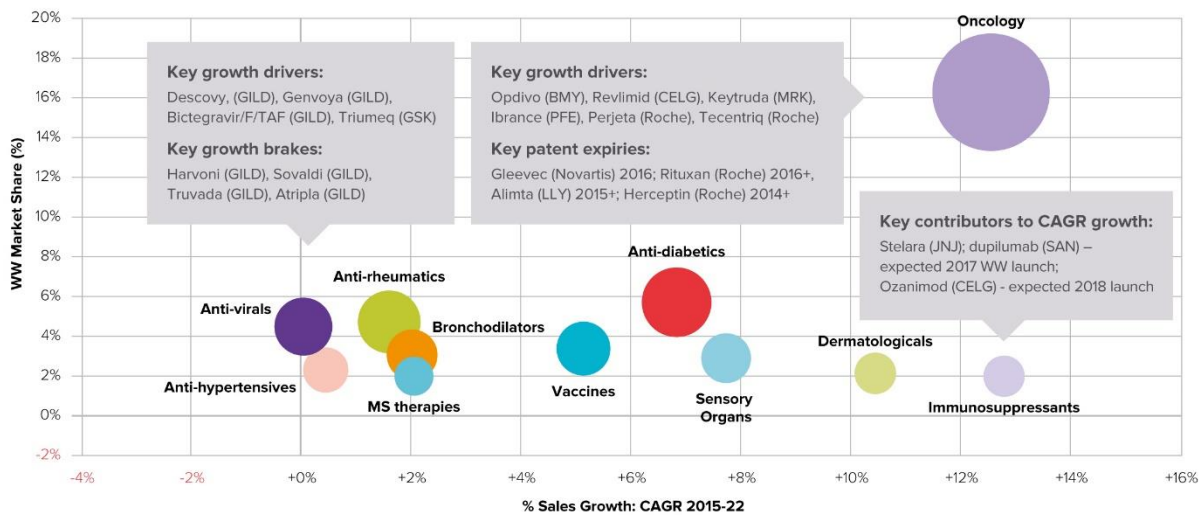


Figure 1.2: Predicted segmental market share in function of the sales growth of the top 10 therapy areas for pharmaceuticals in 2022 [7].

Furthermore, the increasing global population, the fast emerging economies in developing countries such as China or India, and companies losing their product exclusivity due to expiring patent protection will make pharmaceuticals more accessible [8]. Currently, 97% of all drugs available are on the market for more than 10 years [9]. The production of more affordable generic pharmaceuticals will create a market expansion towards a large group of underprivileged people. All top 25 pharmaceutical companies are investing or undertaking opportunities to invest in emerging Asian, South-American or African countries [8]. In addition, thanks to improving healthcare systems in these regions, numerous people that could not afford medicines before, now have access to the most essential drugs. It is expected that over

50% of the global population will consume at least one drug dose per day in 2020 while this was only 33% in 2005 [9]. The lower manufacturing cost will positively influence market prices and production numbers. Therefore, global consumption rates are expected to grow with 24% in 2020, mainly driven by the above mentioned increasing usage in Africa, Middle East, Latin America, Asia and Pacific (Figure 1.3) [9].

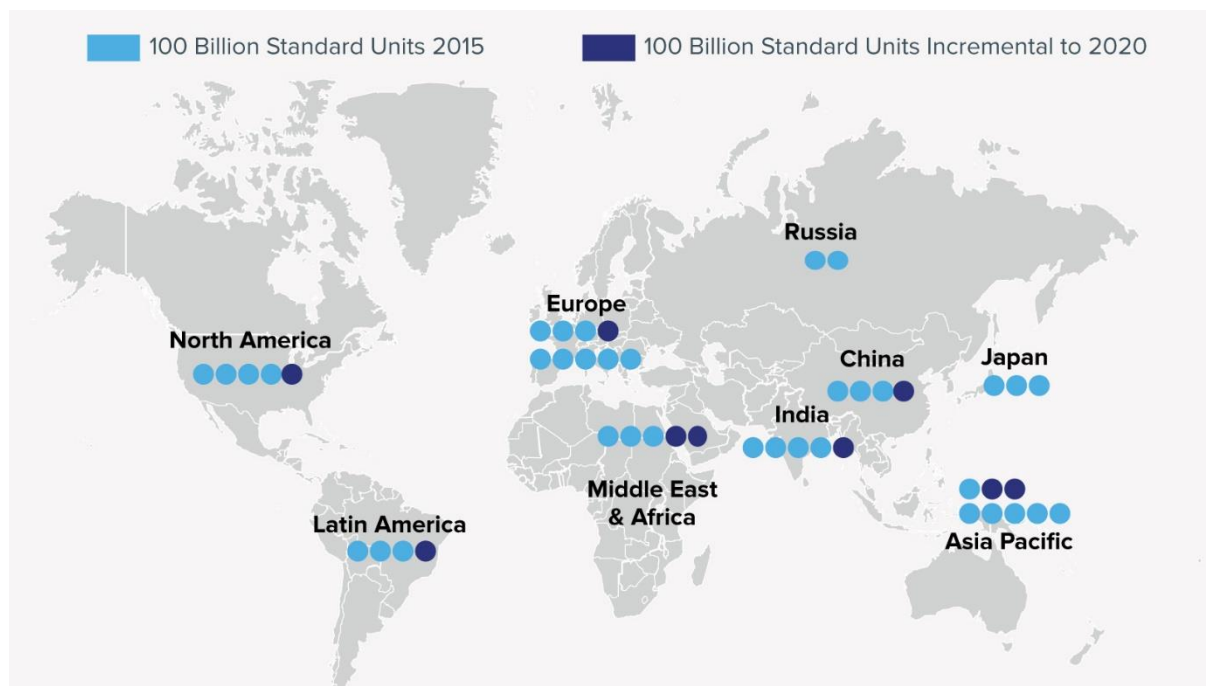


Figure 1.3: Global overview of consumed pharmaceutical doses in 2015 and expected growth rates for 2020. The standard units are defined as a dose of a particular medicine and values are rounded to the nearest whole 100 billion [9].

1.2 Drug appearance and persistence in the environment

1.2.1 Potential entrance pathways of pharmaceuticals into the environment

The increasing production of medicines to improve both human and animal healthcare comes with an important drawback. Many of the drugs used to prevent and treat diseases may end up (after metabolism) in the environment and in particular surface waters that will be used to produce drinking water. Figure 1.4 gives an overview of different routes through which pharmaceuticals can enter the environment [10]. One of the main sources of environmental contamination are the waste streams of pharmaceutical manufacturing sites. Despite thorough purification of in-site treatment facilities to eliminate the large quantities of drugs, drug intermediates and drug by-products, residual amounts of persistent pharmaceuticals or degradation products are discharged in surrounding natural water currents. In developing and

emerging countries such as China and India, pharmaceutical production is booming while waste treatment is not subjected to the strict European legislation. In India for example, pharmaceutical manufacturing or formulation sites only have to adhere to a few basic guidelines concerning organic waste. Indian wastewater effluents should have a maximum chemical and biological oxygen demand of 30 mg/L and 250 mg/L, respectively, and a 90% of fish survival in pure effluent is imposed [11]. Since no maximum drug concentration limits are specified, high (mg/L and even g/L) concentrations of drugs can be found in downstream rivers [12,13]. In 2007, very high levels of active pharmaceutical ingredients were reported in the wastewater effluent (1500 m³/day) of a major production site of generic pharmaceuticals in Patancheru, near Hyderabad, India. The 11 most abundant drugs accounted for a total of 52.5 – 58.4 kg/day released in the environment. In particular ciprofloxacin (up to 31 mg/L and 46.5 kg/day) exceeded toxicity levels for some bacteria by over 1000-fold [14].

Furthermore, accidental leakage or defective good manufacturing practices can also lead to such high concentrations in industrialized countries. For example, due to inappropriate waste management, trimethoprim and ciprofloxacin concentrations of 27.68 and 17.48 mg/L, respectively were reported in the sewage effluent of a Croatian production facility in 2012. Therefore, a site-specific reverse osmosis and nanofiltration membrane treatment technique was developed by Dolar et al. to remove veterinary drugs from pharmaceutical wastewater [15]. However, globally more than 90% of the wastewater is discharged untreated, especially in developing countries [16].

The elimination efficiency of pharmaceutical compounds will vary strongly depending on the drug characteristics and treatment strategies [17,18]. Newly developed drugs show an increased stability to assure their efficacy, making it more and more challenging to remove them in classical wastewater treatment plants (WWTPs) [19]. Therefore, municipal sewer water and wastewater originating from hospitals and nursing homes form another important pathway through which pharmaceutical compounds can enter our water supply. Although exact data are not available and highly dependent on the removal efficiencies of different WWTPs, the total discharge of pharmaceuticals into the environment through municipal WWTPs in Belgium can be estimated by multiplying the total water volume consumed (\pm 450 million m³/annum) with the pharmaceutical concentration levels observed in wastewater effluents. Based on recently published articles wherein multiple pharmaceuticals were detected beyond 100 ng/L and up to 4570 ng/L (carbamazepine) in effluent samples, very high

levels of pharmaceuticals (tens to hundreds of kilograms a day) are estimated to be released into the environment [20,21]. Micro-pollutants can end up in the environment directly via the WWTP effluents or by biological sludge that is regularly used to fertilize agricultural land. Ekpeghere et al. for example reported a pharmaceutical discharge of more than 165 tons per year (of which > 16 tons antibiotics) via municipal and livestock wastewater treatment sludge in Korea [22].

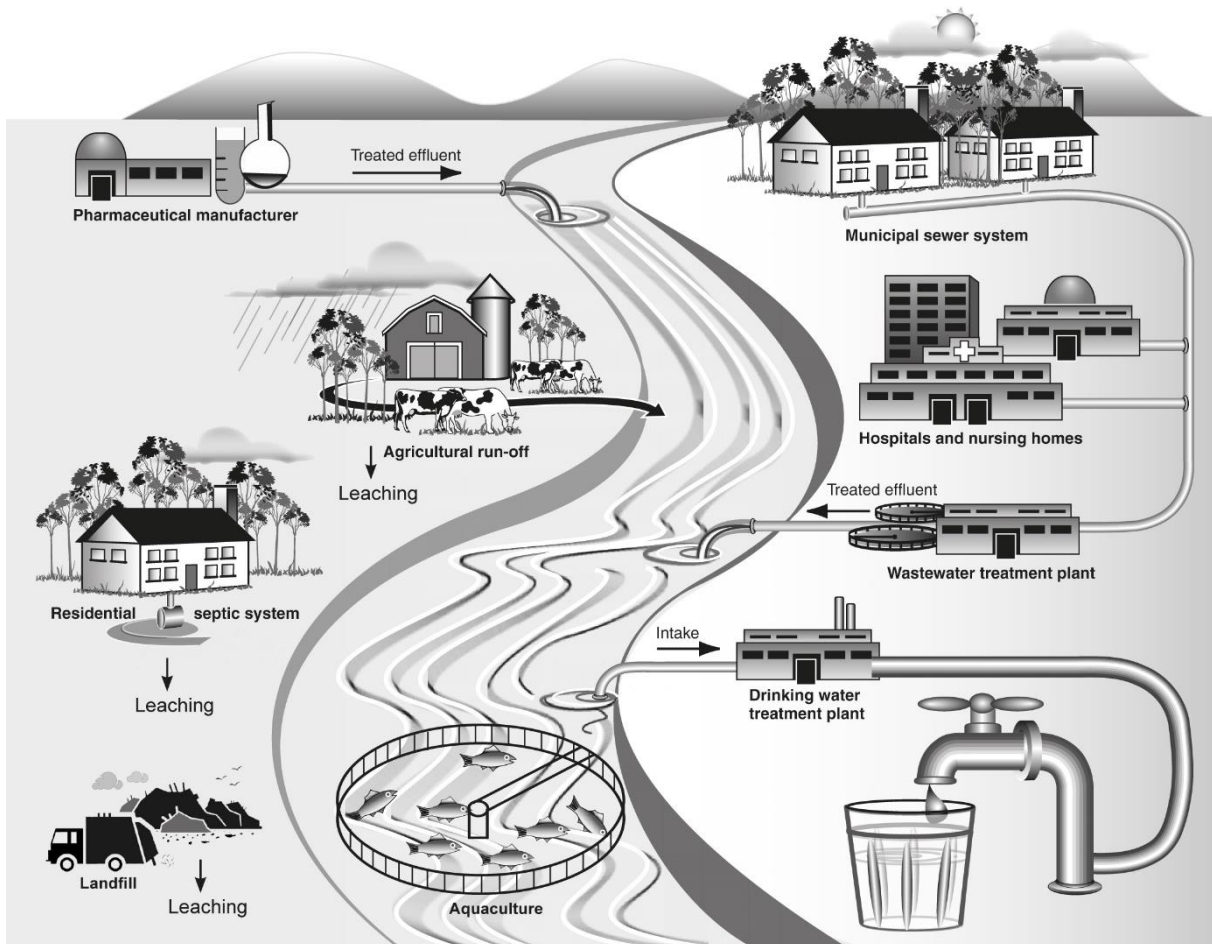


Figure 1.4: Typical pathways how pharmaceuticals may enter drinking water supplies (adjusted figure from [10]).

Moreover, in densely populated areas, there is a higher average consumption of drugs per surface area and a limited availability of natural water to dilute the discarded sewage. Therefore, residents of large cities are potentially more exposed to high concentrations of pharmaceuticals, present in the drinking water. An increased drug exposure is also likely in developing or undeveloped countries, especially in slums, where WWTPs are often lacking. Although the use of pharmaceuticals in these areas is rather limited, direct entrance of pharmaceuticals into the environment appears.

Furthermore, veterinary drugs used in livestock farming to treat or prevent diseases in food-producing animals can enter the ecosystem directly via either excretion or addition in aquaculture, or indirectly by using manure as a fertilizer to grow crops [23,24]. The use of contaminated compost can moreover cause percolation of micro-pollutants into the groundwater. Finally, potential sources of groundwater pollution are leakage of residential septic systems or landfill leaching after inappropriate disposal of unused medicines [10,25,26].

1.2.2 Global occurrence of pharmaceuticals in water

Concentrations of pharmaceuticals observed in European aquatic environments are typically in the ng/L to µg/L range, however, much higher maximum values have also been reported [27–29]. Although the analysis of lower concentrations is generally not feasible, some drugs have been detected in the low pg/L range. Recently, a review article was published wherein the global occurrence of pharmaceuticals in the environment is discussed. More than 1000 research and review articles were combined to compile a database of measured environmental concentrations (MECs) for human and/or veterinary drugs. In total 631 unique substances were detected globally, however, most were reported in industrialized countries (Figure 1.5) [30]. The limited number of pharmaceuticals detected in emerging countries can be associated with a less extensive monitoring program. Moreover, the advanced analytical technology and thus better limits of detection (LODs) in developed countries result in a larger amount of positive detections [30]. Figure 1.5 can therefore be misleading.

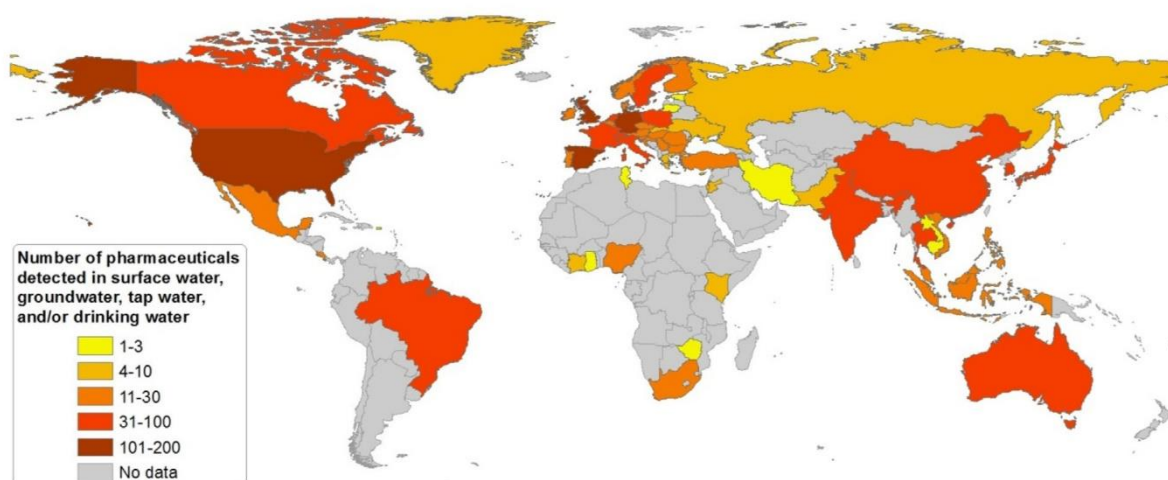


Figure 1.5: Global overview of the number of pharmaceutical compounds detected in surface waters, groundwater, or tap/drinking water [30].

Although some agents are only consumed rarely and most studies focus on drugs that belong to a group of antibiotics, analgesics and estrogens, only a small fraction of the more than 2000 authorized drugs was reported to be found in the environment [1]. Globally, there are over 9000 drugs and a plurality of metabolites and transformation products. The increasing awareness to these emerging pollutants and the ever-improving analytical methodologies will result in a raising number of measurements and will therefore demonstrate additional pharmaceuticals to be present in the aquatic environment.

1.2.3 Persistence of pharmaceutically relevant contaminants

Due to their stability, classical WWTPs are unable to remove pharmaceutical substances entirely from the water. In general, WWTPs consist of a primary mechanical treatment to eliminate large particles, a secondary biological (microbial) cleaning to remove organic compounds such as food and feces. Supplementary, this activated sludge system also reduces phosphates and nitrogen-based nutrients. A tertiary treatment or post-purification aimed to remove specific molecules such as pesticides, personal care products and pharmaceuticals is typically absent. However, additional ultrafiltration techniques or advanced oxidation processes (AOP) such as ozonation and UV irradiation gain more interest to eliminate persistent micro-pollutants [15,19,31,32]. Although these purification strategies can be successfully used to minimize pharmaceuticals, the degradation of medicines remains very challenging. Since complete mineralization is typically not achieved, a wide range of transformation products is formed.

1.3 Adverse biological effects

To date, little information is available about the toxicity of emerging contaminants such as pharmaceuticals. Most metabolites and degradation products are not or less biologically active in comparison with their parent drug, however, cases have been described wherein derivatives are more (eco)toxic [33]. Photo-derivatives of carbamazepine and naproxen are for example more poisonous than their parent drug [34,35] and norfluoxetine, a metabolite of fluoxetine is 50% more toxic for fish [36]. In contrast, only two of five phenolic metabolites of diclofenac are biologically active, however, to a much lesser extent than diclofenac.

1.3.1 Prediction models to define ecological risk

The lack of knowledge about the precise occurrence makes it difficult to perform risk assessments. Therefore, assumptions are made to predict environmental risk based on existing data and physico-chemical characteristics of the different pharmaceuticals. For every substance the metabolism, water solubility, waste treatment, biodegradation, environmental release, dilution and distribution across different compartments such as air and sediments is considered to determine predicted environmental concentrations (PECs) [37]. Ideally, PEC values for different pharmaceuticals are determined with the same PEC calculation model. Unfortunately, the different parameters required are not always available. When multiple PECs are available, the worst-case values are generally used in further risk assessments to avoid underestimation. Based on *in vivo* and *in vitro* studies, no observed effect concentrations (NOECs) are experimentally determined. These NOECs are then divided by a theoretical assessment factor that depends on the strength and availability of eco-toxicity data e.g. acute or chronic toxicity for different species to define predicted no effect concentrations (PNECs) [38,39]. Accordingly, the PEC to PNEC ratio is a fast measure to determine aquatic environmental risk. Additionally, direct human health risk can be predicted by comparing the daily intake based on PECs with the minimum oral toxicity values, the maximum acceptable daily intake or defined daily dose for humans [40,41]. Finally, *in silico* techniques such as Quantitative Structure-Activity Relationships (QSARs) and chemical assisted luciferase gene expression (CALUX) tests are increasingly employed to evaluate ecological risks [42,43]. In QSARs, a quantitative relationship between the structure of a molecule and a certain characteristic is statistically determined by correlating a regression analysis between different descriptors of a set reference molecules and a specific feature. Therefore, it is very important to use a representative selection of reference substances for which the different features are experimentally determined or computationally calculated. CALUX tests are bioassays of modified cell lines wherein a receptor molecule becomes triggered by e.g. an estrogen or dioxin to activate a response element that initiates the transcription of luciferase. In the presence of luciferine chemiluminescence occurs proportional to the amount of toxin present. These ethically more responsible assessment tools minimize animal tests and are much more cost efficient. The major advantage of CALUX tests is, moreover, that they can be used to predict the toxicity or mutagenicity of complex matrices wherein multiple pharmaceuticals are present.

1.3.2 Ecological effects of pharmaceuticals

The concentrations of micro-pollutants in water are generally very low. Studies have been published wherein the lowest observed effect concentrations (LOECs) are about 100 times higher than the drug concentrations in WWTP effluents [44]. Therefore, acute human health issues are not immediately expected. However, the increasing discharge and accumulation of pharmaceutically relevant contaminants in waste, surface, ground and possibly even drinking water have become topics of great concern. Although the low concentrations of individual pharmaceuticals do not cause direct toxicity, carcinogenicity, mutagenicity and effects on reproduction [45], little information is known about the risks of drug cocktails. Figure 1.5 demonstrates that pharmaceuticals always occur in the presence of other drugs and studies have indicated that hormones, antibiotics and non-steroidal anti-inflammatory drugs can reinforce each other's toxicity [43,46]. Exposure to these mixtures of pharmaceuticals, their metabolites and degradation products can possibly lead to chronic health effects. Moreover, when using pharmaceutically enriched water to irrigate agricultural soils, bioaccumulation and thus exposure to higher concentrations may occur [47]. In Pakistan, the extensive use of diclofenac in livestock was associated with the serious decline in vulture populations. Residues of the anti-inflammatory drug diclofenac in carcasses led to visceral gout and renal failure [48]. Furthermore, for certain components the measured environmental concentrations are locally higher than the PNECs [37] and multiple studies have demonstrated negative biological effects on the aqueous environment [49,50]. For example, clotrimazole, a drug to treat fungus infections will influence the biosynthesis of sterols in algae, plants and animals at ng/L concentrations [51]. Besides, Brodin et al. demonstrated that 1.8 µg/L oxazepam influences the behavior and eating pattern of fish. Perch (*Perca fluviatilis*) would be less anxious making them eat more zooplankton, which causes larger algae concentrations [52]. The disturbed growth features of certain organisms such as bacteria, fungi, algae, plants and fish or even their complete extinction can be a direct or indirect result from this micro-pollution [44,53]. Harris et al. predicted the feminization of fish populations due to the presence of female hormones in water [54] and several studies showed kidney, liver and gill injuries in fish caused by diclofenac [50,55]. As a result, the locally elevated presence of pharmaceuticals or the negative ecological impact are harmful for the ecosystem and in addition human population. Therefore, the presence of pharmaceutically relevant contaminants in water should not be tolerated and current concentrations should be reduced to a minimum.

1.4 European regulations

1.4.1 History of the European water policy

To assure a good and safe drinking water quality, the European Union (EU) agreed to impose quality targets for river and lake basins that serve as drinking water sources in 1975. With a *Dangerous Substances Directive*, a first emission control element was set in 1980. In 1988, the legislation was reviewed and improved a first time. As a result, a series of directives including the *Urban Wastewater Treatment Directive (91/271/EEC)*, the *Nitrates Directive (91/676/EEC)*, a *Directive for Integrated Pollution and Prevention Control (96/61/EC)* and a new *Drinking Water Directive (98/83/EC)* were developed to protect the environment and assure industrial, urban and agricultural pollution was minimized [56]. Meanwhile in 1996, the European council and parliament established a new *European Water Policy* in association with all stakeholders. Representatives of EU member state authorities, agriculture, chemical and pharmaceutical industry, water providers, consumers and even environmentalists were consulted and a new *Water Framework Directive (WFD) (2000/60/EC)* was composed in order to protect and improve the quality of all European waters. Besides guidelines to identify and monitor environmental pollutants, a priority list was compiled comprising 33 priority substances for which maximum concentrations were determined. The monitoring of these priority substances was the responsibility of the member states that implemented the guidelines of the WFD in their national legislation to their own understanding. The priority substances were reviewed and a first amendment to the WFD was proposed in 2008 (2008/105/EC). In 2013, the priority list was revised and updated a second time (2013/39/EU). To protect the environment from harmful pollutants the priority list was extended with 15 extra substances. Besides the WFD, an additional control system was introduced in 2006. REACH (Registration, Evaluation and Authorization of Chemicals) registers and manages the production and import of nearly all chemical compounds among which pharmaceuticals (EC No1907/2006).

1.4.2 Composition of the first watch list

Although the priority list only contains heavy metals, pesticides, flame retardants, polyaromatic hydrocarbons, dioxins, alkylphenols and halogenated poly- or hydrocarbons, the European Union is aware of the increasing pharmaceutical pollution. Therefore, a watch list was introduced besides the priority list to monitor a number of additional substances. For

these compounds insufficient data is available, however, they are frequently observed and expected to pose a risk to the human or aquatic environment [57,58]. To select candidate emerging contaminants for the assembly of the first watch list, different databases containing monitoring results such as WATERBASE, IPChem and NORMAN were consulted taking information about production volumes, consumption and stakeholder recommendations into account. Although these databases comprise more than 1000 emerging pollutants, only a limited number of molecules could be included in the watch list due to high monitoring costs, a lack of adequate analytical techniques and/or sufficient knowledge about potential eco-toxic effects. Therefore, a list of de-selection criteria was used to reduce the number of candidates. When sufficient information about the identity, sampling conditions and reported LOD or LOQ values were available to confirm that substance-specific limits or PNECs were not exceeded, substances were filtered out. For example for estrone, carbamazepine, ibuprofen and sulfamethoxazole enough information was available to classify them as not hazardous [37]. The remaining compounds were subjected to an environmental risk assessment (ERA). Based on PEC values for the different environmental compartments (freshwater, sediments and biota) and PNEC calculations to define the toxicity (for freshwater and benthic organisms or via direct drinking water and secondary consumption of fishery products) risk quotients (RQs) were determined for all substances (Figure 1.6) [37]. Based on their risk hazard a ranking was drafted and finally 17 substances, subdivided into 10 different groups, were selected: diclofenac, 17-beta-estradiol, 17-alpha-ethinylestradiol and estrone, oxadiazon, methiocarb, 2,6-ditert-butyl-4-methylphenol, tri-allate, neonicotinoid insecticides as a group (imidacloprid, thiacloprid, thiamethoxam, clothianidin, acetamiprid), macrolide antibiotics (erythromycin, clarithromycin, azithromycin), and 2-ethylhexyl-4-methoxycinnamate [57]. These emerging pollutants are candidate priority substances, but require supplementary research on their eco-toxicity and occurrence before inclusion in routine monitoring programs at European level can be considered [59].

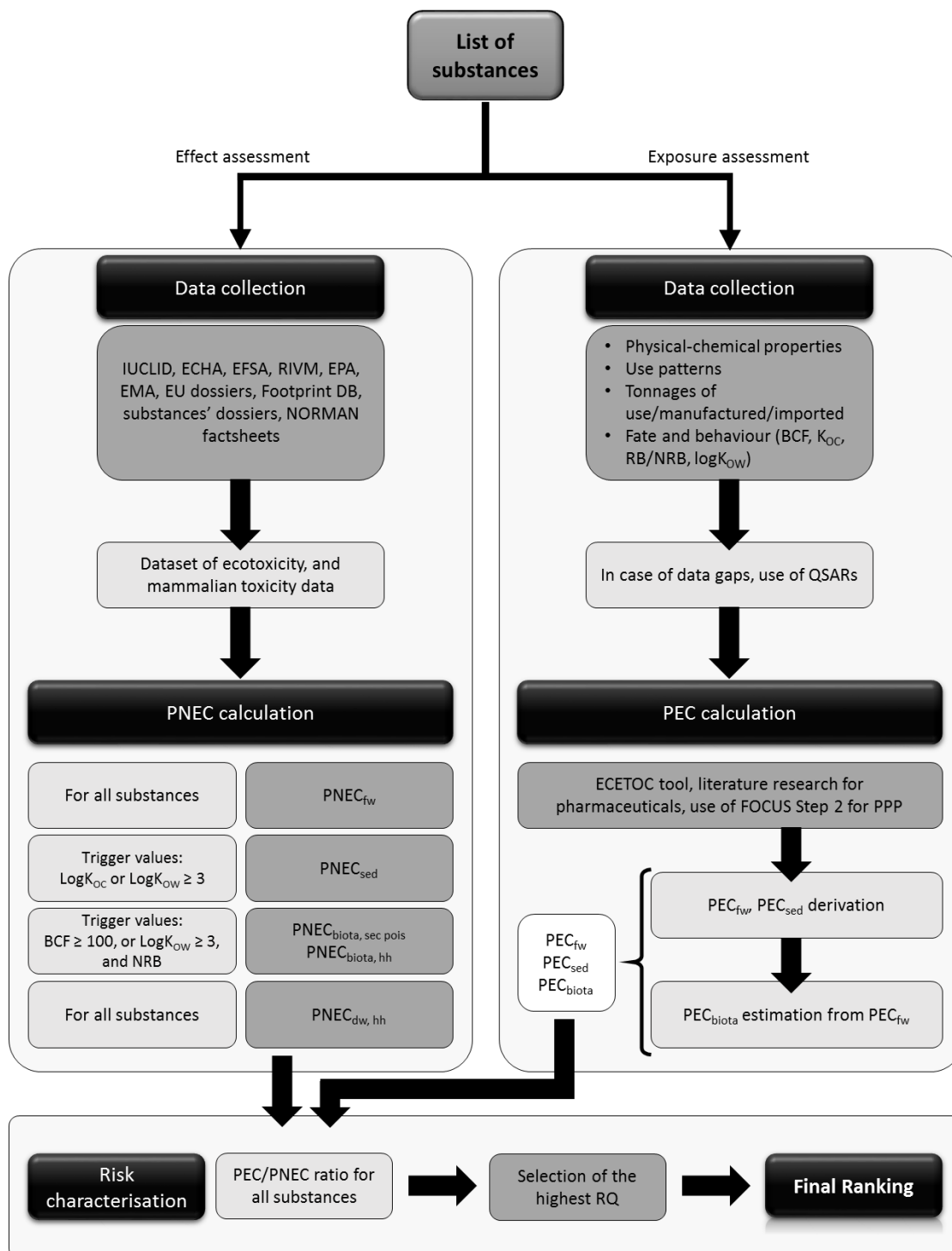


Figure 1.6: Risk assessment methodology for the ranking of candidate substances for the Watch List. Figure based on [37]. Explanatory legend: Predicted No-Effect Concentration (PNEC), Predicted Environmental Concentration (PEC), International Uniform Chemical Information Database (IUCLID), European Chemical Agency (ECHA), European Food Safety Authority (EFSA), Dutch National Institute for Health and Environment (RIVM), Environmental Protection Agency (EPA), European Medicines Agency (EMA), Bioaccumulation Factor (BCF), Organic carbon adsorption coefficient (K_{oc}), Octanol-water partition coefficient ($\log K_{ow}$), Readily Biodegradable (RB), Not Readily Biodegradable (NRB), Quantitative Structure Activity Relationship (QSAR), Freshwater (fw), Sediment (sed), Secondary poisoning (sec pois), Human Health (hh), Drinking Water (dw), Plant Protection Products (PPP), Risk Quotient (RQ)

Since ERA must be carried out for both existing priority substances and newly reported substances in active ingredients or biocidal products, EU member states also monitor other pharmaceuticals besides the ones included in the watch list. To further refine the priority and watch list, the identification and detection of drugs, metabolites and their different transformation products remains a great challenge. Thanks to advanced analytical techniques, simultaneous identification and quantitation of a wide variety of compounds in aqueous samples is possible. Therefore, it is expected that a growing number of pharmaceutically relevant contaminants will be included in European legislation.

1.5 Analytical methodologies for pharmaceuticals in water

To evaluate the presence, degradation and removal of various drugs, the availability of appropriate analytical methods with sufficient sensitivity is important. Currently, there are no standardized protocols to obtain high-quality data on pharmaceutical MECs and PNECs and thus determine the safety of emerging contaminants. This is due to the high complexity of divergent matrices and the diverse components of interest in different monitoring studies. Moreover, different laboratories are typically dedicated to measure a certain group of emerging pollutants since a full analysis of the whole range is not feasible [60]. Frequently used approaches combine a sample preparation technique with selective chromatography hyphenated to a mass spectrometer.

1.5.1 Mass spectrometry

1.5.1.1 Mass analyzer

A mass spectrometer has the ability to identify pharmaceutical substances by fragmenting molecules into smaller building blocks or by obtaining very accurate masses. Quantitation, however, is generally done by adding (isotopically labeled) internal standards and comparing the obtained intensities with a pre-prepared calibration curve. Since different mass spectrometry instruments have other specifications [61,62], the choice for a specific type depends particularly on the type of research that will be conducted. A triple quadrupole (QQQ) that has a high scan rate and low resolution and a time-of-flight (TOF) or orbitrap instrument with the opposite specifications (Figure 1.7), are mainly used to study different things. In general, water analysis studies can be subdivided into two categories; untargeted identification to determine the sample composition and targeted quantification to define

exact concentrations. Qualitative analyses are mainly done with high-resolution mass spectrometry (HRMS) using orbitrap or TOF instruments [63,64]. These high resolution mass spectrometers allow the identification of unknown molecules by measuring specific m/z -ratios with very high accuracy. Once the composition of a sample is known, a triple quadrupole is the instrument of choice to quantify the compounds of interest using specific MS/MS transitions. In a first quadrupole a small fraction of precursor ions are selected by subjecting the different molecules to orthogonally varying electromagnetic fields. Subsequently, these precursor ions are dissociated in the second quadrupole to be finally analyzed in the third quadrupole that filters out a specific number of product ions [65]. The high scan speed of these quadrupoles allows a continuous multiple reaction monitoring (MRM) of unique precursor/product ion pairs to assure a sensitive quantification of the targeted components.

Since different mass analyzers are rather complementary, they should be used together or alternately in an ideal scenario [66,67]. Given the high cost of a mass spectrometer, many research labs lack the financial resources to purchase various state-of-the-art devices. Moreover, the cumbersomeness of using different instruments to analyze one sample is preferably avoided. The recent development of hybrid devices combining the benefits of multiple instruments therefore allows researchers to use the same tool for various purposes [68,69]. Two interesting examples are the quadrupole linear ion trap (QLIT) and the quadrupole time-of-flight (QTOF) which are in fact triple quadrupoles wherein the last quadrupole is replaced by a linear ion trap or a TOF tube, respectively. As a result, the high speed and sensitivity of a conventional QQQ is combined with a higher resolution in case of a QTOF or with MS_n-capability in case of a QLIT. When comparing these two instruments, it should be noted that both devices are extremely suitable for both identification and quantification [70,71]. The QTOF can be used in HRMS, but its slightly lower scan speed limits the duty cycle when multiple analytes have to be quantified. Therefore, a triple quadrupole is still the instrument of choice for the simultaneous quantification of numerous pharmaceuticals. Working in MRM mode can drastically decrease the background noise of a spectrum and will have a positive influence on the signal-to-noise ratio which leads to an increased sensitivity [72]. However, sensitivity remains particularly related to the formation and guidance of analyte ions [62,73].

| | QQQ | IT | QLIT | QTOF | Orbitrap |
|--|--|---|---|---|--|
| Mass range | ++ | +++ | ++/+++ | +++ | ++++ |
| Resolving power | + | ++ | ++ | ++/+++ | +++ |
| Dynamic range | ++++ | +++ | +++ | ++++ | +++/++++ |
| Mass accuracy | + | + | ++/++++ (depending on scan mode) | +++ | ++++ |
| Data acquisition rate (for fast chromatography) | +/++++ (depending on scan mode) | +/++ | +++ | +++ | +/++ |
| Cost | ++/+++ | ++ | +++ | +++ | ++++/++++ |
| Advantages | <ul style="list-style-type: none"> • High selectivity and sensitivity in SRM mode | <ul style="list-style-type: none"> • Moderate to high sensitivity in full-scan mode • Moderate sensitivity in SIM mode • Multiple-stage MS • Compact size | <ul style="list-style-type: none"> • High sensitivity and selectivity in SRM mode • Moderate to high sensitivity in full-scan mode • MS³ capabilities • Higher capacity for ion storage than QIT | <ul style="list-style-type: none"> • High sensitivity in full-scan mode | <ul style="list-style-type: none"> • Moderate to high sensitivity in full-scan mode • Multiple-stage MS • Large space charge capacity |
| limitations | <ul style="list-style-type: none"> • Low sensitivity in full-scan mode | <ul style="list-style-type: none"> • Limited capacity for ion storage | <ul style="list-style-type: none"> • Low accurate nominal mass | <ul style="list-style-type: none"> • Less sensitive than QQQ for quantitative purposes | <ul style="list-style-type: none"> • Not fully UPLC compatible at high resolution |

+: low; ++: moderate; +++: high; ++++: very high.

Figure 1.7: Comparison of characteristics of different tandem-mass analyzers [74]. Explanatory legend: triple quadrupole (QQQ), ion trap (IT), quadrupole-linear ion trap (QLIT), quadrupole time-of-flight (QTOF), quadrupole ion trap (QIT), selected ion monitoring (SIM), selected reaction monitoring (SRM), ultra-performance liquid chromatography.

1.5.1.2 Ionization source

During ionization, only a certain fraction of all molecules is ionized and only part of them will subsequently reach the mass analyzer [75]. In pharmaceutical analysis atmospheric pressure chemical ionization (APCI), atmospheric pressure photo-ionization (APPI) and in particular electrospray ionization (ESI) are still the ionization methods of choice. These types of ionization can easily atomize the mobile phase when hyphenated with liquid chromatography, even in highly aqueous conditions and at high flow rates [73]. Polar pharmaceuticals are mainly ionized using electrospray ionization [76,77]. The desolvation efficiency during electrospray ionization depends on the mobile phase, the matrix wherein the analyte is dissolved and the ionization source design as demonstrated by Periat et al. [73]. High concentrations of organic solvents used in hydrophilic interaction liquid chromatography (HILIC) separations for example can easily evaporate and will promote ionization relative to the highly aqueous mobile phases used in reversed-phase liquid chromatography (RPLC) [73,78]. Since the ions produced by an APCI and/or APPI interface are not necessarily the same as the ones formed in an ESI source, these techniques are alternately used depending on the type of analytes. For the analysis of rather apolar/volatile compounds, ions are preferably produced by an APCI source as they can evaporate in the ESI spray without being charged [79]. Therefore, Waters (ESCI), AB Sciex (IonDrive DuoSpray) and Agilent (Multimode Source) came up with a multimode ionization source which combines ESI and APCI to ionize every analyte in the sample [62,76,80,81]. This allows the successful analysis of both polar and non-polar compounds. The simultaneous use of APCI and ESI has recently been improved by Cheng et al. with the development of a concentric ESI+APCI dual ionization source which can be operated in ESI only, APCI only and ESI+APCI mode [82].

To perform a reliable quantification in MS experiments, it is of great importance that there is no aberration in the fraction of ionized analytes during different analytical runs. The variation in ion suppression or enhancement between samples can influence the reliability of the analysis. Highly complex matrices may cause interferences that can lead to incorrect determinations and even false positive or negative results. Therefore, it is recommended to perform an additional separation step such as liquid chromatography to minimize co-elution. Further, every methodology should be validated to obtain reliable quantitative results, even when actions are taken to compensate for matrix effects [83,84].

1.5.2 Separation of complex samples

1.5.2.1 Gas chromatography

In environmental analysis, gas chromatography (GC) and liquid chromatography (LC) are the most commonly used techniques to ensure not all molecules enter the MS ionization source simultaneously. Since GC is limited to the measurement of volatile or semi-volatile compounds and most pharmaceuticals are relatively polar, non-volatile molecules, derivatization reactions are required to make them suitable for GC analysis. To simplify and make this laborious process less time consuming, derivatization is sometimes conducted simultaneous with the sample preparation [85]. In order to enable multi-residue analysis, Kumirska *et al.* introduced a derivatization approach which allows the simultaneous analysis of pharmaceuticals from six different drug classes in the ng/L range [86]. The often toxic and non-selective derivatization reactions necessary to analyze pharmaceutical components have, however, caused LC to be the most prominent technique to separate complex water samples prior to multi-residue MS analysis.

1.5.2.2 Liquid chromatography

1.5.2.2.1 Basic principles of chromatography

High performance liquid chromatography (HPLC) is a powerful technique for the separation of pharmaceutical substances. Typically, an organic or aqueous mobile phase is used to pass a sample under high pressure through a column filled with a stationary phase. Depending on their physico-chemical properties, the components in the sample will show a different affinity for the stationary phase and elute sequentially from the column to the detector. Compounds with a higher affinity will have a larger retention time (t_R) and elute later. Molecules that are not retained elute in the void volume of the column and have a retention/elution time t_0 (dead time), which represents the time that the mobile phase needs to pass the column. The retentive force of a column can be expressed by the retention factor k (eq. 1.1). It represents the equilibration ratio of a compound in the mobile and stationary phase.

$$k = \frac{t_R - t_0}{t_0} \quad (1.1)$$

Since not all molecules of the same compound elute simultaneously due to different forms of diffusion, a detector will register Gaussian-like peaks according to the compound distribution. The longer a compound remains in a column, the more band broadening will appear. Therefore, longer columns will result in higher retention times and larger peak widths. The variance of a peak (σ^2) is proportional to the column length (L) and can be expressed via the height equivalent of a theoretical plate (H) (eq. 1.2).

$$H = \frac{\sigma^2}{L} \quad (1.2)$$

To prevent or minimize co-elution and hence matrix effects in LC-MS, the highest possible peak capacities are pursued by increasing the efficiency of the columns. Efficient columns have smaller base peak widths (w_t) and can separate a large number of molecules in a short time. Column efficiency (N) can therefore be expressed as the number of theoretical plates per length unit (eq. 1.3) and is mainly influenced by the theoretical plate height (H).

$$N = \frac{L}{H} = 16 \frac{t_R^2}{w_t^2} \quad (1.3)$$

Since band broadening mainly depends on the retention time of a substance, plate heights depend on the linear velocity (u) of the mobile phase. To define optimum flow velocities and thus efficiency, this relationship is typically plotted in a van Deemter curve (Figure 1.8) and expressed by the van Deemter equation (eq. 1.4) wherein the different (A, B and C) terms that contribute to band broadening are displayed.

$$H = A + \frac{B}{u} + C \cdot u \quad (1.4)$$

The A-term or eddy dispersion describes the uniformity of the stationary phase. Efficiently packed columns result in more homogenous beds reducing the disparity in flow path lengths of different molecules of the same compound. Therefore, plate heights are largely influenced by the particle size (d_p) of the stationary phase. As shown in Figure 1.8, smaller particles will positively affect the plate height, in particular at the optimum velocity.

When a sample is injected onto a column, a highly concentrated plug will migrate through the column and move to low-concentrated areas. This phenomenon is named longitudinal diffusion (B-term) and is inversely proportional to the linear velocity. Slow flow rates will therefore result in high longitudinal diffusion.

The C-term or resistance to mass transfer is a measure for the exchange speed of a molecule between stationary and mobile phase. This mass transfer is directly proportional with the linear velocity and depends on the diffusion coefficients of the analytes in the mobile and stationary phase. Since the interparticle volume and thus exchange time of analytes between small particles decreases, plate heights are less influenced by enhanced flow rates in columns packed with small particles. Therefore, small particle columns have a broad linear velocity optimum, which allow them to perform fast analyses.

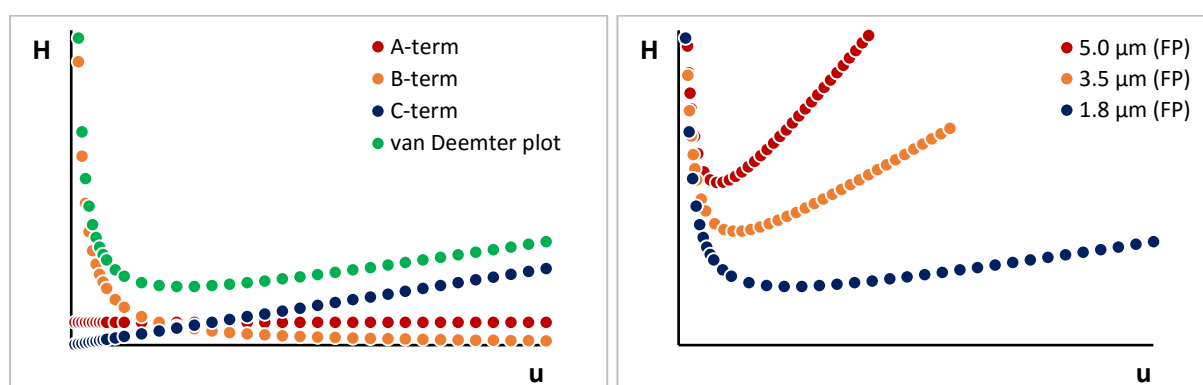


Figure 1.8: van Deemter curve with associated A, B and C terms (left). Comparison of van Deemter plots for columns packed with fully porous (FP) particles with different particle sizes (right).

To obtain the best possible separation of different substances, highly efficient columns are pursued and this is mainly done by decreasing the particle size (< 2 μm) of the stationary phase [87]. However, as can be deduced from the Kozeny-Carman law (eq. 1.5), smaller particles result in higher backpressures when the column length (L), mobile phase viscosity (η), bed porosity (ε_e) and flow velocity (u) remain similar.

$$\frac{\Delta p}{L} = - \frac{180 \eta}{d_p^2} \cdot \frac{(1 - \epsilon_e)^2}{\epsilon_e^3} \cdot u \quad (1.5)$$

Since, the pressure is inversely proportional to the square of the particle size, a new generation of UHPLC equipment has been developed to carry out chromatographic runs at sufficiently high velocities [88].

Alternatively, using core-shell particles with a solid core and a porous shell, the backpressure can be reduced with similar or better efficiencies than smaller fully porous particles (Figure 1.9) [89,90]. Due to the manufacturing process, the particle size distribution of superficially porous particles is much smaller than that of fully porous particles [91]. Consequently, the packing of these particles is more homogeneous and eddy diffusion is minimized.

Using core-shell particles, the intraparticle volume decreases which results in smaller column voids and the solid cores act as an additional obstruction inhibiting longitudinal diffusion. Furthermore, these impermeable cores lead to fast partitioning between mobile and stationary phase resulting in a decreased C-term and enhanced efficiency [92].

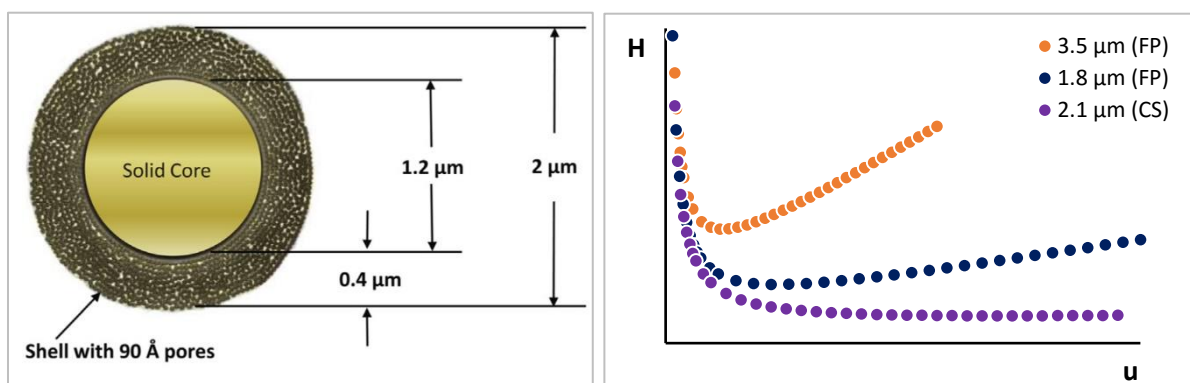


Figure 1.9: Schematic section of a core-shell particle with dimensions (left) [93] and van Deemter plot comparison of columns packed with fully porous (FP) and core-shell (CS) particles.

Another option to reduce the backpressure is the use of monolithic columns which have a stationary phase made of one single rod of porous silica-based or polymer material. Therefore, this material can be used at high flow rates to elevate the sample throughput or in longer dimensions to increase the efficiency. Despite these benefits, monoliths are not commonly used. The limited number of available selectivities and column geometries, low maximum backpressures (200 bar) and problems with the structural homogeneity of the rod should first be overcome before these columns can compete with currently available sub-2 μm and core-shell particles. Further research is thus necessary to improve the production process and provide a wide selection of monoliths with repeatable performances [94,95].

Although column efficiency is of major importance to obtain a good sample separation, analytes can only be separated when they have a different affinity for the stationary phase. Therefore, it is recommended to select an optimal column selectivity that results in a high resolution (R_s) between two separated peaks (eq. 1.6). The selectivity factor (α) can be defined as the ratio of the retention factors k_1 and k_2 for respectively the first and second eluting peak between which the resolution is determined. For Gaussian peaks a baseline separation is obtained when the resolution exceeds 1.5, however, a minimum resolution of 2.0 is preferred to ensure a robust separation method.

$$R_s = \frac{\sqrt{N}}{4} \cdot \left(\frac{k_2}{1 + k_2} \right) \cdot \left(\frac{\alpha - 1}{\alpha} \right) \quad (1.6)$$

Based on the physico-chemical features of the analytes an appropriate surface chemistry of the sorbent particles can be chosen. Typically, molecules are separated by different electrostatic bonds that are formed in ion-exchange chromatography or the formation of van der Waals forces and dipole-dipole interactions during partitioning between stationary and mobile phase [88].

1.5.2.2.2 Reversed phase and hydrophilic interaction liquid chromatography

Due to the robustness and broad application range of the columns, most water analyses are still done using reversed-phase liquid chromatography (RPLC) [87,96–98]. The hydrophobic stationary phases (e.g. C18, hexyl-phenyl or alkyl-amide), which can have polar embedded functional groups to extend the applicability, efficiently retain non-polar and semi-polar substances. In general, retention in RPLC is caused by partitioning of the molecules between the stationary and mobile phase and the different compounds are sequentially eluted according to their hydrophobicity using an aqueous mobile phase containing an organic modifier.

With numerous improvements in stationary phase material and a better understanding of the retention principles in hydrophilic interaction liquid chromatography (HILIC), the use of HILIC for the analysis of polar pharmaceuticals has increased drastically in the last decade [67,99,100]. In HILIC, a hydrophilic stationary phase (e.g. bare silica, cyano or amide) in combination with a mixture of an aqueous buffer (3% - 40%) and a high percentage of organic solvent as mobile phase, are used to separate polar substances that are not or only little retained in RPLC. Although the retention mechanisms are not yet fully understood, it is assumed that the analytes are distributed between the highly organic mobile phase and a water-enriched multilayer adsorbed on the stationary phase [101,102]. Separation of the different substances occurs by a combination of partitioning, electrostatic interactions and hydrogen bonding with the stationary phase and is highly depending on the type of stationary phase modifications, organic solvent, pH and buffer conditions such as the type of salt and concentration.

Therefore, HILIC and RPLC are two orthogonal, but complementary separation principles to analyze complex samples such as water samples that contain a large number of chemicals, pesticides, personal care products, pharmaceuticals, metabolites and transformation

products [103]. These compounds have strongly differing physico-chemical characteristics such as polarity and require highly efficient and selective separation techniques to minimize matrix interferences. For the multi-residue analyses of such complex environmental samples, simultaneous separation of both polar and non-polar components is of great importance. To allow the simultaneous analysis of these substances, both RPLC and HILIC columns can be combined. Most studies wherein pharmaceuticals are examined in combination with their generally more hydrophilic metabolites and degradation products use multiple LC-MS methodologies to analyze the entire sample [99]. In this way, highly polar substances are subjected to an improved separation and interferences will be spread more resulting in reduced matrix effects [98]. This approach, however, requires numerous injections of a sample that is not always compatible with the solvent conditions required for the individual analysis on different columns. Therefore, preference is generally given to a single method that allows a complete analysis of the entire sample.

1.5.2.3 Sample preparation

In general, pharmaceuticals are only present in very low concentrations ($\mu\text{g/L}$ to sub ng/L range) in waste and surface water [28]. However, hormones such as 17α -ethinylestradiol already show adverse effects on the aquatic environment at extremely low concentration [54]. To monitor the occurrence and determine potential adverse effects, analytical methodologies with extremely high sensitivities are thus required. For certain emerging pollutants, in particular when no state-of-the-art instruments are available, the limits of detection are deficient to acquire reliable eco-toxicity data. Therefore, sample preparation techniques are commonly used to pre-concentrate the analytes. Frequently used sample preparation strategies such as liquid/liquid extraction (LLE) and solid-phase extraction (SPE) are based on partitioning between two phases. Due to a higher affinity for a small volume of e.g. organic solvent or hydrophobic sorbent, the analytes of interest are extracted from a voluminous aqueous matrix. In environmental analysis, SPE is commonly used to analyze pharmaceuticals in water [87,104]. The large selection of different sorbents and volumes encompasses a high selectivity and capacity, thus resulting in a high sensitivity. Based on the physico-chemical properties of the pharmaceuticals and matrix interferences, a sorbent with hydrophobic or ionic characteristics can be selected to extract the substances from the water. Furthermore, SPE allows combining sorbents with different selectivities to enlarge the range in which multi-

residue analysis can be performed [98,105]. A major disadvantage of sample preparation is the large impact on the total analysis time. To improve sample throughput and minimize the analysis time, parallel offline or less time consuming online SPE procedures can be performed [106]. The development of a good sample preparation procedure is of major importance and remains a challenge. To assure a correct representation of the obtained result, the influence of the sample composition on the accuracy, repeatability and reliability should be negligible.

1.6 References

- [1] V. Law, C. Knox, Y. Djoumbou, T. Jewison, A.C. Gua, Y. Liu, et al., <https://www.drugbank.ca/> (accessed August 4, 2017).
- [2] EU, <http://ec.europa.eu/health/documents/community-register/html/atc.htm> (accessed August 1, 2017).
- [3] FAGG, https://www.fagg-afmps.be/nl/DIERGENEESKUNDIG_gebruik/geneesmiddelen/geneesmiddelen/goed_gebruik/wachttijden (accessed July 25, 2017).
- [4] A. Adriaensen, L. Bauduin, D. Boissy, K. Bonnarens, A. Cady, O. Christiaens, et al., FAGG jaarverslag 2015, 2015.
- [5] J. Van der Heyden, D. Walckiers, S. Drieskens, L. Gisle, Gezondheidsenquête 2013, 2013.
- [6] RIZIV, Farmaceutische kengetallen 2014, 2015.
- [7] EvaluatePharma, World Preview 2016 , Outlook to 2022, 2016.
- [8] E. Moorkens, N. Meuwissen, I. Huys, P. Declerck, A.G. Vulto, S. Simoens, *Front. Pharmacol.* **8**, Article 314 (2017).
- [9] K. Pennente, J. Lyle, B. Gardocki, M. Aitken, Global Medicines Use in 2020 Outlook and Implications, 2015.
- [10] D.B. Raynes, E.R. Beardsley, M.A. Braza, T.L. Doriss, C.T. Egan, B. Keith-Jennings, et al., ENVIRONMENTAL HEALTH - Action Needed to Sustain Agencies' Collaboration on Pharmaceuticals in Drinking Water, 2011.
- [11] GoI, http://www.cpcb.nic.in/Industry_Specific_Standards.php (accessed August 9, 2017).
- [12] O. Cardoso, J. Porcher, W. Sanchez, *Chemosphere.* **115**, 20–30 (2014).
- [13] D.G.J. Larsson, *Philos. Trans. R. Soc. B.* **369**, (2014).
- [14] D.G.J. Larsson, C. de Pedro, N. Paxeus, *J. Hazard. Mater.* **148**, 751–755 (2007).
- [15] D. Dolar, T. Ignjati, *Environ. Sci. Pollut. Res.* **19**, 1033–1042 (2012).
- [16] C. Gadipelly, A. Pérez-González, G.D. Yadav, I. Ortiz, R. Ibáñez, V.K. Rathod, et al., *Ind. Eng. Chem. Res.* **53**, 11571–11592 (2014).
- [17] N. Tadkaew, F.I. Hai, J.A. Mcdonald, S.J. Khan, L.D. Nghiem, *Water Res.* **45**, 2439–2451 (2011).
- [18] B. Petrie, E.J. Mcadam, M.D. Scrimshaw, J.N. Lester, E. Cartmell, *Trends Anal. Chem.* **49**, 145–159 (2013).
- [19] J. Rivera-Utrilla, M. Sánchez-Polo, M.Á. Ferro-García, G. Prados-Joya, *Chemosphere.* **93**, 1268–1287 (2013).
- [20] L. Vergeynst, A. Haeck, H. Van Langenhove, P. De Wispelaere, K. Demeestere, *Chemosphere.* **119**, 2–8 (2015).
- [21] H. Auvinen, I. Havran, L. Hubau, L. Vanseveren, W. Gebhardt, V. Linnemann, et al., *Ecol. Eng.* **100**, 157–164 (2017).
- [22] K.I. Ekpeghere, J.-W. Lee, H.-Y. Kim, S.-K. Shin, J.-E. Oh, *Chemosphere.* **168**, 1211–1221 (2017).

- [23] X.Y. Guo, L.J. Hao, P.Z. Qiu, R. Chen, J. Xu, X.J. Kong, et al., *J. Environ. Sci. Heal. Part B.* **51**, 383–392 (2016).
- [24] X. Liu, J. Caleb, X. Meng, *Environ. Pollut.* **223**, 161–169 (2017).
- [25] J.R. Masoner, D.W. Koplín, E.T. Furlong, I.M. Cozzarelli, J.L. Gray, *Environ. Tox.* **35**, 906–918 (2016).
- [26] K. Kümmerer, *J. Environ. Manage.* **90**, 2354–2366 (2009).
- [27] B. Petrie, R. Barden, B. Kasprzyk-Hordern, *Water Res.* **72**, 3–27 (2015).
- [28] B. Petrie, J. Youdan, R. Barden, B. Kasprzyk-Hordern, *J. Chromatogr. A.* **1431**, 64–78 (2015).
- [29] K. Kuroda, R. Itten, L. Kovalova, C. Ort, D.G. Weissbrodt, C.S. Mcardell, *Environ. Sci. Technol.* **50**, 4742–4751 (2016).
- [30] T. aus der Beek, F.-A. Weber, A. Bergmann, S. Hickmann, I. Ebert, A. Hein, et al., *Environ. Toxicol. Chem.* **35**, 823–835 (2016).
- [31] M. Pomiès, J. Choubert, C. Wisniewski, M. Coquery, *Sci. Total Environ.* **443**, 733–748 (2013).
- [32] C. Grandclément, I. Seyssiecq, A. Píram, P. Wong-Wah-Chung, G. Vanot, N. Tiliacos, et al., *Water Res.* **111**, 297–317 (2017).
- [33] D. Fatta-Kassinos, M.I. Vasquez, K. Kümmerer, *Chemosphere.* **85**, 693–709 (2011).
- [34] E. Donner, T. Kosjek, S. Qualmann, K. Ole, E. Heath, D.M. Revitt, et al., *Sci. Total Environ.* **443**, 870–876 (2013).
- [35] M. Isidori, M. Lavorgna, A. Nardelli, A. Parrella, L. Previtiera, M. Rubino, *Sci. Total Environ.* **348**, 93–101 (2005).
- [36] G. Nałecz-Jawecki, **70**, 29–35 (2007).
- [37] R.N. Carvalho, L. Ceriani, A. Ippolito, T. Lettieri, Development of the first Watch List under the Environmental Quality Standards Directive water policy, Report EUR 27142 EN, 2015.
- [38] V. Varano, E. Fabbri, A. Pasteris, *Ecotoxicology.* **26**, 711–728 (2017).
- [39] W. Zhao, B. Wang, Y. Wang, S. Deng, J. Huang, G. Yu, *Ecotoxicol. Environ. Saf.* **144**, 537–542 (2017).
- [40] A. Kumar, I. Xagorarakí, *Regul. Toxicol. Pharmacol.* **57**, 146–156 (2010).
- [41] V.L. Cunningham, S.P. Binks, M.J. Olson, *Regul. Toxicol. Pharmacol.* **53**, 39–45 (2009).
- [42] E. Mendonc, A. Picado, S. Maria, L. Silva, M. Ana, S. Leitão, et al., *J. Ha.* **163**, 665–670 (2009).
- [43] M. Cleuvers, *Ecotoxicol. Environ. Saf.* **59**, 309–315 (2004).
- [44] K. Fent, A.A. Weston, D. Caminada, *Aquat. Toxicol.* **76**, 122–159 (2006).
- [45] V. de Jesus Gaffney, C.M.M. Almeida, A. Rodrigues, E. Ferreira, M.J. Benoliel, V.V. Cardoso, *Water Res.* **72**, 199–208 (2015).
- [46] F. Pomati, C. Orlandi, M. Clerici, F. Luciani, E. Zuccato, *Toxicol. Sci.* **102**, 129–137 (2008).
- [47] A. Christou, P. Karaolia, E. Hapeshi, C. Michael, D. Fatta-Kassinos, *Water Res.* **109**, 24–34 (2017).

- [48] J.L. Oaks, M. Gilbert, M.Z. Virani, R.T. Watson, C.U. Meteyer, B.A. Rideout, et al., *Nature*. **427**, 630–633 (2004).
- [49] C.M. De Jongh, P.J.F. Kooij, P. De Voogt, T.L. Laak, *Sci. Total Environ.* **427–428**, 70–77 (2012).
- [50] R. Triebkorn, H. Casper, V. Scheil, J. Schwaiger, *Anal. Bioanal. Chem.* **387**, 1405–1416 (2007).
- [51] T. Porsbring, H. Blanck, H. Tjellström, T. Backhaus, *Aquat. Toxicol.* **91**, 203–211 (2009).
- [52] T. Brodin, J. Fick, M. Jonsson, J. Klaminder, *Science (80-.)*. **339**, 814–816 (2013).
- [53] M.E. Monge, G.A. Harris, P. Dwivedi, F.M. Fernández, *Chem. Rev.* **113**, 2269–2308 (2013).
- [54] C.A. Harris, P.B. Hamilton, T.J. Runnalls, V. Vinciotti, A. Henshaw, D. Hodgson, et al., *Environ. Health Perspect.* **119**, 306–311 (2011).
- [55] B. Hoeger, B. Köllner, D.R. Dietrich, B. Hitzfeld, *Aqua*. **75**, 53–64 (2005).
- [56] [Http://eur-lex.europa.eu](http://eur-lex.europa.eu), (accessed August 4, 2017).
- [57] R. Loos, Analytical methods for possible WFD 1 watch list substances st, European Commission, Report EUR 27046 EN, 2015.
- [58] V. Geissen, H. Mol, E. Klumpp, G. Umlauf, M. Nadal, M. van der Ploeg, et al., *Int. Soil Water Conserv. Res.* **3**, 57–65 (2015).
- [59] NORMAN, <http://www.norman-network.net/?q=node/19> (accessed July 18, 2017).
- [60] A. Van Eeckhaut, K. Lanckmans, S. Sarre, I. Smolders, Y. Michotte, *J. Chromatogr. B Anal. Technol. Biomed. Life Sci.* **877**, 2198–2207 (2009).
- [61] A. Kaufmann, *TrAC - Trends Anal. Chem.* **63**, 113–128 (2014).
- [62] L. Lin, H. Lin, M. Zhang, X. Dong, X. Yin, C. Qu, et al., *RSC Adv.* **5**, 107623–107636 (2015).
- [63] J. Wang, P.R. Gardinali, *Chemosphere.* **107**, 65–73 (2014).
- [64] L. Vergeynst, H. Van Langenhove, P. Joos, K. Demeestere, *Anal. Bioanal. Chem.* **406**, 2533–2547 (2014).
- [65] R.A. Yost, C.G. Enke, *Anal. Chem.* **51**, 1251–1264 (1979).
- [66] D. Chen, S. Lin, W. Xu, M. Huang, J. Chu, F. Xiao, et al., *Molecules.* **20**, 18597–18619 (2015).
- [67] T. Letzel, A. Bayer, W. Schulz, A. Heermann, T. Lucke, G. Greco, et al., *Chemosphere.* **137**, 198–206 (2015).
- [68] G. Hopfgartner, D. Tonoli, E. Varesio, *Anal. Bioanal. Chem.* **402**, 2587–2596 (2012).
- [69] H.-J. Kim, K.-A. Seo, H.-M. Kim, E.-S. Jeong, J.L. Ghim, S.H. Lee, et al., *J. Pharm. Biomed. Anal.* **102**, 9–16 (2015).
- [70] C. Vom Eyser, K. Palmu, R. Otterpohl, T.C. Schmidt, J. Tuerk, *Anal. Bioanal. Chem.* **407**, 821–830 (2014).
- [71] A. Masia, J. Campo, C. Blasco, Y. Pico, *J. Chromatogr. A.* **1345**, 86–97 (2014).
- [72] B. Van Bavel, D. Geng, L. Cherta, J. Nacher-Mestre, T. Portolés, M. Ábalos, et al., *Anal. Chem.* **87**, 9047–9053 (2015).
- [73] A. Periat, I. Kohler, A. Bugey, S. Bieri, F. Versace, C. Staub, et al., *J. Chromatogr. A.* **1356**, 211–220 (2014).

- [74] M. Farré, L. Kantiani, M. Petrovic, S. Pérez, D. Barceló, *J. Chromatogr. A.* **1259**, 86–99 (2012).
- [75] A.N. Krutchinsky, J.C. Padovan, H. Cohen, B.T. Chait, *J. Am. Soc. Mass Spectrom.* **26**, 649–658 (2015).
- [76] R.T. Gallagher, M.P. Balogh, P. Davey, M.R. Jackson, I. Sinclair, L.J. Southern, *Anal. Chem.* **75**, 973–977 (2003).
- [77] P. Jackson, M.I. Attalla, *Rapid Commun. Mass Spectrom.* **24**, 3567–3577 (2010).
- [78] A. Periat, J. Boccard, J.-L. Veuthey, S. Rudaz, D. Guillarme, *J. Chromatogr. A.* **1312**, 49–57 (2013).
- [79] R. King, R. Bonfiglio, C. Fernandez-Metzler, C. Miller-Stein, T. Olah, *J. Am. Soc. Mass Spectrom.* **11**, 942–950 (2000).
- [80] A. Schreiber, *Appl. Note AB Sciex.* # 7200213-02 (2013).
- [81] S. Fischer, *Appl. Note Agil. Technol.* # 5989-6463EN (2007).
- [82] S.C. Cheng, S.S. Jhang, M.Z. Huang, J. Shiea, *Anal. Chem.* **87**, 1743–1748 (2015).
- [83] F. Gosetti, E. Mazzucco, D. Zampieri, M.C. Gennaro, *J. Chromatogr. A.* **1217**, 3929–3937 (2010).
- [84] M.J. Ruiz-Angel, M.C. García-Alvarez-Coque, A. Berthod, S. Carda-Broch, *J. Chromatogr. A.* **1353**, 2–9 (2014).
- [85] U. Kotowska, J. Kapelewska, J. Sturgulewska, *Environ. Sci. Pollut. Res.* **21**, 660–673 (2014).
- [86] J. Kumirska, A. Plenis, P. Łukaszewicz, M. Caban, N. Migowska, A. Białk-Bielińska, et al., *J. Chromatogr. A.* **1296**, 164–178 (2013).
- [87] A. Jakimska, A. Kot-Wasik, J. Namieśnik, *Crit. Rev. Anal. Chem.* **44**, 277–298 (2014).
- [88] U.W. Neue, *HPLC Columns: theory, technology and practice*, Wiley-VCH Inc., Milford, USA, 1997.
- [89] J.O. Omamogho, J.P. Hanrahan, J. Tobin, J.D. Glennon, *J. Chromatogr. A.* **1218**, 1942–1953 (2011).
- [90] D. Cabooter, F. Lestremau, F. Lynen, P. Sandra, G. Desmet, *J. Chromatogr. A.* **1212**, 23–34 (2008).
- [91] L.E. Blue, J.W. Jorgenson, *J. Chromatogr. A.* **1380**, 71–80 (2015).
- [92] F. Gritti, A. Cavazzini, N. Marchetti, G. Guiochon, *J. Chromatogr. A.* **1157**, 289–303 (2007).
- [93] J.J. DeStefano, B.E. Boyes, S.A. Schuster, W.L. Miles, J.J. Kirkland, *J. Chromatogr. A.* **1368**, 163–172 (2014).
- [94] D. Cabooter, K. Broeckhoven, R. Sterken, A. Vanmessen, I. Vandendael, K. Nakanishi, et al., *J. Chromatogr. A.* **1325**, 72–82 (2014).
- [95] J. Urban, *J. Sep. Sci.* **39**, 51–68 (2016).
- [96] A.K. Brown, C.S. Wong, *Trends Environ. Anal. Chem.* **5**, 8–17 (2015).
- [97] M. Caban, J. Kumirska, A. Białk-Bielinska, P. Stepnowski, *Curr. Anal. Chem.* **12**, 1–1 (2015).

- [98] E.L. Schymanski, H.P. Singer, J. Slobodnik, I.M. Ipolyi, P. Oswald, M. Krauss, et al., *Anal. Bioanal. Chem.* **407**, 6237–6255 (2015).
- [99] L. Havlíková, H. Vlčková, P. Solich, L. Nováková, *Bioanalysis*. **5**, 2345–2357 (2013).
- [100] M.-E. Beaudoin, E.T. Gangl, *Bioanalysis*. **8**, 111–122 (2016).
- [101] B. Buszewski, S. Noga, *Anal. Bioanal. Chem.* **402**, 231–247 (2012).
- [102] P. Hemström, K. Irgum, *J. Sep. Sci.* **29**, 1784–1821 (2006).
- [103] S.D. Richardson, S.Y. Kimura, *Anal. Bioanal. Chem.* **88**, 546–582 (2016).
- [104] L. Vergeynst, H. Van Langenhove, K. Demeestere, *TrAC - Trends Anal. Chem.* **67**, 192–208 (2015).
- [105] S. Huntscha, H.P. Singer, C.S. McArdell, C.E. Frank, J. Hollender, *J. Chromatogr. A.* **1268**, 74–83 (2012).
- [106] S. Idder, L. Ley, P. Mazellier, H. Budzinski, *Anal. Chim. Acta.* **805**, 107–115 (2013).

CHAPTER 2

Objectives

To date, little is known about pharmaceutical water pollution worldwide, nevertheless, the occurrence and potential ecological harm of pharmaceuticals has become a major topic of interest. New techniques to eliminate pharmaceuticals from water are being developed continuously, however, appropriate analytical methods to evaluate the presence, degradation and removal of various drugs with a wide range of polarities are lacking. Due to the very low concentrations wherein these molecules are present in water bodies, assays with an extremely high sensitivity are required.

To refine wastewater treatment strategies, a small selection of frequently observed pharmaceuticals in environmental water bodies will be subjected to advanced oxidation processes using a boron-doped diamond electrode in Chapter 3. Different parameters will be tested to optimize the removal efficiency of these pharmaceuticals in simulated wastewater and real wastewater effluent. Since the formation of multiple transformation products that are generally more hydrophilic than the parent compounds is expected, a methodology to accelerate and simplify the screening of pharmaceuticals and their degradation products in wastewater is required. Therefore, a new generic analytical methodology with the potential to separate complex environmental samples will be developed in Chapter 4. With the objective to analyze polar and non-polar molecules in a single analytical run, the combination of orthogonal stationary phases will be explored. With a setup wherein reversed-phase and hydrophilic interaction liquid chromatography stationary phases are coupled in series, the analyses of samples containing pharmaceuticals with a large variety in polarity will be pursued. The use of a single solvent delivery pump is envisaged to make the setup more economical and robust. To deal with the mobile phase incompatibility of the orthogonal stationary phases, commercially available mixers will be used for intermediate solvent exchange. However, since these commercial mixers are bulky, expensive and not flexible, an innovative mixing unit will be evaluated in Chapter 5. A flexible and cheap mixing unit is envisaged by combining restriction capillaries with different flow resistances allowing various dilution volumes. Furthermore, columns of different internal diameter will be combined to demonstrate the repeatability and flexibility of the restriction capillaries. Complementary to the analytical setup, a generic sample preparation method capable of extracting compounds with a large variety in polarity is required for the analysis of pharmaceutically relevant contaminants in wastewater. Therefore, a generic SPE procedure will be developed in Chapter 6 for the simultaneous extraction of polar and non-polar pharmaceuticals from simulated wastewater.

CHAPTER 3

Electrochemical oxidation of key pharmaceuticals using a Boron Doped Diamond electrode

Based on:

Loos G., Scheers T., Van Eyck K., Van Schepdael A., Adams E., Van der Bruggen B., Cabooter D., Dewil R. (2017). Electrochemical oxidation of key pharmaceuticals using a Boron Doped Diamond electrode. Submitted article

3.1 Introduction

Preventing, counteracting and remediating wastewater from polluting our environment has been one of the main topics in water research for the last decades. Pollutants that are receiving special attention lately are pharmaceutical products originating from care centers, hospitals and civil use [1,2]. As described in § 1.2.1, these products enter the environment through sewage systems and wastewater treatment plants causing a wide variety of unwanted effects on organisms that live in surface and ground water. Some of these products have already been reported in drinking water thus creating the possibility to affect the human population [3].

The possibility to use advanced oxidation processes (AOP) as viable methods for the removal of these substances from wastewater has been reported in the literature [2,4,5]. One type of AOP is electrochemical oxidation, which has some distinct benefits such as the sole use of electricity for pollutant degradation (without the need to add chemicals), no waste production and operation at ambient temperature [6]. Initial studies for its use in wastewater treatment have already been reported decades ago, however, an effective degradation has only been achieved since diamond coated anodes were applied [7,8]. The main advantage this type of anodes has over others is the high overpotential for water hydrolysis. This property facilitates a highly efficient generation of hydroxyl radicals at the anode's surface, which serve as oxidants for the degradation of the organic compounds [9]. Next to oxidation via these radicals, other mechanisms were shown to take place, such as (i) oxidation mediated by other oxidizing species generated from salts present in the wastewater such as hypochlorite and peroxosulphates and (ii) direct oxidation at the anode's surface [10]. In contrast, when using typical anode materials such as platinum and carbon, the oxidation mainly takes place at the anode's surface via direct electron transfer after adsorption of the organic compound at the anode or oxidation via physically or chemically adsorbed hydroxyl radicals (depending on the applied voltage) [11]. These mechanisms are much slower than the indirect oxidation via free hydroxyl radicals, mainly because these reactions do not only take place at the surface of the anode, but also in the bulk liquid surrounding the anode. Basically, diffusional aspects are the only processes that are limiting the degradation rate at high pollutant concentrations [12]. Additionally, these anodes are highly stable, both chemically and electrochemically, resulting in a long lifetime [12]. A full overview of the electrochemical degradation technology is provided in [13]. An overview of some recent publications is included in Table 3.1.

Table 3.1: Overview of some recent publications on the degradation of pharmaceuticals via BDD.

| Reference | Substances studied | Main conclusions |
|-------------------------------|---|--|
| Lan et al. (2018) [14] | Ciprofloxacin Sulfamethoxazole Salbutamol | <ul style="list-style-type: none">– Complete removal of pharmaceuticals observed– No significant impact of common organics in the wastewater– Model developed with excellent correlation with experimental results |
| Frontistis et al. (2017) [15] | Amoxicillin | <ul style="list-style-type: none">– Initial COD concentration, current density and treatment time were most important parameters governing amoxicillin degradation– Major transformation products were identified– Degradation pathways were defined |
| Pérez et al. (2017) [16] | Mixed real effluents | <ul style="list-style-type: none">– Comparison between Fenton oxidation and BDD was made– For 80% of the effluents studied, BDD degradation was found to be more efficient |
| Sopaj et al. (2016) [17] | Sulfamethazine | <ul style="list-style-type: none">– BDD was found to be the best anode material, compared to Ti/RuO₂-IrO₂ and graphite felt– Almost complete mineralization was achieved |
| Salazar et al. (2016) [18] | losartan | <ul style="list-style-type: none">– Full removal of losartan was achieved– Four aromatic intermediates were identified and short-linear carboxylic acids were determined as degradation products |
| Zhu et al. (2016) [19] | Ciprofloxacin Norfloxacin Ofloxacin | <ul style="list-style-type: none">– Eight oxidation products for each parent component were identified and oxidation pathways were proposed– Toxicity after oxidation remained constant for ciprofloxacin and norfloxacin, and increased for ofloxacin (algae inhibition tests)– Oxidation mixture retained antibacterial properties |
| Brillas et al. (2016) [20] | Dopamine | <ul style="list-style-type: none">– BDD anodes yielded a faster decomposition of dopamine than Pt anodes due to greater oxidation of OH[•] generated by BDD– Short-linear carboxylic acids were identified as oxidation products |

In this Chapter, the use of a boron doped diamond (BDD) electrode for the degradation of four representative pharmaceuticals is evaluated: iopromide (IOP), an x-ray contrast agent; sulfamethoxazole (SMX), a sulfonamide based antibacterial agent; 17 α -ethinylestradiol (EE₂), a steroid derivate used in contraceptives and diclofenac (DCF), a nonsteroidal anti-inflammatory drug. The influence of operating conditions such as flow rate, temperature and current are evaluated. For this purpose, the four pharmaceutical products are dissolved in simulated effluent wastewater. The results are moreover compared with tests using real effluent wastewater originating from a hospital wastewater treatment plant.

3.2 Materials and methods

3.2.1 Chemicals

Diclofenac (DCF), sulfamethoxazole (SMX) and 17 α -ethinylestradiol (EE₂) were purchased from Sigma-Aldrich (Overijse, Belgium). Iopromide (IOP) was purchased from VWR International (Leuven, Belgium). Deionized water was produced with a reverse osmosis water filtration device (VWR International, Leuven, Belgium) that maintained an electrical conductivity of 5 μ S/cm. Simulated wastewater (SWW) was prepared according to the composition provided in Table 3.2.

Table 3.2: Composition of SWW used in the experiments.

| Substances | Concentration (mg/L) | Supplier |
|--|----------------------|---|
| NaHCO ₃ | 96 | Fisher Scientific (Loughborough, UK) |
| NaCl | 7 | Fisher Scientific (Loughborough, UK) |
| CaSO ₄ · 2H ₂ O | 60 | Merck (Darmstadt, Germany) |
| Urea | 6 | S.C. Federa S.V. (Brussels, Belgium) |
| KCl | 4 | ChemLab (Zedelgem, Belgium) |
| CaCl ₂ | 3 | Sigma-Aldrich (Steinheim, Germany) |
| Peptone | 32 | BD Biosciences (Le Pont-de-Claix, France) |
| MgSO ₄ · 7H ₂ O | 125 | Acros Organics (Geel, Belgium) |
| NH ₄ H ₂ PO ₄ | 1.2 | Merck (Darmstadt, Germany) |
| Meat extract | 22 | Sigma-Aldrich (Steinheim, Germany) |

The chemical oxygen demand (COD) of the SWW was 53.2 mg/L. Real effluent wastewater (RWW) was taken from the effluent ditch of the Pellenberg hospital WWTP (Kortenbergh, Belgium), and had a COD of around 78.4 mg O₂/L. COD was measured using Hach COD test kits and a DR3900 spectrophotometer from Hach (Mechelen, Belgium).

3.2.2 Electrochemical setup and experiments

The experimental setup consisted of a flow-through electrochemical cell, a circulation tank and a centrifugal pump as depicted in Figure 3.1. For each experiment, the buffer tank was filled with 10 L of the experimental solution, which was circulated through the electrochemical

cell at a fixed flow rate (controlled via a membrane valve). The electrodes were made of a conductive substrate of silicon, coated with the BDD layer, and yielded a surface area of 189 cm². The electrodes were connected to a power source with a maximum voltage of 55 V and a maximum current of 10 A. The conductivity was measured with a WTW Microprocessor Conductivity meter LF 537 from VWR (Haasrode, Belgium) while the pH and temperature were monitored with a HI2211 pH meter from Hanna Instruments (Temse, Belgium).

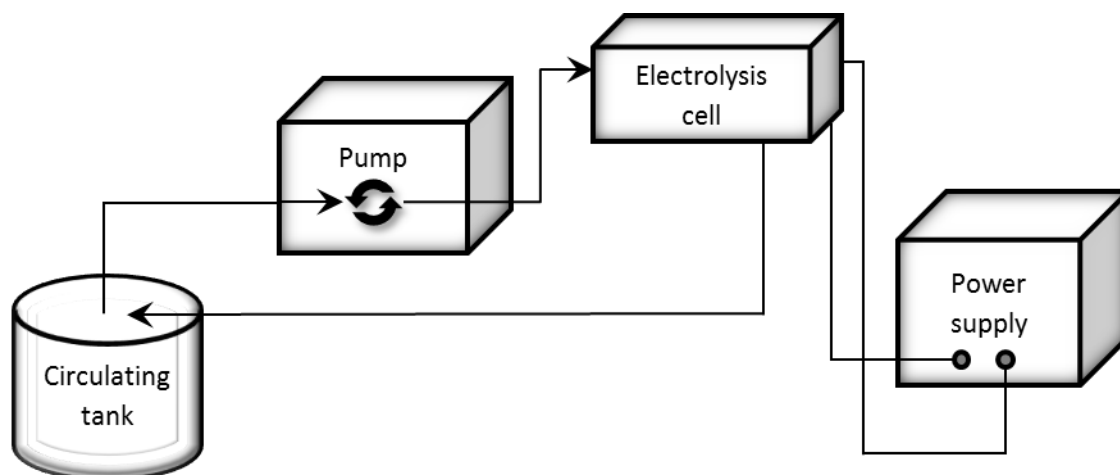


Figure 3.1: Schematic representation of the lab scale experimental setup.

Experimental solutions were prepared by measuring out the appropriate mass of IOP, SMX, EE₂ and DCF gravimetrically in concentrations of 0.5 mg/L or 10 mg/L. Complete dissolution of the components was guaranteed by mixing the solution for 2 h on a stir plate before introducing it in the circulation tank. To start the experiment, the circulation pump was activated and the flow rate adjusted using the valve. Once the flow rate was stable, the BDD cell was turned on. The polarization of the electrodes was switched every 10 min to prevent scaling. Samples were taken at regular time intervals in the circulation tank and analyzed using liquid chromatography (see § 3.2.3).

3.2.3 LC-MS experiments

All samples were analyzed on a Dionex Ultimate 3000 HPLC system (ThermoFisher Scientific, Germering, Germany) equipped with an autosampler, a quaternary pump and a variable wavelength detector with a cell volume of 11 µL. The column temperature was controlled at 40 °C with a static air oven compartment (Waters, Bedford, MA, USA). The maximum operating pressure of the system was 400 bar. Peeksil viper tubing (75 µm I.D.) (ThermoFisher

Scientific) was used to connect the column to the injector and detector of the system. The tubing was not altered during the experiments to avoid changing the extra-column volume. Analyses were performed using a Poroshell 120 Bonus-RP (2.1 x 100 mm; 2.7 μ m) column (Agilent Technologies, Waldbronn, Germany) in gradient mode using 0.5% formic acid in H₂O as mobile phase A and 0.5% formic acid in ACN as mobile phase B. After an equilibration of 7 min at the initial mobile phase condition of 100% A, the mobile phase was changed to 30:70 A:B in 10 min, held for 2 min at 30:70 A:B and returned to 100% A in 1 min. The flow rate was 0.3 mL/min and the injection volume 100 μ L. The absorbance was measured at wavelengths of 254 nm (IOP) and 280 nm (SMX, EE₂ and DCF). For the identification of the transformation products, the HPLC was connected to an LCQ ion trap mass spectrometer (ThermoFinnigan) with ESI interface operated in positive ion mode. The ESI needle voltage was set at 4.5 kV and the heated capillary was held at 300°C. Following voltages were applied to obtain an optimal signal: capillary voltage 19.0 V, tube lens offset voltage -15.0 V, octopole 1 offset voltage -3.0 V, octopole 2 offset voltage -10.0 V, and interoctopole lens voltage -16.0 V. Nitrogen (Air Liquide, Liège, Belgium) served as sheath at a flow rate of 100 arb and auxiliary gas at a flow rate of 60 arb. Helium was used as damping gas. Xcalibur 1.3 software (ThermoFinnigan) was used for instrument control, data acquisition, and processing. The experimental m/z values of the parent compounds were obtained with a resolving power of 500 – 1000 based on the full width at half maximum methodology and subsequently compared with literature data to suggest a tentative structure for some transformation products.

3.2.4 Kinetic evaluation

Because of the very short lifetime of the generated hydroxyl radicals (limited to a few nanoseconds) [21], their concentration can be described via a quasi-stationary state and pseudo first-order reaction kinetics can be considered, following eq. 3.1.

$$-\frac{dC}{dt} = k_{\text{abs}} \cdot [\text{OH}^{\bullet}] \cdot C = k \cdot C \quad (3.1)$$

where C is the concentration of the organic compound to be degraded, k_{abs} is the absolute reaction rate constant and k the apparent first-order reaction rate constant. After integration of this reaction rate equation, the corresponding representation of the logarithm in function of time was used to determine the k for the oxidation of the compounds at each experiment.

3.3 Results and discussion

3.3.1 Degradation kinetics in simulated wastewater

The kinetics for the degradation of IOP, SMX, EE₂ and DCF were first assessed separately in simulated wastewater (mono) and then compared to the kinetics of a mixture of the components (mixed). The initial concentration of each component in all tests was 0.5 mg/L, and the BDD treatment was carried out at an applied current (I) of 0.9 A and a flow rate (Q) in the electrochemical cell of 250 L/h. The results of the degradation experiments are reported in Figure 3.2.

Only small differences were observed between the degradation curves of SMX, EE₂ and DCF when the compounds were individually added to the SWW, with a degradation of 72.9%, 69.7% and 73.7% after 180 min reaction time, respectively. The IOP degradation occurred much slower. Only 32.3% of the initial IOP concentration was degraded after 180 min. For all components, a considerable decrease in degradation rate was observed when all components were present simultaneously. The degradation after 180 min reaction time was reduced to 27.8%, 67.7%, 39.5% and 66.9% for IOP, SMX, EE₂ and DCF, respectively. Especially for EE₂ a considerable drop was noticed. For the other components, the decrease was limited.

To quantify these differences in degradation rate, the first order reaction rate constants were determined and are listed in Table 3.3 for all compounds. The high correlation coefficients (R^2) for the linear approximation of $\ln(c)$ versus t confirms the validity of the assumption that pseudo first-order kinetics are applicable for all degradation curves. It moreover confirms the high accuracy of the concentration measurements.

The reaction rate constants k are all in the same order of magnitude (10^{-3}), but differences between the exact values are observed. For the individual compounds, the order of reaction rate constants is DCF > SMX > EE₂ > IOP. The same order is observed when all compounds are present simultaneously: DCF > SMX > EE₂ > IOP. Further, a decrease in k by 17.4%, 32.4%, 54.7% and 22.7% is observed for IOP, SMX, EE₂ and DCF, respectively, when the compounds are simultaneously present in the SWW. Especially for EE₂, this decrease is substantially higher than for the other components. This observation cannot be explained by the experimental results obtained in this study.

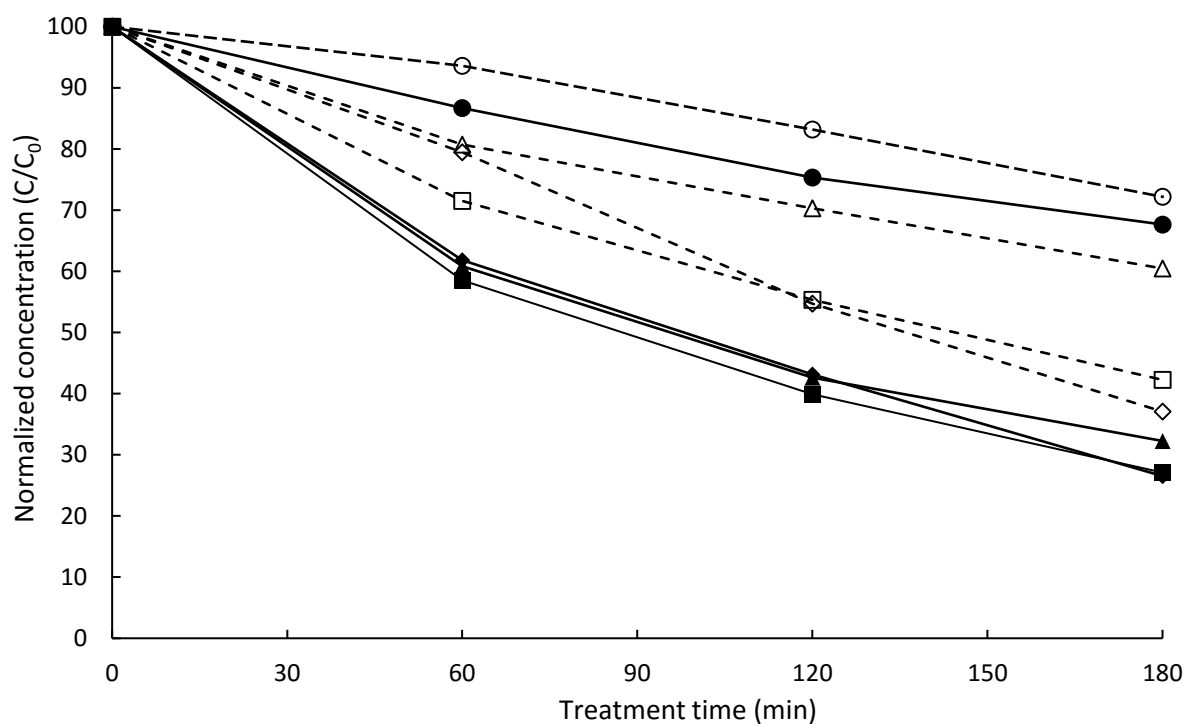


Figure 3.2: Time course of the compound concentration during BDD treatment for the SSW with each compound individually (mono, closed symbols and full lines) and a mixture of all compounds (mixed, open symbols and dashed lines) ($I= 0.9$ A; $Q= 250$ L/h; $T=$ room temperature). Symbols indicate IOP (●/○), SMX (■/□), EE_2 (▲/△) and DCF (◆/◇).

Table 3.3: Pseudo first-order reaction rate constants for the degradation of IOP, SMX, EE_2 and DCF in SSW for each individual compound and for the mixture of all compounds ($I= 0.9$ A; $Q= 250$ L/h; $T=$ room temperature).

| Sample | k (min^{-1}) | R^2 |
|----------------|---------------------------|-------|
| IOP (mono) | 0.0023 | 0.996 |
| IOP (mixed) | 0.0019 | 0.972 |
| SMX (mono) | 0.0074 | 0.990 |
| SMX (mixed) | 0.0050 | 0.996 |
| EE_2 (mono) | 0.0064 | 0.980 |
| EE_2 (mixed) | 0.0029 | 0.989 |
| DCF (mono) | 0.0075 | 0.997 |
| DCF (mixed) | 0.0058 | 0.989 |

The decrease in k is explained by the competitive degradation of the components. Given a set of process conditions (i.e., $I= 0.9$ A, $Q= 250$ L/h and $T=$ room temperature), the amount of hydroxyl radicals generated in the BDD cell is constant. A competitive use of these oxidants for the degradation of the compounds hence occurs if more compounds are added simultaneously. The SWW (without addition of the pharmaceutical compounds) already contains 60 mg/L of organic material (combination of urea, peptone and meat extract that is included in the wastewater). When simultaneously adding all compounds, the total organic matter concentration in the SWW increases from 60.5 mg/L (0.5 mg/L if one pharmaceutical compound is added) to 62.0 mg/L (0.5 mg/L of each of the 4 pharmaceutical compounds when added together), but this increase is limited compared to the overall concentration of organics. The observed decrease in k values is hence induced by only a minor increase of organic matter, suggesting that this type of organics is more prone to oxidative degradation than the organic matter already present in the SWW. In other words, the large decrease in k , for only a limited increase in total organic matter of the SWW suggests that the pharmaceuticals are preferentially targeted by the BDD treatment.

3.3.2 Influence of flow rate

The influence of the flow rate Q in the electrochemical cell on the observed degradation was tested by measuring the degradation of the pharmaceutical compounds over time at three different flow rates, i.e., 125, 250 and 500 L/h. Tests were carried out in SWW, to which a concentration of 0.5 mg/L of all four pharmaceutical compounds was added simultaneously. The applied current was 0.9 A and all experiments were performed at room temperature. The results of the degradation tests are shown in Figure 3.3. The pseudo first-order reaction rate constants are listed in Table 3.4. Again, high R^2 values confirm the assumption of pseudo first-order reaction kinetics.

Table 3.4: Pseudo first-order reaction rate constants for the degradation of IOP, SMX, EE₂ and DCF in SSW for different flow rates Q ($I= 0.9$ A; $T=$ room temperature).

| Flow rate Q (L/h) | IOP | | SMX | | EE ₂ | | DCF | |
|------------------------|--------------------------|-------|--------------------------|-------|--------------------------|-------|--------------------------|-------|
| | k (min ⁻¹) | R^2 | k (min ⁻¹) | R^2 | k (min ⁻¹) | R^2 | k (min ⁻¹) | R^2 |
| 125 | 0.0019 | 0.987 | 0.0052 | 0.963 | 0.0023 | 0.998 | 0.0052 | 0.996 |
| 250 | 0.0019 | 0.972 | 0.0050 | 0.996 | 0.0029 | 0.989 | 0.0058 | 0.989 |
| 500 | 0.0021 | 0.991 | 0.0054 | 0.998 | 0.0037 | 0.996 | 0.0068 | 0.992 |

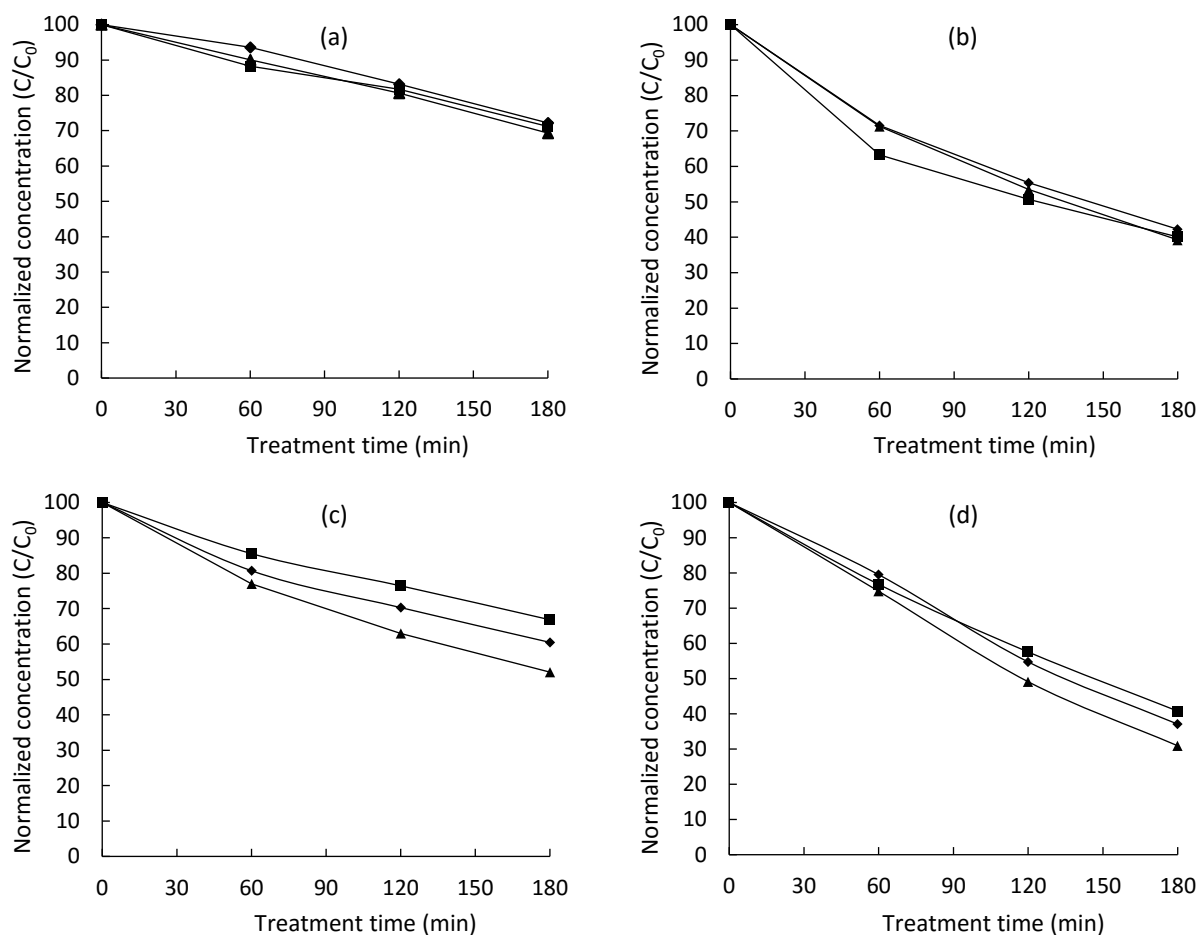


Figure 3.3: Time course of compound degradation for different flow rates: ■ 125 L/h, ◆ 250 L/h, ▲ 500 L/h for (a) IOP, (b) SMX, (c) EE₂ and (d) DCF ($I = 0.9$ A; $T = \text{room temperature}$).

Overall, only a limited influence of Q on the degradation kinetics is observed. There is no substantial change in k for IOP and SMX. The values of k remain within a 10% margin, irrespective of the flow rate applied. For EE₂, an increase from 0.0023 min^{-1} to 0.0029 min^{-1} and 0.0037 min^{-1} is present when Q increases from 125 L/h to 250 L/h and 500 L/h, respectively. This represents a relative increase by 26% and 61%, respectively. The k values for DCF increase from 0.0052 min^{-1} to 0.0058 min^{-1} and 0.0068 min^{-1} for a Q increase from 125 L/h to 250 L/h and 500 L/h, respectively (relative increase by 12% and 31%). It was previously described [22,23] that the flow rate in the cell determines the mass transfer coefficient. Racaud et al. even described a linear relationship between flow rate and mass transfer coefficient. A limited influence of the flow rate in the cell indicates that the occurring reactions are not mass transfer limited, but rather reaction rate limited (chemical reaction is slower than mass transfer). Hence an improvement of the mass transfer coefficient only influences the overall observed kinetic constant k to a limited extent [23].

3.3.3 Temperature dependency

The temperature dependency of the degradation reaction was evaluated by carrying out tests at 18°C, 30°C and 50°C. Tests were carried out on SWW, to which a concentration of 0.5 mg/L of all 4 pharmaceutical compounds was added simultaneously. The applied current was 0.9 A and the flow rate through the electrolysis cell was 500 L/h. The results of the degradation tests are shown in Figure 3.4. The pseudo first-order reaction rate constants are listed in Table 3.5.

For all components, the reaction rate increased with increasing temperature. Between 18°C and 50°C, an increase in k was observed of 44%, 186%, 58% and 64% for IOP, SMX, EE₂ and DCF, respectively. With an increase of 186%, a prominent increase was observed for SMX when the temperature was elevated. In contrast, the other 3 components had a less pronounced increase for k and showed a very similar temperature dependency.

The availability of the reaction rate constants at different temperatures further enabled to calculate the activation energy E_a for all degradation reactions. Indeed, as is the case for most chemical reaction systems, the electrochemical degradation is assumed to follow the Arrhenius law, which is displayed in eq. 3.2:

$$k = A \cdot \exp\left(-\frac{E_a}{R \cdot T}\right) \quad (3.2)$$

with k the reaction rate constant (min^{-1}), A the pre-exponential factor (min^{-1}), E_a the activation energy (J/mol), T the absolute temperature (K) and R the universal gas constant (8.314 J/mol.K).

E_a can further be calculated by taking the natural logarithm of both sides of the equation, which recasts it into the form of an equation for a straight line (eq. 3.3):

$$\ln(k) = \ln(A) - \frac{E_a}{R} \cdot \frac{1}{T} \quad (3.3)$$

A plot of $\ln k$ in function of $1/T$ gives a straight line whose slope is $-E_a/R$ and whose y-intercept is $\ln(A)$. The results of this evaluation are reported in Table 3.6. The Arrhenius assumption was confirmed by the systematically high R^2 values for the linear fit of the experimental data to eq. 3.3, which were 0.99, 0.94, 0.99 and 0.89 for IOP, SMX, EE₂ and DCF, respectively. The highest value of E_a was obtained for SMX (24914 J/mol), followed by 12696 J/mol for DCF, 11182 J/mol for EE₂ and 8950 J/mol for IOP.

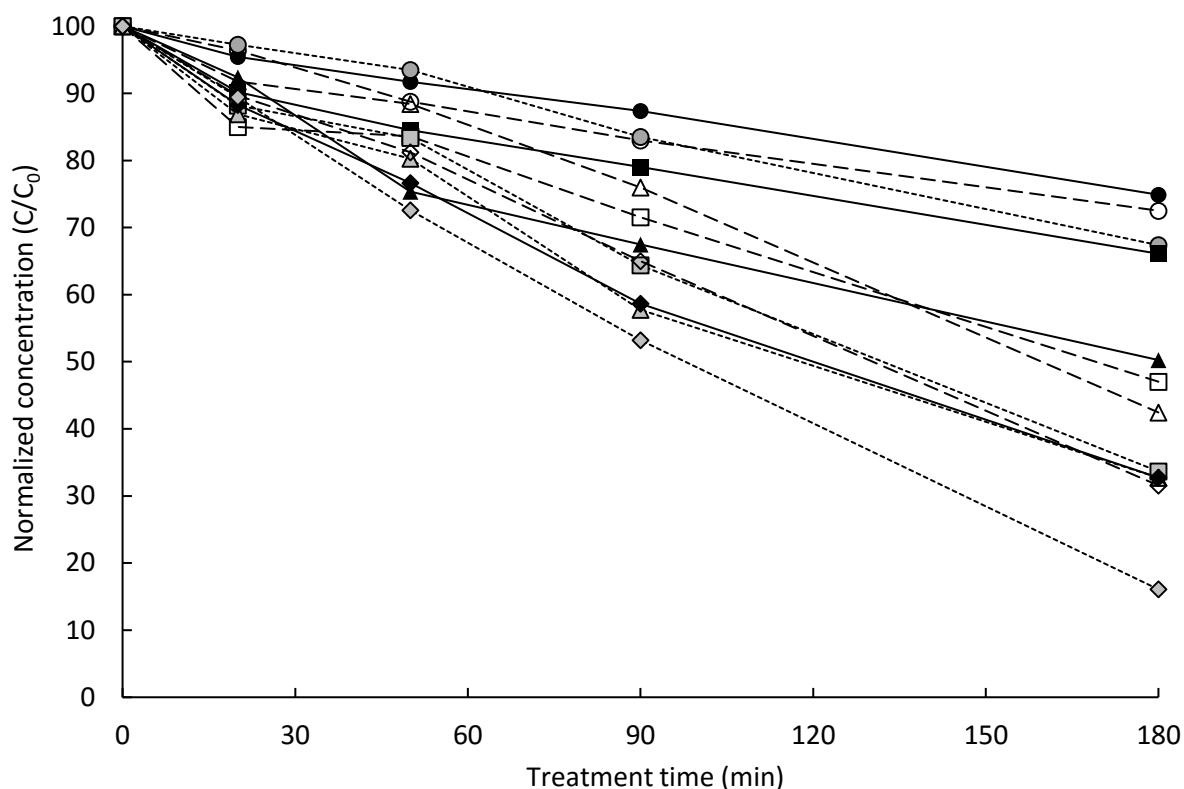


Figure 3.4: Time course of compound degradation at different temperatures: 18°C (full symbols and full lines), 30°C (open symbols and dashed lines), 50°C (grey symbols and dotted lines) for IOP (●), SMX (■), EE₂ (▲) and DCF (◆) at $I = 0.9$ A and $Q = 500$ L/h.

Table 3.5: Pseudo first-order reaction rate constants for the degradation of IOP, SMX, EE₂ and DCF in SSW at different temperatures ($I = 0.9$ A; $Q = 500$ L/h).

| Temp (°C) | IOP | | SMX | | EE ₂ | | DCF | |
|-----------|------------------------|----------------|------------------------|----------------|------------------------|----------------|------------------------|----------------|
| | k (min ⁻¹) | R ² | k (min ⁻¹) | R ² | k (min ⁻¹) | R ² | k (min ⁻¹) | R ² |
| 18 | 0.0016 | 0.995 | 0.0021 | 0.973 | 0.0039 | 0.964 | 0.0062 | 0.976 |
| 30 | 0.0018 | 0.986 | 0.0040 | 0.976 | 0.0049 | 0.977 | 0.0064 | 0.998 |
| 50 | 0.0023 | 0.989 | 0.0060 | 0.976 | 0.0062 | 0.991 | 0.0102 | 0.972 |

Table 3.6: Pre-exponential factor A and activation energy E_a for the degradation of IOP, SMX, EE₂ and DCF.

| | IOP | SMX | EE ₂ | DCF |
|------------------------|--------|-------|-----------------|-------|
| A (min ⁻¹) | 0.0640 | 68.1 | 0.403 | 1.10 |
| E _a (J/mol) | 8950 | 24914 | 11182 | 12696 |

3.3.4 Degradation in real effluent wastewater

Degradation experiments were also performed using real effluent wastewater (RWW). The wastewater was spiked with the four pharmaceutical compounds simultaneously at concentrations of 0.5 mg/L and 10 mg/L. For the 10 mg/L concentration, the treatment time was extended to 540 min to achieve a sufficient degradation of the compounds. The current I was set at 0.9 and 3.1 A while the temperature was kept at 50°C. The results of the degradation experiments are presented in Figure 3.5. The calculated pseudo first-order reaction rate constants k are included in Table 3.7.

Table 3.7: Pseudo first-order reaction rate constants for the degradation of IOP, SMX, EE₂ and DCF in RWW. ($Q= 500$ L/h; $T= 50^{\circ}\text{C}$).

| Compound | 0.5 mg/L, 0.9 A | | 0.5 mg/L, 3.1 A | | 10 mg/L, 3.1 A | |
|-----------------|--------------------------|----------------|--------------------------|----------------|--------------------------|----------------|
| | k (min ⁻¹) | R ² | k (min ⁻¹) | R ² | k (min ⁻¹) | R ² |
| IOP | 0.0025 | 0.962 | 0.0088 | 0.973 | 0.0087 | 0.976 |
| SMX | 0.0252 | 0.990 | - | - | - | - |
| EE ₂ | 0.0177 | 0.908 | - | - | 0.0095 | 0.899 |
| DCF | 0.0117 | 0.992 | 0.0241 | 0.894 | 0.0248 | 0.962 |

To evaluate the difference in degradation efficiency between SWW and RWW as wastewater matrix, the k -values of the pharmaceutical compounds at the following process conditions were compared: $C_0= 0.5$ mg/L, $I= 0.9$ A, $T= 50^{\circ}\text{C}$ and $Q= 500$ L/h. For all four compounds, a much higher k was observed in the RWW. The relative increase for the different compounds, however, largely differed: k increased with 19%, 367%, 378% and 72% for IOP, SMX, EE₂ and DCF, respectively. The systematically higher k for all compounds in the RWW is remarkable since the COD of the RWW (78.4 mg/L) was approximately 50% higher than the COD of the SWW. Similar to the discussion on the selectiveness of the oxidation in section 3.1, it seems that the type of organic matter in the RWW consumes less oxidative species, and the selectiveness towards the oxidation of the added pharmaceuticals is higher for the RWW.

An increase of I to 3.1 A resulted in a considerably faster degradation of all compounds. The concentration of SMX and EE₂ already dropped below the detection limit at the first sampling point (at a reaction time of 60 min). Therefore, k could not be determined for these components. For IOP and DCF, k increased by 252% and 106%, respectively. At the same I , increasing the C_0 to 10 mg/L only had a marginal effect on k . Because of the very fast degradation of SMX and EE₂ (as mentioned above), no comparison could be made for these compounds. For IOP and DCF, no prominent difference in k was observed.

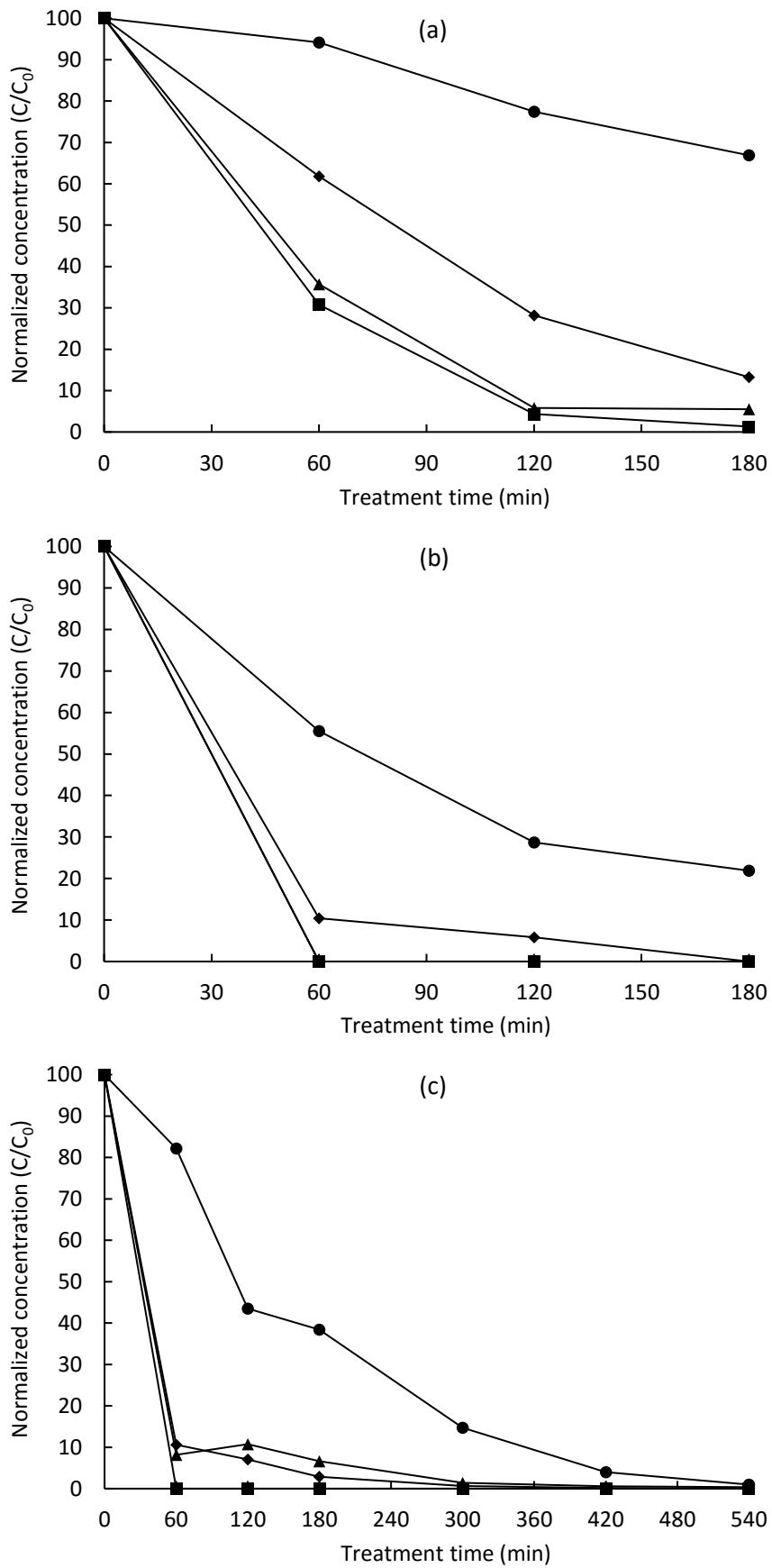


Figure 3.5: Time course of compound degradation in real effluent wastewater. **(a)** $C_0 = 0.5 \text{ mg/L}$, $Q = 500 \text{ L/h}$, $I = 0.9 \text{ A}$; **(b)** $C_0 = 0.5 \text{ mg/L}$, $Q = 500 \text{ L/h}$, $I = 3.1 \text{ A}$; **(c)** $C_0 = 10 \text{ mg/L}$, $Q = 500 \text{ L/h}$, $I = 3.1 \text{ A}$ for IOP (●), SMX (■), EE₂ (▲) and DCF (◆). All experiments were performed at 50°C.

3.3.5 Fate of the degradation products

So far, only the degradation of the parent compounds has been discussed. However, when these pharmaceuticals are oxidized, a large number of degradation/transformation products is formed. Figure 3.6 (a) shows a representative chromatogram obtained for DCF after 0, 60, 120, 180 and 300 min of treatment, using the same experimental conditions as in Figure 3.5. Note that a number of transformation products (TPs) can clearly be observed in the chromatogram. Some transformation products were tentatively identified based on their m/z and literature data [24–26]. The suggested structures are shown in Table 3.8. Since standard compounds of these TPs were not available, an accurate quantitation of their concentration was not feasible. Therefore, the evolution of their concentration as a function of degradation time is merely represented as the observed area under the curve versus the maximum obtained area under the curve of the chromatographic peak (A/A_{\max}) in Figure 3.6 (b). These results indicate that whereas DCF is completely removed from the solution after 180 min, it takes two to three times longer to remove all the degradation products from the solution.

Similar results were obtained for SMX, EE₂ and IOP (data not shown), where it was also observed that the order wherein the degradation products are removed, is similar to their parent compounds: i.e., the degradation products of DCF are easier to remove than those of SMX, EE₂ and IOP. These observations indicate that monitoring the removal efficiency of the parent compounds is not sufficient when dealing with persistent degradation products, especially when these have a higher toxicity than the parent compound.

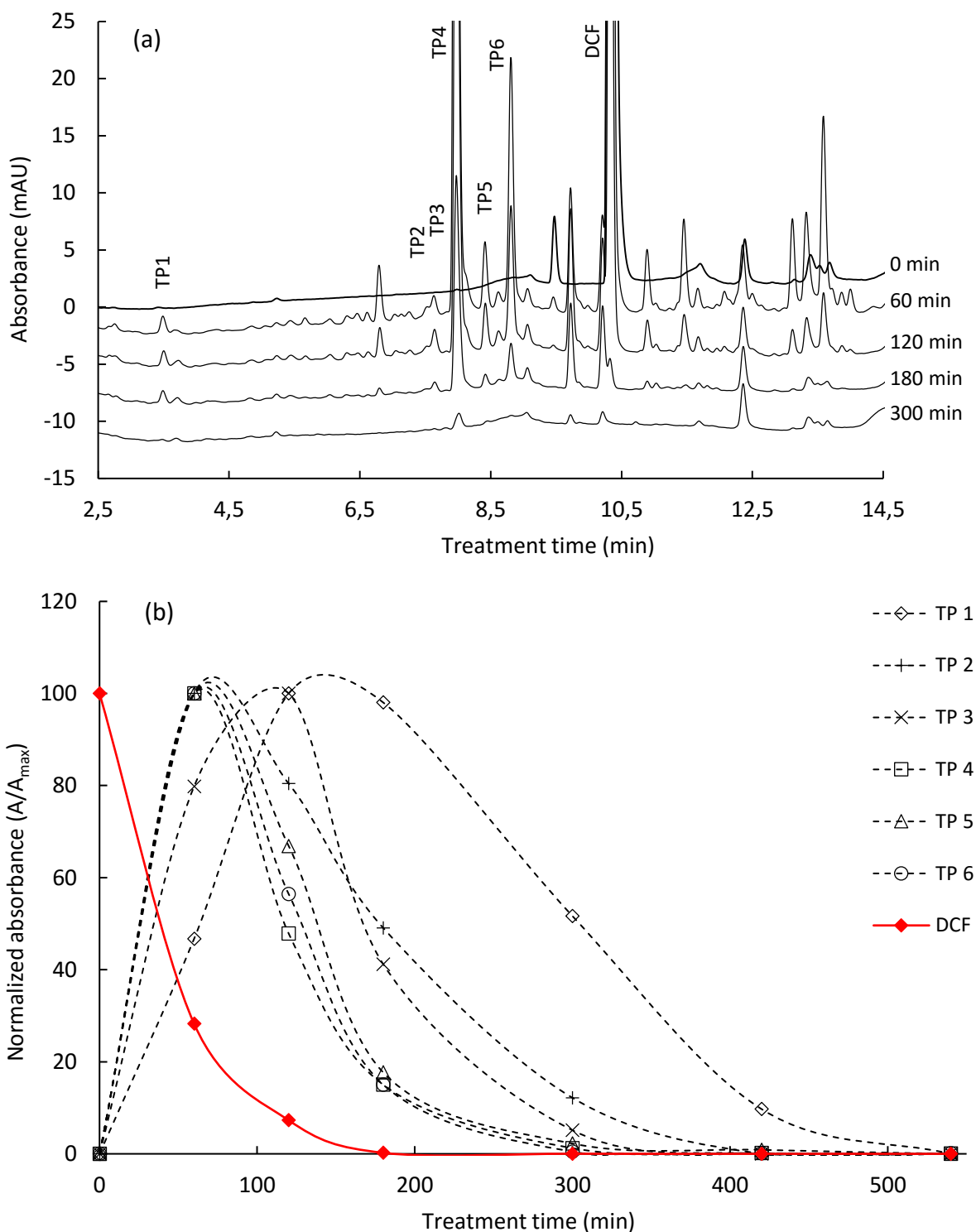
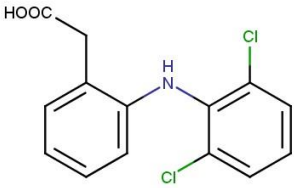
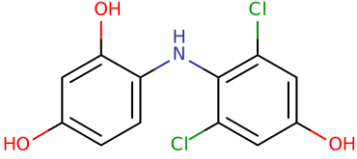
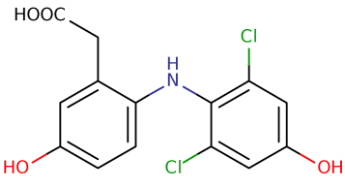
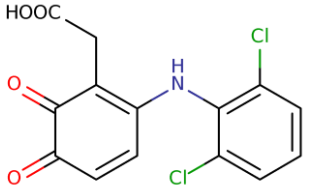
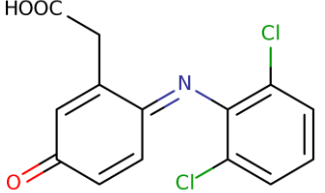
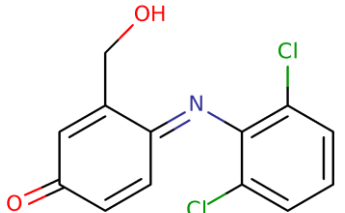
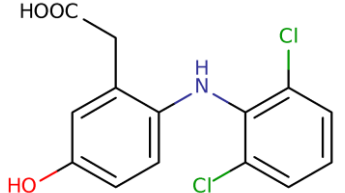


Figure 3.6: (a) Chromatogram showing DCF and its main transformation products after 0, 60, 120, 180 and 300 minutes of treatment time. The original gradient was adapted to optimize the peak distribution of the different transformation products and went from 75:25 (v/v%) 0.5% FA in H₂O:0.5% FA in ACN to 15:85 (v/v%) 0.5% FA in H₂O:0.5% FA in ACN in 10 min and was held for 2 min at 15:85, F= 0.3 mL/min. (b) Evolution of DCF and its main transformation products as a function of treatment time. The observed area under the curve (A) of the chromatographic peak is plotted as a function of the maximum observed area under the curve (A_{max}) for each compound separately.

Table 3.8: Tentative structures of the main transformation products of diclofenac, based on their m/z.

| Compound name | Retention time (min) | m/z | Proposed structure |
|------------------|----------------------|-----|---|
| Diclofenac (DCF) | 10.38 | 297 |  |
| TP1 | 3.53 | 286 |  |
| TP2 | 7.54 | 328 |  |
| TP3 | 7.65 | 326 |  |
| TP4 | 7.97 | 310 |  |
| TP5 | 8.42 | 282 |  |
| TP6 | 8.82 | 312 |  |

3.4 Conclusions

In this Chapter, the degradation by electrochemical oxidation via boron doped diamond electrodes was assessed for the selected pharmaceutical compounds iopromide (IOP), sulfamethoxazole (SMX), 17 α -ethinylestradiol (EE₂) and diclofenac (DCF) in simulated wastewater and real hospital effluent wastewater. The influence of the flow rate in the electrochemical cell, applied current, initial compound concentration and wastewater matrix (simulated (SWW) versus real effluent (RWW) wastewater) was evaluated. A kinetic evaluation confirmed that the degradation can be described via pseudo first-order reaction kinetics for all experimental conditions tested. It was shown that SMX, EE₂ and DCF degraded readily in SWW and RWW. The degradation of IOP was much slower, which is in agreement with previously reported slow degradation kinetics using typical advanced oxidation processes. Activation energies for the degradation reactions were calculated. The flow rate in the electrochemical cell only had a moderate effect on the degradation rate of EE₂ and DCF. The applied current, however, had a major effect. BDD was shown to be an effective technique for removing pharmaceutical components from the effluent of a biological hospital wastewater treatment plant. However, when a full mineralization of the pharmaceuticals is envisaged, it should be taken into account that the degradation of transformation products can take some 2-3 times longer. Moreover, due to the oxidation reactions, these transformation products are generally more hydrophilic than their parent compounds. This considerably increases the difficulty to analyze all substances simultaneously, especially when the monitoring of other pharmaceuticals in real environmental water samples is envisioned. To monitor the occurrence of (eco)toxic substances and to evaluate the degradation efficiency of various AOP, a generic methodology is required to simplify the analysis of such complex samples. Therefore, a novel approach wherein orthogonal hydrophilic interaction liquid chromatography (HILIC) and reversed-phase liquid chromatography (RPLC) columns are coupled in series will be suggested in Chapters 4 and 5.

3.5 References

- [1] J. Wang, S. Wang, *J. Environ. Manage.* **182**, 620–640 (2016).
- [2] J. Rivera-Utrilla, M. Sánchez-Polo, M.Á. Ferro-García, G. Prados-Joya, *Chemosphere.* **93**, 1268–1287 (2013).
- [3] Y. Yang, Y. Sik Ok, K.-H. Kim, E.E. Kwon, Y. Fai Tsang, *Sci. Total Environ.* **596–597**, 303–320 (2017).
- [4] G. Márquez, E.M. Rodríguez, F.J. Beltrán, P.M. Álvarez, *Chemosphere.* **113**, 71–78 (2014).
- [5] A. Mirzaei, Z. Chen, F. Haghghat, L. Yerushalmi, *Chemosphere.* **174**, 665–688 (2017).
- [6] R. Dewil, D. Mantzavinos, I. Poulios, M.A. Rodrigo, *J. Environ. Manage.* **195**, 93–99 (2017).
- [7] P. Cañizares, R. Paz, C. Sáez, M.A. Rodrigo, *Electrochim. Acta.* **53**, 2144–2153 (2008).
- [8] M.A. Rodrigo, P.A. Michaud, I. Duo, M. Panizza, G. Cerisola, C. Comninellis, *J. Electrochem. Soc.* **148**, 60–64 (2001).
- [9] B. Marselli, J. Garcia-Gomez, P. Michaud, M.A. Rodrigo, C. Comninellis, *J. Electrochem. Soc.* **150**, 79–83 (2003).
- [10] P. Cañizares, J. Lobato, R. Paz, M.A. Rodrigo, C. Sáez, *Wa.* **39**, 2687–2703 (2005).
- [11] J. De Coster, W. Vanherck, L. Appels, R. Dewil, *J. Environ. Manage.* **190**, 61–71 (2017).
- [12] P. Cañizares, C. Sáez, J. Lobato, R. Paz, M.A. Rodrigo, *J. Electrochem. Soc.* **154**, 37–44 (2007).
- [13] G. Chen, *Sep. Purif. Technol.* **38**, 11–41 (2004).
- [14] Y. Lan, C. Coetsier, C. Causser, K. Groenen Serrano, *Chem. Eng. J.* **333**, 486–494 (2018).
- [15] Z. Frontistis, M. Antonopoulou, D. Venieri, I. Konstantinou, D. Mantzavinos, *J. Environ. Manage.* **195**, 100–109 (2017).
- [16] J.F. Pérez, J. Llanos, C. Sáez, C. López, P. Cañizares, M.A. Rodrigo, *J. Environ. Manage.* **195**, 216–223 (2017).
- [17] F. Sopaj, N. Oturan, J. Pinson, F. Podvorica, M.A. Oturan, *Appl. Catal. B Environ.* **199**, 331–341 (2016).
- [18] C. Salazar, N. Contreras, H.D. Mansilla, J. Yáñez, R. Salazar, *J. Hazard. Mater.* **319**, 84–92 (2016).
- [19] L. Zhu, B. Santiago-Schübel, H. Xiao, H. Hollert, S. Kueppers, *Water Res.* **102**, 52–62 (2016).
- [20] E. Brillas, A. Thiam, S. Garcia-Segura, *J. Electroanal. Chem.* **775**, 189–197 (2016).
- [21] M. Haidar, A. Dirany, I. Sirés, N. Oturan, M.A. Oturan, *Chemosphere.* **91**, 1304–1309 (2013).
- [22] Y. Lan, C. Coetsier, C. Causserand, K. Groenen Serrano, *Electrochim. Acta.* **231**, 309–318 (2017).
- [23] C. Racaud, A. Savall, P. Rondet, N. Bertrand, K. Groenen Serrano, *Chem. Eng. J.* **211–212**, 53–59 (2012).
- [24] L.A. Pérez-Estrada, S. Malato, W. Gernjak, A. Agüera, E.M. Thurman, I. Ferrer, et al., *Environ. Sci. Technol.* **39**, 8300–8306 (2005).
- [25] H. Yu, E. Nie, J. Xu, S. Yan, W.J. Cooper, W. Song, *Water Res.* **47**, 1909–1918 (2013).
- [26] L. Minetto, F.M. Mayer, C.A. Mallmann, A.F. Martins, *Clean - Soil, Air, Water.* **40**, 950–957 (2012).

CHAPTER 4

Generic UHPLC methodology for the simultaneous analysis of compounds with a wide range of polarities

Based on:

Loos G., Dittmann M., Shoykhet K., Desmet G., Cabooter D. (2016). Generic UHPLC Method for the Simultaneous Analysis of Compounds with a Wide Range of Polarities. LC GC Europe, 29 (5), 240-247.

Loos G., Dittmann M., Shoykhet K., Desmet G., Cabooter D. (2016). Generic UHPLC Method for the Simultaneous Analysis of Compounds with a Wide Range of Polarities. LC GC Asia Pacific, 19 (2), 6-15.

Loos G., Dittmann M., Shoykhet K., Desmet G., Cabooter D. (2017). Generic UHPLC Method for the Simultaneous Analysis of Compounds with a Wide Range of Polarities. LC GC North America, 35 (2), 123-131.

4.1 Introduction

Due to the presence of metabolites, transformation and degradation products, environmental water samples typically display a large variety in polarity. To analyze such complex samples, multiple separations operating under different separation conditions are required. In principle, and provided the number of compounds in the sample is not too large, such analyses can be achieved by injecting the same sample several times on different columns operating under varying conditions [4–6]. This approach requires the development of adequate separation methods for each analysis on each individual column. Besides the fact that each analysis will require a new sample injection (which can be problematic when only limited sample is available) the original sample composition will not necessarily be compatible with the solvent conditions required for each analysis. A switch in sample solvent composition will be required in this case, making the approach difficult to automate.

Two-dimensional approaches (2D-LC), wherein column-switching techniques are used to transfer fractions from a first to a second dimension column automatically, have proven powerful to separate complex samples. This is especially the case when columns operating under largely differing separation mechanisms, such as reversed-phase liquid chromatography (RPLC) and hydrophilic interaction liquid chromatography (HILIC) are considered [7–9]. When first and second dimension columns are coupled online, all fractions eluting from the first dimension are immediately analyzed in the second dimension. This can put strong demands on the methods in terms of column dimensions and flow rates when both columns operate under strongly differing mobile phase conditions. In some cases this can lead to dilution problems resulting in sensitivity issues and methods being used sub-optimally [10]. The outcome of the separation moreover presents itself as a combination of chromatograms that require dedicated analysis software, making two-dimensional approaches currently less interesting for routine analyses. As a more up-front alternative to online two-dimensional approaches, the serial coupling of different separation conditions has been suggested [11–15]. This approach entails splitting the sample online in a limited number of fractions that are sequentially analyzed on a second column under different separation conditions. Since the individual separations are performed in sequence, they are visualized in a single chromatogram amenable for direct analysis and interpretation.

When combining separation mechanisms operating under largely differing mobile phase conditions, both two-dimensional and serially coupled approaches suffer from the problem that an online change in mobile phase is required before any subsequent separation can be commenced. A number of setups for the online changing and/or mixing of mobile phases in between analyses have been described in literature [11,13,15]. However, most of the proposed setups require elaborate instrumentation with multiple trap columns, solvent delivery pumps and switching valves that often involve multiple system controllers, making it challenging to implement these setups routinely.

Very recently, a novel setup was proposed for the online coupling of HILIC and RPLC columns in series to separate a sample consisting of compounds with a wide range of polarities [16]. The setup was entirely made up of commercially available equipment that could be controlled using the system's software. An Agilent 1290 UHPLC system was equipped with two switching valves that were used to couple HILIC and RPLC columns either in series or in parallel to the system. The sample was first injected onto the HILIC column. The non-polar compounds that were not retained on this column and eluted close to the void of the HILIC column were redirected towards a sample loop by changing the configuration of the valves. Meanwhile, the polar compounds were retained and separated on the HILIC column. Once the separation of the polar compounds on the HILIC column was completed, the configuration of the valves was altered again to redirect the non-polar compounds from the sample loop to the reversed-phase column.

Commercially available Jet Weaver mixers were integrated into the setup for the online conversion of the mobile phase composition between both analyses. This was done to ensure the non-polar compounds would be trapped adequately on the top of the reversed-phase column before analysis. The entire analysis was carried out on a single UHPLC system containing a single quaternary pump and a single detector. Since both HILIC and RPLC analyses were performed sequentially, the final separation of the polar and non-polar compounds could be displayed into a single chromatogram. The main drawback of the system was the large dwell volume generated by the mixers, manifesting itself as a large additional delay time between the analysis of the polar and non-polar compounds and increasing the total analysis time drastically [16].

In this Chapter, the simple addition of a small trap column to the setup is proposed to intercept the compounds eluting from the mixers, before directing them to the analytical column (Figure 4.1). The short length of the trap column and its concomitant low backpressure, allow operating the mixers in combination with the trap column at much higher flow rates than would be possible in combination with the analytical column. This leads to a substantial reduction in delay time and hence overall analysis time as is demonstrated for the analysis of 32 pharmaceuticals with a wide range of polarities.

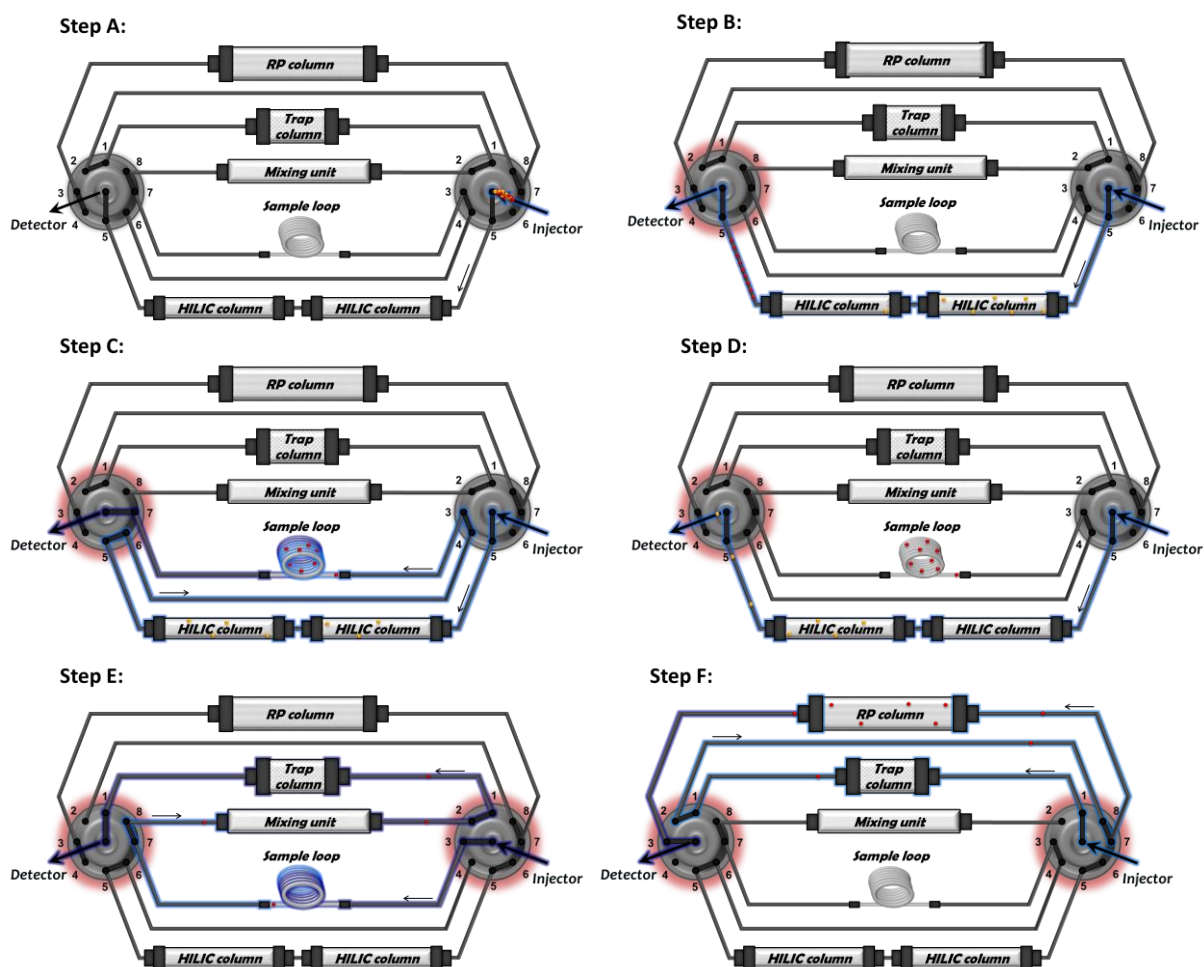


Figure 4.1: Setup and methodology employed to connect the HILIC and RPLC columns in series. Step A-B: injection of the sample consisting of polar (●) and non-polar compounds (●) on two serially coupled HILIC columns (each 1.0 x 100 mm, $d_p = 1.7 \mu\text{m}$), $F = 0.25 \text{ mL/min}$, mobile phase: 97:3 (v/v%) ACN:10 mM ammonium formate (AF) (pH= 3.0). Step C: switching of the left valve to direct the non-polar compounds (●) towards the sample loop at $t = 0.60 \text{ min}$. Step D: switching of the left valve to direct the polar compounds (●) eluting from the HILIC columns towards the detector at $t = 1.00 \text{ min}$. Gradient conditions: 97:3 (v/v%) ACN:10 mM AF (pH= 3.0) to 92:3:5 (v/v%) ACN:10 mM AF (pH= 3.0):0.02% formic acid (FA) in H_2O in 12 min. Step E: switching of the valves to direct the non-polar compounds (●) from the sample loop through the mixing unit towards the trap column. Mobile phase: 0.02% FA in H_2O , $F = 1.9 \text{ mL/min}$. Step F: switching of the valves to direct the non-polar compounds from the trap column to the analytical phenyl-hexyl column (3.0 x 100 mm). Gradient conditions: (100%) 0.02% FA in H_2O to 70:30 (v/v%) ACN:0.02% FA in H_2O in 8 min, $F = 0.5 \text{ mL/min}$.

4.2 Experimental

4.2.1 Chemicals and columns

The following pharmaceuticals were selected as test compounds: atenolol, bezafibrate, clozapine, diclofenac, pipamperone, progesterone, sulfamethoxazole, metformin hydrochloride and β -estradiol were from Sigma-Aldrich (Steinheim, Germany); diazepam, propranolol and carbamazepine were from Alpha Pharma (Braine-l'Alleud, Belgium); ticlopidine was from Sanofi (Diegem, Belgium); lorazepam from Fagron (Waregem, Belgium). Ibuprofen and lidocaine were from Certa (Braine-l'Alleud, Belgium). Naproxen was from Acros Organics (Geel, Belgium). Sertraline was from Apex Pharma (Cairo, Egypt) and escitalopram and venlafaxine from NODCAR (Cairo, Egypt). Cilostazol, caffeine, codeine phosphate, metoprolol, trimethoprim, vidarabine, oxazepam and iopromide were available in the lab as USP reference standards (Rockville, MD, USA), while pentoxifylline was available as an EDQM reference standard (Strasbourg, France). Fluoxetine, irbesartan and phenazone were available in the lab. These compounds were selected to represent common pharmaceuticals with a wide range of polarities, as can be witnessed from their log D-values that are displayed in Table 4.1.

Acetonitrile (ACN, HPLC grade) and ammonium acetate were from Fisher Chemical (Loughborough, UK), ethanol (EtOH) was from VWR (Leuven, Belgium). Ammonium formate (AF) (Fluka) was purchased from Sigma-Aldrich. Anhydrous acetic acid (100%) was from Merck (Darmstadt, Germany) and formic acid (FA) (99%) from Acros Organics. High purity water (conductivity= 0.3 μ S/cm, pH= 5.97) (H_2O) was prepared in the laboratory using a Milli-Q gradient (Millipore, Bedford, MA, USA) water purification system.

For the subdivision of the sample, an Acquity BEH HILIC with an inner diameter (I.D.) of 2.1 mm, a length of 100 mm and a particle size (d_p) of 1.7 μ m (Waters, Wexford, Ireland) was used. Method development for the polar compounds was done by evaluating their retention and separation on Acquity BEH HILIC, Amide and Cyano columns (Waters) with an I.D. of 2.1 mm, a length of 100 mm and d_p = 1.7 μ m. For the method development of the non-polar compounds, Acquity BEH C18 d_p = 1.7 μ m (Waters), Acquity polar embedded BEH d_p = 1.7 μ m (RP-18) (Waters) and Zorbax Eclipse Plus phenyl-hexyl d_p = 1.8 μ m columns (Agilent Technologies, Little Falls, CA, USA) with an I.D. of 2.1 mm and a length of 100 mm were evaluated.

In the final setup, a Zorbax Eclipse Plus phenyl-hexyl column (Agilent Technologies) with an I.D. of 3.0 mm, a length of 100 mm and $d_p = 1.8 \mu\text{m}$ was used for the separation of the non-polar compounds. Two serially coupled Acquity BEH HILIC columns (Waters) with an I.D. of 1.0 mm, a length of 100 mm and $d_p = 1.7 \mu\text{m}$ were used for the separation of the polar compounds. A Zorbax Eclipse Plus phenyl-hexyl trap column (Agilent Technologies) with an I.D. of 3.0 mm, a length of 30 mm and $d_p = 1.8 \mu\text{m}$ was used to intercept the non-polar compounds eluting from the mixers.

4.2.2 Apparatus

All experiments were executed on an Agilent Infinity UHPLC 1290 system (Agilent Technologies, Waldbronn, Germany). The system consisted of a 1290 quaternary pump, a 1290 autosampler and a 1290 DAD detector with a 1.0 μL flow cell (path length: 10 mm). The system was equipped with two 9-port/8-position ultra-high pressure valves (max. pressure 1200 bar). System operation, valve configuration, data acquisition and analysis were handled using Chemstation software (Agilent Technologies). All connections between pump, valves, columns, mixers and detector were made using Viper tubing (Thermo Scientific, Germering, Germany) with an I.D. of 75 μm and the shortest possible length.

4.2.3 Methodology

Stock solutions of the compounds were prepared in a concentration between 2 and 20 mg/mL in either water or an organic solvent (details see Table 4.1). A working solution for method development was prepared by mixing the appropriate amounts of solutions and adding ACN to a final volume of 1.5 mL with a final composition of ~95% organic solvent. The concentrations of the compounds in this working solution can also be found in Table 4.1.

4.2.3.1 Subdivision of the sample

Following the procedure elaborated in [16], a generic gradient was run on a HILIC column (Acquity BEH HILIC) at a flow rate of 0.4 mL/min, using a detection wavelength of 210 nm and an injection volume of 1.0 μL . For this purpose, an isocratic hold of 95% ACN for 5 min was followed by a gradient wherein the mobile phase composition varied from 95% ACN to 50% ACN in 10 min. The aqueous component of the mobile phase consisted of 10 mM AF, brought to pH= 3.0 using FA. Subdivision of the sample into polar and non-polar compounds was based on the retention obtained for the different compounds under these conditions.

4.2.3.2 Method development for the polar and non-polar compounds

After the subdivision of the sample into polar and non-polar compounds, a method was developed for the non-polar compounds on reversed-phase columns and for the polar compounds on HILIC columns. For this purpose, generic scouting runs were conducted on each available stationary phase (see § 4.2.1) at a flow rate of 0.4 mL/min to identify the most promising separation conditions. The organic modifier percentage was varied between 5% ACN and 95% ACN for the reversed-phase stationary phases and between 95% ACN and 50% ACN for the HILIC stationary phases in 10 min. The pH-value of the aqueous component of the mobile phase was altered between pH= 3.0 and pH= 6.8 using ammonium formate and ammonium acetate, respectively, with a total concentration of 10 mM. The best runs for the separation of the polar compounds on HILIC columns and for the non-polar compounds on reversed-phase columns were selected as the runs that led to the largest number of separated peaks with the highest critical pair resolution. These runs were subsequently optimized by varying the gradient parameters (start- and end concentration of the organic modifier, gradient time), the flow rates and the column lengths [17,18].

4.2.3.3 Hyphenation of the final obtained methods

The HILIC stationary phase leading to the best separation of the polar compounds was subsequently serially coupled to the stationary phase leading to the best separation of the non-polar compounds using the setup shown in Figure 4.1.

The entire sample (containing both polar and non-polar compounds) was first injected on the HILIC columns (step A-B, Figure 4.1) operated at a flow rate of 0.25 mL/min and using a mobile phase composition of 97:3 (v/v%) ACN:10 mM AF (pH= 3.0). While the polar compounds were retained on the HILIC columns, the configuration of the valves was changed at $t= 0.60$ min to direct the non-polar compounds eluting in the void of the HILIC columns towards a sample loop (step C, Figure 4.1). Once the non-polar compounds were contained in the sample loop, the configuration of the valves was changed again at $t= 1.00$ min to direct the separated polar compounds eluting from the HILIC column towards the detector (step D, Figure 4.1). For this purpose, the mobile phase composition was changed from 97:3 (v/v%) ACN:10 mM AF (pH= 3.0) to 92:3:5 (v/v%) ACN:10 mM AF (pH= 3.0):0.02% FA in H₂O in 12 min. After this, the configuration of both valves was altered to direct the non-polar compounds from the sample loop through the mixing unit towards the trap column. A new mobile phase (consisting of 0.02% FA in H₂O) was used at a high flow rate ($F= 1.9$ mL/min) to dilute the ACN plug containing

the non-polar compounds, allowing to adequately retain the non-polar compounds on the trap column (step E, Figure 4.1). Finally, the configuration of the valves was changed one last time to couple the trap column in series with the analytical reversed-phase column for the separation of the non-polar compounds (step F, Figure 4.1). For this purpose, the mobile phase composition was changed from 0.02% FA in H₂O to 70:30 (v/v%) ACN:0.02% FA in H₂O in 8 min at a flow rate of 0.5 mL/min.

The mixing unit consisted of four serially coupled Jet Weaver mixers (Agilent Technologies). These Jet Weaver mixers are high performance mixers based on multilayer microfluidics technology that combine high mixing efficiencies with low delay volumes. A schematic representation of a Jet Weaver mixer can be found in the supporting information of [16]. Jet Weaver mixers with volumes of 380 μ L (2x) and 1140 μ L (2x) were used in the setup, resulting in a total mixing volume of approximately 3.04 mL.

4.3 Results and discussion

4.3.1 Subdivision of the sample

Following the methodology elaborated in [16], the sample was subdivided into polar and non-polar compounds based on their retention obtained on the HILIC column, using the generic gradient described in § 4.2.3.1. All compounds eluting in or near the void of the column were classified as non-polar compounds. These compounds are denoted with letters A-N in Table 4.1. All other compounds with clear retention on the HILIC column (denoted with numbers 1-18 in Table 4.1) were classified as polar.

4.3.2 Method development for the polar and non-polar compounds

Initial method development efforts were performed on column dimensions of 2.1 x 100 mm, since a large selection of column selectivities were available in the lab in these dimensions. To obtain a satisfactory separation for all polar compounds, two identical Acquity BEH HILIC columns (each 2.1 x 100 mm) were coupled in series. A gradient separation wherein the mobile phase composition was first held at 97:3 (v/v%) ACN:10 mM AF (pH= 3.0) for 4 min and subsequently varied to 92:3:5 (v/v%) ACN:10 mM AF (pH= 3.0):0.02% FA in H₂O in 12 min at a flow rate of 1.1 mL/min was employed to adequately separate all polar compounds. For the non-polar compounds, baseline separation was obtained on a 100 mm phenyl-hexyl column operating under gradient conditions wherein the solvent composition was altered from (100%) 0.02% FA in H₂O to 70:30 (v/v%) ACN:0.02% FA in H₂O in 8 min at a flow rate of 0.25

mL/min. Once the optimal separation conditions were identified for the polar and non-polar compounds, the HILIC separation was converted to 1.0 mm I.D. column formats and the RPLC separation to a 3.0 mm I.D. column format by scaling the flow rates according to the column diameters. This was done to limit the volume of the ACN-rich plug wherein the non-polar compounds would elute from the HILIC column and ensure this ACN-rich plug would be sufficiently diluted when passing through the mixing unit [16]. The final separations obtained for the polar and non-polar compounds on HILIC and RPLC columns, respectively, are shown in Figure 4.2.

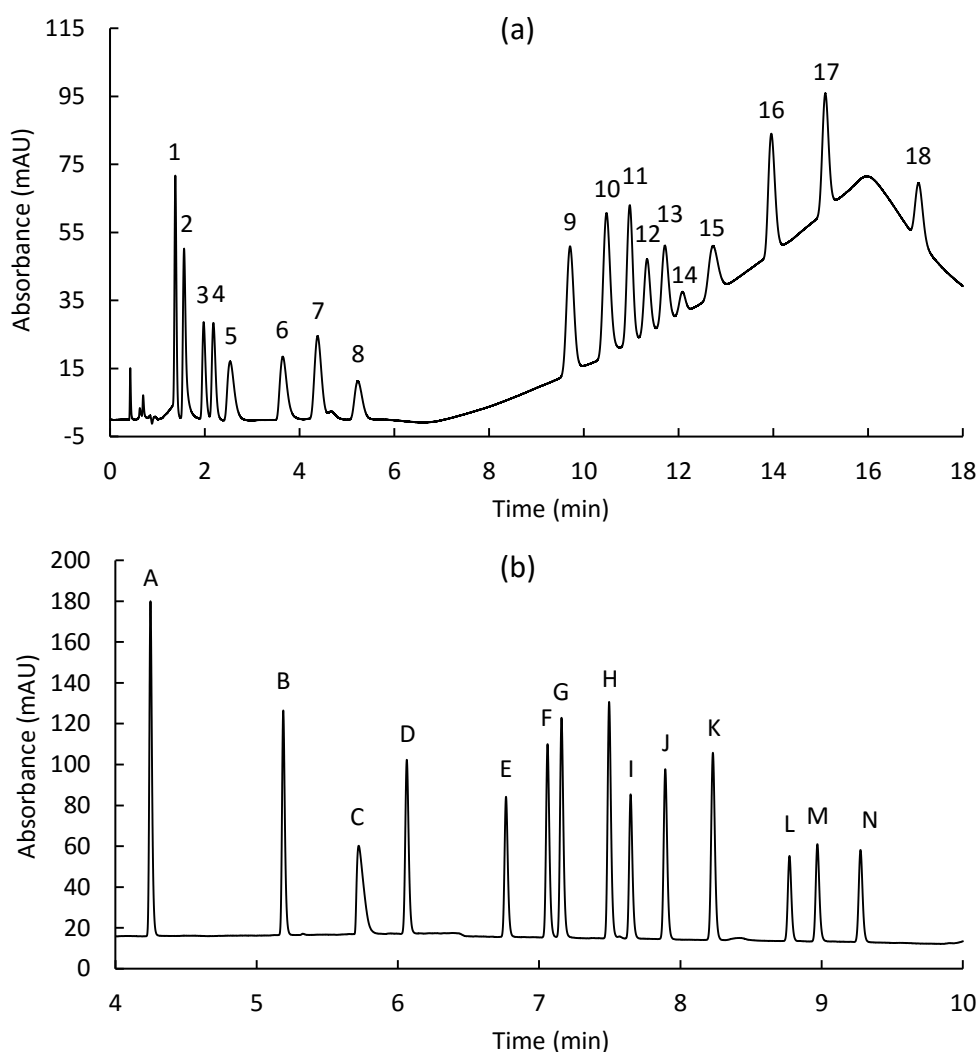


Figure 4.2: Final separation obtained for (a) polar compounds on HILIC columns and (b) non-polar compounds on a reversed-phase column after scaling to the appropriate column dimensions. Separation conditions in (a) two serially coupled Acquity HILIC columns (each 1.0 x 100 mm, $d_p = 1.7 \mu\text{m}$), gradient conditions: isocratic hold of 4 min at 97:3 (v/v%) ACN:10 mM AF (pH= 3.0), followed by a change to 92:3:5 (v/v/v%) ACN:10 mM AF (pH= 3.0):0.02% FA in H_2O in 12 min, $F = 0.25 \text{ mL/min}$. Separation conditions in (b) Zorbax Eclipse Plus phenyl-hexyl column (3.0 x 100 mm, $d_p = 1.8 \mu\text{m}$), gradient conditions: (100%) 0.02% FA in H_2O to 70:30 (v/v%) ACN:0.02% FA in H_2O in 8 min, $F = 0.5 \text{ mL/min}$. Peak annotation as in Table 4.1.

Table 4.1: Pharmaceutical compounds considered in this Chapter. Drug class, sample stock solvents and respective concentrations in the working solution are given. Log D-values at pH= 3.0 were calculated with Chemaxon Marvin software (www.chemaxon.com). The letters and numbers in the first column refer to the peak annotation in the figures.

| # | Pharmaceutical | Drug Class | Sample stock solvent | Stock solution (mg/mL) | Working solution (µg/mL) | Log D (pH= 3.0) |
|----|------------------|------------------------------------|----------------------|------------------------|--------------------------|-----------------|
| 1 | Phenazone | Nonsteroidal anti-inflammatory | H ₂ O | 10 | 33.3 | 1.22 |
| 2 | Bezafibrate | Anti-cholesterol | EtOH | 10 | 33.3 | 3.93 |
| 3 | Irbesartan | Angiotensin II receptor antagonist | EtOH | 5 | 16.7 | 3.80 |
| 4 | Lidocaine | Antiarrhythmic | EtOH | 10 | 33.3 | -0.63 |
| 5 | Iopromide | Contrast agent | H ₂ O | 10 | 50.0 | 0.48 |
| 6 | Vidarabine | Anti-viral | 0.5 M HCl | 10 | 33.3 | -3.78 |
| 7 | Trimethoprim | Antibiotic | EtOH | 2.5 | 16.7 | 0.19 |
| 8 | Clozapine | Antipsychotic | MeOH | 10 | 33.3 | -0.96 |
| 9 | Sertraline | Antidepressive | EtOH | 10 | 33.3 | 1.91 |
| 10 | Propranolol | Anti-hypertensive | H ₂ O | 10 | 33.3 | -0.66 |
| 11 | Fluoxetine | Antidepressive | MeOH | 15 | 75.0 | 0.93 |
| 12 | Escitalopram | Antidepressive | H ₂ O | 10 | 33.3 | 0.26 |
| 13 | Metoprolol | Anti-hypertensive | H ₂ O | 20 | 133.3 | -1.48 |
| 14 | Venlafaxine | Antidepressive | MeOH | 10 | 33.3 | 0.46 |
| 15 | Codeine | Anti-tussive | H ₂ O | 10 | 33.3 | -2.16 |
| 16 | Pipamperone | Antipsychotic | H ₂ O | 10 | 133.3 | -4.60 |
| 17 | Metformin | Anti-diabetic | H ₂ O | 20 | 66.7 | -5.75 |
| 18 | Atenolol | Anti-hypertensive | EtOH | 10 | 133.3 | -2.82 |
| A | Caffeine | CNS stimulant | H ₂ O | 10 | 33.3 | -0.55 |
| B | Pentoxifylline | Xanthine derivative | H ₂ O | 10 | 50.0 | 0.23 |
| C | Ticlopidine | Antiplatelet | H ₂ O | 10 | 33.3 | 0.76 |
| D | Sulfamethoxazole | Antibacterial | EtOH | 5 | 33.3 | 0.75 |
| E | Carbamazepine | Anti-convulsant | ACN | 5 | 16.7 | 2.77 |
| F | Oxazepam | Anti-anxiety | MeOH | 2 | 33.3 | 2.92 |
| G | Lorazepam | Anti-anxiety | ACN | 5 | 33.3 | 3.53 |
| H | β-estradiol | Hormone | EtOH | 5 | 83.3 | 3.75 |
| I | Cilostazol | Platelet-aggregation inhibitor | MeOH | 2.5 | 8.3 | 3.31 |
| J | Naproxen | Nonsteroidal anti-inflammatory | EtOH | 10 | 33.3 | 2.96 |
| K | Diazepam | Anti-anxiety | EtOH | 10 | 33.3 | 2.81 |
| L | Ibuprofen | Nonsteroidal anti-inflammatory | ACN | 10 | 33.3 | 3.84 |
| M | Diclofenac | Nonsteroidal anti-inflammatory | EtOH | 5 | 16.7 | 4.22 |
| N | Progesterone | Hormone | EtOH | 10 | 166.7 | 4.15 |

4.3.3 Hyphenation of the final obtained methods

To hyphenate these two methods, the setup shown in Figure 4.1 was used to redirect the non-polar compounds from the HILIC column towards the sample loop. For this purpose, the configuration of the left valve was changed from the position shown in step B (Figure 4.1) to the position in step C (Figure 4.1) just before the non-polar compounds started eluting from the HILIC column. To accurately determine the timing upon which the configuration of this valve should be switched, the sample was first injected in its entirety and under the optimized mobile phase conditions on the coupled HILIC columns (obtained separation shown in Figure 4.1). This allowed defining the window wherein the non-polar compounds eluted from these columns (and hence the timing upon which the valve should be switched) between 0.60 and 1.00 min (denoted by the red frame).

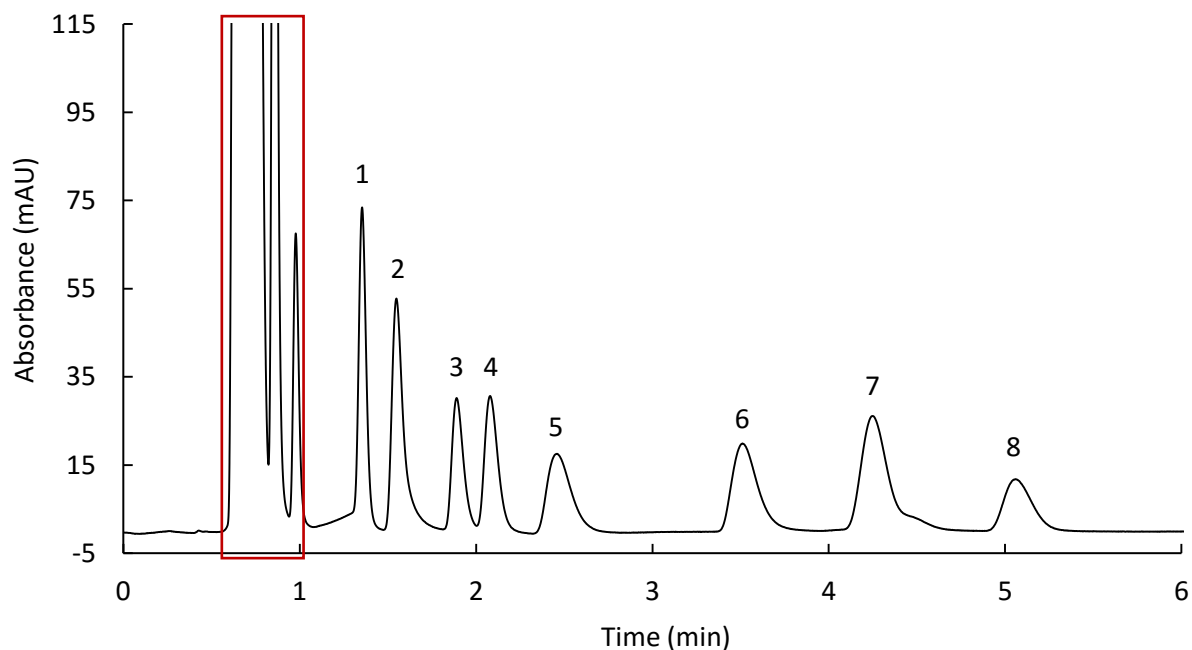


Figure 4.3: Zoom on the first part of the HILIC separation with determination of the elution window of the non-polar compounds (denoted by the red frame) using the optimized separation conditions specified in Figure 4.2. The configuration of the setup and separation conditions are as in Step A-B in Figure 4.1. Peak annotation as in Table 4.1.

The entire sample was subsequently injected on the HILIC columns again, but this time the configuration of the left valve was actually altered from the position in step B to step C (Figure 4.1) at 0.60 min to direct the non-polar compounds to the sample loop and from the position in step C to step D (Figure 4.1) at 1.00 min to ensure the polar compounds would be directed towards the detector once they started eluting from the HILIC column. It was already

demonstrated in [16] that changing the configuration of the valves during the HILIC separation had no effect on the separation of the polar compounds (see also Figure 4.4). Note that under the specified conditions ($F= 0.25$ mL/min), the non-polar compounds will elute in a solvent plug with a volume of ~ 100 μ L (see also below). To ensure the non-polar compounds would be adequately captured in the sample loop, the volume of the sample loop was chosen sufficiently large (200 μ L) to avoid the non-polar compounds from eluting towards the detector before the configuration of the left valve was switched back to the position in step D.

After elution of the polar compounds from the HILIC column, the configuration of both valves was switched to the configuration shown in step E of Figure 4.1 to redirect the non-polar compounds from the sample loop towards the trap column. The non-polar compounds are dissolved in a large plug of ACN at this stage. The volume of this plug can roughly be calculated from the applied flow rate on the HILIC columns, the percentage of ACN in the HILIC mobile phase and the switching times of the valves as 0.25 mL/min $\times 0.97 \times (1.00 - 0.60$ min) = 97 μ L. To ensure the non-polar compounds can be adequately withheld on the trap column, the amount of ACN in this plug needs to be reduced drastically. For this purpose, a mixing unit consisting of commercially available Jet Weaver mixers with a total volume of approximately 3 mL was coupled between the sample loop and the trap column. The mixing unit was prefilled with an aqueous mobile phase by coupling the mixing unit directly to the instrument and pumping 0.02% FA in H₂O (pH ~ 3.0) through it at a high flow rate (1 mL/min). The configuration of the valves was subsequently switched to the configuration in step E of Figure 4.1 and a high flow of 0.02% FA in H₂O (1.9 mL/min) was applied to elute the non-polar compounds towards the trap column. By prefilling the mixing unit with an aqueous solvent and using the same solvent to elute the non-polar compounds from the sample loop towards the mixing unit, the ACN-rich plug containing the non-polar compounds was virtually sandwiched between two layers of aqueous solvent. The design of the Jet Weaver mixers is such that this will result in an adequate dilution of the ACN-rich plug when passing through the mixing unit and before reaching the trap column. The low backpressure of both the mixing unit and the short trap column, moreover ensure that the entire dilution process can occur at a high flow rate, reducing the delay time required to pass through the mixing unit to only 1.6 min (3 mL / 1.9 mL/min).

Finally, the configuration of the valves was altered one last time to the configuration shown in step F of Figure 4.1 to elute the non-polar compounds from the trap column to the analytical column for separation.

The final separation obtained in this way is shown in Figure 4.4. Note that the separations that were previously obtained for the polar and non-polar compounds separately in Figure 4.2 are nearly perfectly maintained in the coupled setup, while the delay time caused by the mixing unit is drastically reduced with 8 min by including a small trap column in the setup to intercept the non-polar compounds eluting from the mixing unit.

To verify whether the repeated valve and column switching would have an effect on the repeatability of the final obtained method, the same separation was executed 6 times successively. As can be deduced from Table 4.2, the repeatability of the retention times of all compounds was excellent, with a maximum variation of 0.4% RSD. For the areas, slightly larger variations were observed but in general these were still below 1.0% RSD. These findings suggest that the presented approach has potential to be used in routine applications.

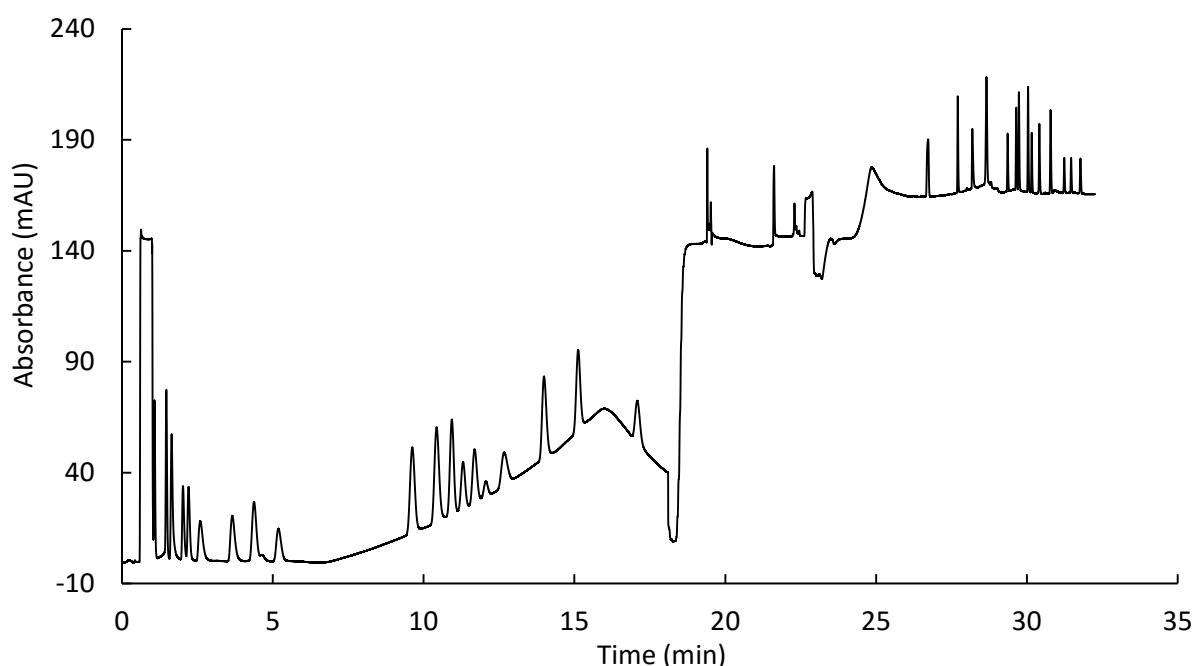
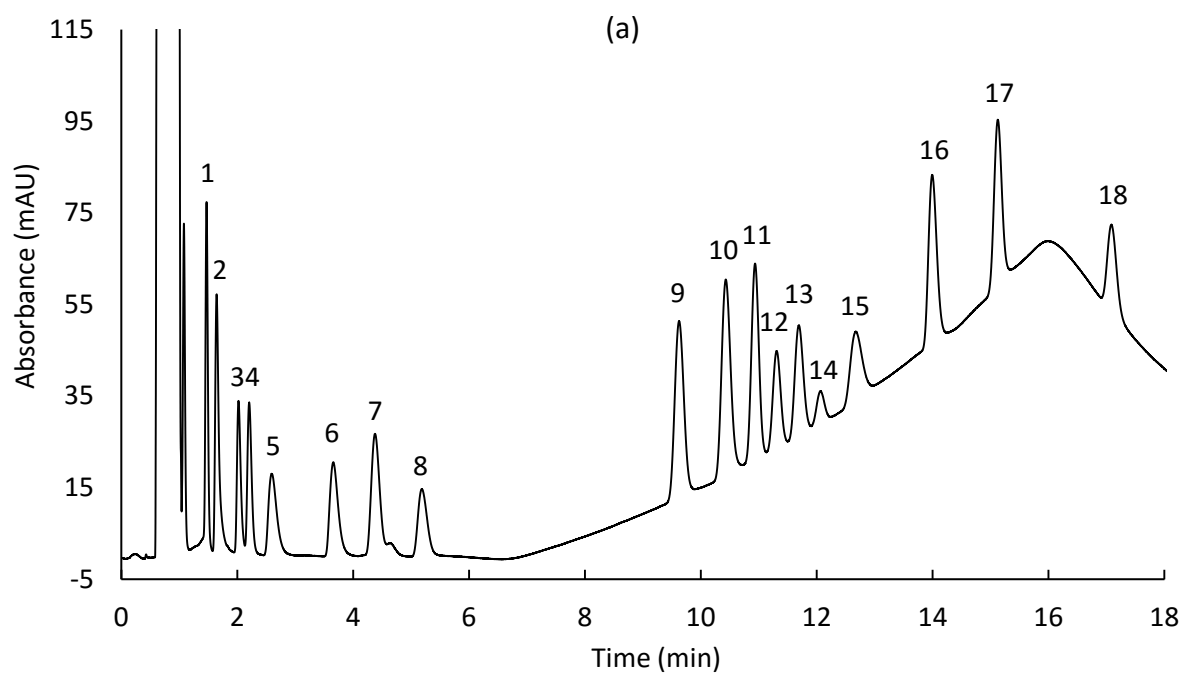


Figure 4.4: Final obtained separation for the polar and non-polar compounds using the setup shown in Figure 4.1. Column dimensions, separation conditions and switching times of the valves are as in Figure 4.1. Peak annotation as in Table 4.1.

Zoom on separation of polar compounds:



Zoom on separation of non-polar compounds:

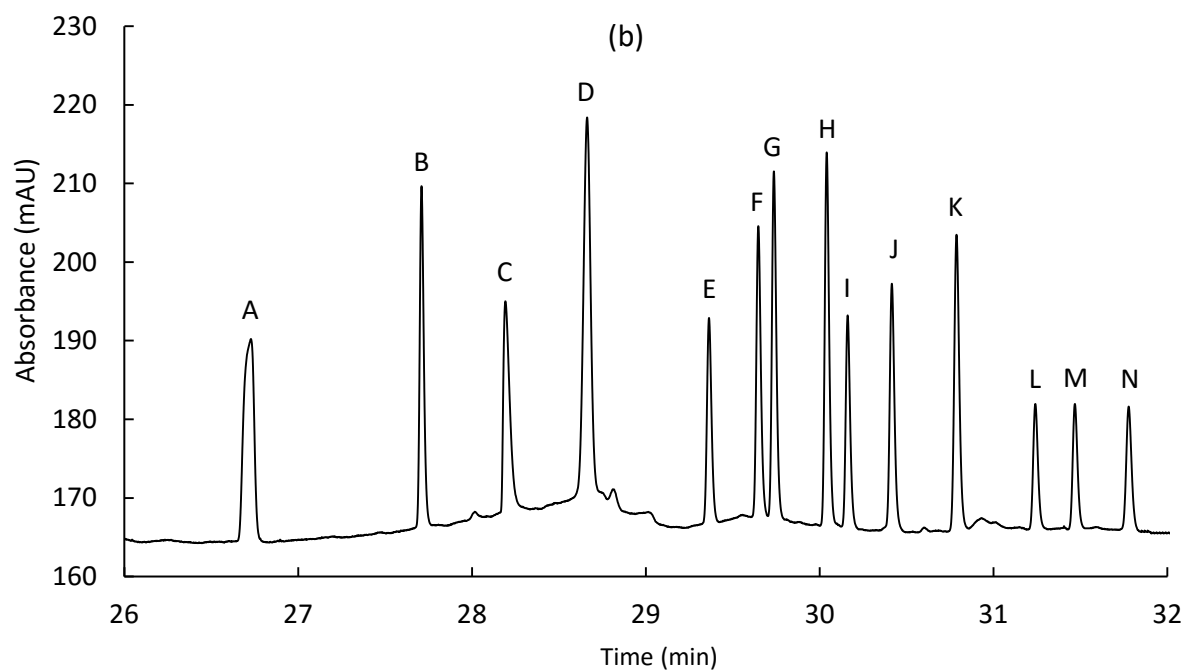


Figure 4.4: Continued

Table 4.2: Average values of retention times (t_r) and peak areas obtained for all compounds in the working mixture from six consecutive injections. Standard deviations (stdev) and relative standard deviations (RSD) are also given.

| Compound | t_r (min) (n= 6) | | | area (n= 6) | | |
|--------------------|--------------------|-------|---------|-------------|-------|---------|
| | average | stdev | RSD (%) | average | stdev | RSD (%) |
| Phenazone | 1.34 | 0.00 | 0.12 | 3.40 | 0.02 | 0.60 |
| Bezafibrate | 1.55 | 0.00 | 0.28 | 4.23 | 0.02 | 0.51 |
| Irbesartan | 1.88 | 0.01 | 0.31 | 2.14 | 0.02 | 0.71 |
| Lidocaine | 2.04 | 0.01 | 0.30 | 2.54 | 0.02 | 0.63 |
| Iopromide | 2.34 | 0.01 | 0.25 | 2.90 | 0.03 | 0.93 |
| Vidarabine | 3.40 | 0.01 | 0.22 | 3.53 | 0.02 | 0.57 |
| Trimethoprim | 4.14 | 0.01 | 0.26 | 4.52 | 0.02 | 0.48 |
| Clozapine | 4.96 | 0.02 | 0.37 | 1.67 | 0.03 | 1.85 |
| Sertraline | 9.21 | 0.02 | 0.17 | 7.04 | 0.02 | 0.32 |
| Propranolol | 9.95 | 0.01 | 0.08 | 7.82 | 0.04 | 0.49 |
| Fluoxetine | 10.46 | 0.01 | 0.08 | 6.39 | 0.02 | 0.30 |
| Escitalopram | 10.84 | 0.01 | 0.10 | 3.31 | 0.01 | 0.31 |
| Metoprolol | 11.19 | 0.01 | 0.10 | 4.11 | 0.03 | 0.69 |
| Venlafaxine | 11.59 | 0.01 | 0.11 | 1.11 | 0.01 | 0.55 |
| Codeine | 12.17 | 0.03 | 0.23 | 3.53 | 0.03 | 0.86 |
| Pipamperone | 13.47 | 0.03 | 0.22 | 6.16 | 0.02 | 0.40 |
| Metformin | 14.55 | 0.04 | 0.27 | 5.78 | 0.03 | 0.54 |
| Atenolol | 16.50 | 0.06 | 0.36 | 3.49 | 0.01 | 0.28 |
| Caffeine | 26.74 | 0.01 | 0.03 | 1.98 | 0.01 | 0.27 |
| Pentoxifylline | 27.71 | 0.01 | 0.02 | 1.37 | 0.02 | 1.38 |
| Ticlopidine | 28.14 | 0.01 | 0.04 | 1.27 | 0.02 | 1.22 |
| Sulfamethoxazole | 28.67 | 0.02 | 0.06 | 1.91 | 0.11 | 5.52 |
| Carbamazepine | 29.35 | 0.01 | 0.03 | 0.91 | 0.01 | 1.01 |
| Oxazepam | 29.64 | 0.01 | 0.02 | 1.24 | 0.01 | 0.80 |
| Lorazepam | 29.74 | 0.01 | 0.02 | 1.39 | 0.01 | 0.66 |
| β -estradiol | 30.06 | 0.01 | 0.03 | 1.41 | 0.01 | 0.38 |
| Cilostazol | 30.18 | 0.01 | 0.02 | 0.85 | 0.00 | 0.34 |
| Naproxen | 30.45 | 0.01 | 0.03 | 1.15 | 0.01 | 0.46 |
| Diazepam | 30.82 | 0.01 | 0.02 | 1.39 | 0.01 | 0.75 |
| Ibuprofen | 31.30 | 0.01 | 0.03 | 0.57 | 0.00 | 0.49 |
| Diclofenac | 31.49 | 0.01 | 0.03 | 0.53 | 0.00 | 0.21 |
| Progesterone | 31.84 | 0.01 | 0.03 | 0.62 | 0.00 | 0.63 |

Since HILIC and RPLC analyses are done in series, the peak capacity of the overall separation can be calculated by adding the peak capacities of the individual separations. The individual peak capacities ($n_{p,RPLC}$ and $n_{p,HILIC}$) were calculated as in eq. 4.1 [19]:

$$n_p = 1 + \sum_{i=1}^n \frac{t_{R,i} - t_{R,i-1}}{4\sigma_i} \quad (4.1)$$

With $t_{R,i}$ the retention time of peak i and $t_{R,i-1}$ the retention time of peak $i-1$ and σ_i the square root of the variance of peak i (σ^2), related to the width of the peak. This leads to a peak capacity of $n_{p,HILIC} = 61$ for the HILIC separation and $n_{p,RPLC} = 100$ for the RPLC separation, resulting in a total peak capacity of $n_{p,total} = 161$. Such peak capacity can be considered as intermediate to typical peak capacities that are obtained under one-dimensional and two-dimensional conditions.

4.4 Conclusions

A novel approach to the serial coupling of HILIC and RPLC columns based on equipment that is commercially available is presented. For this purpose, a UHPLC instrument is equipped with two switching valves that can be controlled using the system's software. These valves are used to redirect non-polar compounds that are not withheld on a HILIC column and hence elute near the void of this column towards a sample loop, where they are stored while the separation of the polar compounds on the HILIC column is carried out. Once the separation of the polar compounds is complete, the switching valves are used to direct the non-polar compounds from the sample loop through a mixing unit consisting of a number of serially connected mixers, wherein the sample solvent is modified to a large percentage of water. The mixing unit is connected to a small trap column to intercept the non-polar compounds eluting from the mixing unit. In this way, the mixing unit can be operated at a high flow rate, reducing the delay time caused by the high dwell volume of the mixers considerably. The trap column is finally connected to an analytical column by switching the valves one more time, to separate the non-polar compounds on the analytical column.

The proposed setup is shown to result in an adequate and repeatable separation of both polar and non-polar compounds in the sample and can therefore potentially be used for routine applications. Intermediate peak capacities to one-dimensional and two-dimensional separations are obtained, making the proposed setup a promising alternative for the analysis of samples of intermediate complexity.

4.5 References

- [1] M.G.M. Kok, G.W. Somsen, G.J. De Jong, *Trends Anal. Chem.* **61**, 223–235 (2014).
- [2] J.R. Griffiths, S. Perkins, Y. Connolly, L. Zhang, M. Holland, V. Barattini, et al., *J. Chromatogr. A.* **1232**, 276–280 (2012).
- [3] M. Meyer-monath, C. Chatellier, D. Cabooter, F. Rouget, I. Morel, F. Lestremau, *Talanta.* **138**, 231–239 (2015).
- [4] R. Hirsch, T.A. Ternes, K. Haberer, A. Mehlich, F. Ballwanz, *J. Chromatogr. A.* **815**, 213–223 (1998).
- [5] T.A. Ternes, M. Bonerz, N. Herrmann, L. Dirk, E. Keller, *J. Chromatogr. A.* **1067**, 213–223 (2005).
- [6] P. Kubica, A. Kot-Wasik, A. Wasik, J. Namieśnik, *J. Chromatogr. A.* **1289**, 13–18 (2013).
- [7] Y.S. Ling, H.J. Liang, M.H. Lin, C.H. Tang, K.Y. Wu, M.L. Kuo, et al., *Biomed. Chromatogr.* **28**, 1284–1293 (2014).
- [8] A. Mihailova, H. Malerød, S.R. Wilson, B. Karaszewski, R. Hauser, E. Lundanes, et al., *J. Sep. Sci.* **31**, 459–467 (2008).
- [9] K.M. Kalili, A. De Villiers, *J. Chromatogr. A.* **1289**, 69–79 (2013).
- [10] D.R. Stoll, X. Li, X. Wang, P.W. Carr, S.E.G. Porter, S.C. Rutan, *J. Chromatogr. A.* **1168**, 3–43 (2007).
- [11] Y. Wang, X. Lu, G. Xu, *J. Sep. Sci.* **31**, 1564–1572 (2008).
- [12] S. Louw, A.S. Pereira, F. Lynen, M. Hanna-brown, P. Sandra, **1208**, 90–94 (2008).
- [13] M.P.Y. Lam, S.O. Siu, E. Lau, X. Mao, H.Z. Sun, P.C.N. Chiu, et al., *Anal. Bioanal. Chem.* **398**, 791–804 (2010).
- [14] G. Greco, S. Grosse, T. Letzel, *J. Sep. Sci.* **37**, 630–634 (2014).
- [15] Y. Wang, R. Lehmann, X. Lu, X. Zhao, G. Xu, *J. Chromatogr. A.* **1204**, 28–34 (2008).
- [16] D. Cabooter, K. Choikhet, F. Lestremau, M. Dittmann, G. Desmet, *J. Chromatogr. A.* **1372**, 174–186 (2014).
- [17] G. Desmet, D. Cabooter, *LC-GC Eur.* **22**, 70–77 (2009).
- [18] D. Cabooter, D. Clicq, F. De Boever, R. Szucs, G. Desmet, *Anal. Chem.* **83**, 966–975 (2011).
- [19] K. Broeckhoven, D. Cabooter, S. Eeltink, G. Desmet, *J. Chromatogr. A.* **1228**, 20–30 (2012).

CHAPTER 5

Restriction capillaries as an innovative mixing unit for intermediate mobile phase exchange in multidimensional analysis

Based on:

Loos G., Shoykhet K., Dittmann M., Cabooter D. (2017). Restriction capillaries as an innovative mixing unit for intermediate mobile phase exchange in multidimensional analysis. *Journal of Chromatography A*, 1497, 70–80.

5.1 Introduction

The increasing demand for multi-residue analyses has led to numerous improvements in column and instrument technology [1–3]. The analysis of complex matrices such as blood, urine or environmental samples, however, remains challenging, especially when the multi-residue analysis of both polar and non-polar components is required. Most studies in e.g. toxicology, pharmacokinetics or environmental analysis, wherein pharmaceuticals are examined in combination with their generally more hydrophilic metabolites and degradation products, are performed using multiple liquid chromatography-mass spectrometry (LC-MS) methodologies [4–6]. Although manufacturers have modified and optimized conventional reversed-phase (RP) stationary phases with hydrophilic functional groups to accommodate the analysis of polar compounds, these stationary phases are generally not capable of retaining very polar analytes with water/octanol partition ($\log K_{ow}$) or water/octanol distribution ($\log D$) coefficients well below zero [7,8]. These values represent the concentration ratio of a certain molecule at equilibrium when dissolved in two immiscible phases. However, $\log K_{ow}$ only corresponds with the un-ionized form of a compound while $\log D$ takes into account the various forms of a solute at a certain pH value. As described in §1.5.2.2.2 such hydrophilic analytes can be retained using hydrophilic interaction liquid chromatography (HILIC). The recent revival of HILIC has resulted in a large number of applications in different fields of analysis demonstrating its capability to analyze polar compounds [9–15].

A complete multi-residue analysis of complex matrices can in principle be accomplished using orthogonal stationary phases, such as RP and HILIC columns to separate non-polar and polar compounds, respectively. Therefore, one sample is often analyzed by different orthogonal methods consecutively. However, in most cases, preference is given to a single, efficient and generic method that allows the complete analysis of the entire sample, in particular when only small sample amounts are available. Although the largely differing mobile phase requirements can be a major challenge when orthogonal methods are combined into a single analysis, different strategies have been elaborated to overcome this difficulty.

In two-dimensional (2D) analyses, fractions of the first dimension eluent are collected in vials (offline) or sample loops (online) and re-injected onto an orthogonal second dimension column [16,17]. To prevent peak shape disturbances by the mobile phase composition of the

first dimension in the second dimension separation, a dilution step is required [18–20]. In online 2D-LC, a counter gradient or a high flow of a diluting solvent using a second LC pump in combination with a large bore second dimension column is generally applied to optimize the second dimension performance [21,22]. Furthermore, microbore columns are generally used in the first dimension to reduce the amount of incompatible solvent that is transferred to the second dimension. This results in reduced extra-column band broadening by reducing the volume injected onto the second dimension column and improves peak focusing [23,24]. Disadvantages of a 2D-LC setup are the need for a second pump to dilute the eluate of the first dimension column and the laborious method optimization process, since the first and second dimension separation are mutually dependent. Interpretation of the generated chromatograms is moreover not straightforward.

Alternatively, orthogonal columns can be coupled in series to obtain a semi-2D-LC analysis resulting in a single chromatogram. It has been demonstrated that the serial coupling of RP and HILIC combines the separation characteristics of both methods and allows a simultaneous analysis of hydrophobic and hydrophilic components. This can be achieved by injecting a sample, containing polar and non-polar compounds, on a RP column in the first dimension. Non-polar compounds will be retained and separated on this column, while unretained polar compounds will move directly to a HILIC column, coupled in series with the RP column. To allow the analysis of these polar compounds on the HILIC column, a second pump is used to dilute the aqueous mobile phase with a high flow of ACN [25–27]. Although the peak capacity of such a serial analysis is lower compared to that obtained in 2D-LC, this approach is convenient due to its ability to optimize both dimensions independently. This leads to a more generic method development procedure and simplifies the data interpretation. The major disadvantages of such semi-2D-LC setups are the need for a second pump and the high dilution of the polar components in the second dimension.

Therefore, a setup wherein HILIC and RP columns are coupled in series using a single pump and two switching valves was developed in Chapter 4. To assure a compatible “sample solvent” for the sequential analysis on HILIC and RPLC columns, commercially available mixers were used to dilute the organic solvent with pure water. Although this approach has been demonstrated to result in the successful analysis of a mixture of 20 pharmaceuticals with log D-values ranging between -5.75 and 4.22 in a total analysis time of 20 min [29], the use of

commercially available mixers for online solvent dilution still has a number of drawbacks. Since the mixers are available in fixed and limited volumes only, several mixers need to be coupled in series to obtain a large enough mixing volume. This increases both the cost and the bulkiness of the setup.

The fixed volumes of the mixers also prevent a continuous tuning of the mixing volume, since the mixing volume can only be altered in discrete steps (corresponding to the volume of one mixer). The current study therefore focuses on the elaboration of an alternative mixing unit for online solvent dilution that is more flexible and less expensive in comparison with commercial mixing units. For this purpose, cheap and commonly available restriction capillaries with different dimensions and hence different flow resistances are used. The proof-of-concept is demonstrated for a simple but representative test sample containing a number of pharmaceuticals with a wide variety in polarity.

5.2 Experimental

5.2.1 Chemicals

The pharmaceuticals used to prepare a representative sample for the method development were: 17 α -ethinylestradiol, β -estradiol, atenolol, diclofenac, estrone, metformin hydrochloride, progesterone, sulfamethoxazole and testosterone from Sigma-Aldrich (Diegem, Belgium). Carbamazepine and propranolol were from Alpha Pharma (Zwevegem, Belgium) and lorazepam was from Fagron (Waregem, Belgium). Caffeine, codeine phosphate, ibuprofen, metoprolol, oxazepam, pentoxifylline, trimethoprim and vidarabine were available in the lab as USP reference standards. The drug classes and their predicted log D values (at pH 3.0 using Marvin Sketch software) are shown in Table 5.1. Since the focus in this Chapter is the new mixing unit, an adjusted sample was used for the method development compared with Chapter 4. The majority of pharmaceuticals separated on HILIC was omitted to allow isocratic runs in the first dimension and correspondingly reduce the equilibration time. Therefore, the same sample was used as in Cabooter et al. [28], however, ticlopidine was substituted by the slightly more hydrophilic pentoxifylline.

The solvents used to prepare sample stock solutions or mobile phases were: acetonitrile (ACN, HPLC grade), ethanol (EtOH, absolute, analytical reagent grade), isopropanol (IPA, analytical

reagent grade) and HCl solution (37.5 w/w%), purchased from Fisher Chemical (Loughborough, UK). Methanol (MeOH, HPLC grade) and formic acid (FA, 99%) were from Acros Organics (Geel, Belgium) and ammonium formate (AF, $\geq 99.995\%$) was from Sigma-Aldrich. Ultrapure water (H_2O , conductivity = $0.1 \mu\text{S}/\text{cm}$, pH 6.00) was produced in the laboratory using a Milli-Q gradient purification system from Millipore (Bedford, MA, USA).

5.2.2 Columns and materials

Analysis of the polar compounds was performed on an Acquity UPLC BEH HILIC column (1.0 x 100 mm; $1.7 \mu\text{m}$ or 2.1 x 100 mm; $1.7 \mu\text{m}$) from Waters (Wexford, Ireland). Trapping of the non-polar compounds was done on a Cortecs phenyl trap column (3.0 x 30 mm; $2.7 \mu\text{m}$ or 2.1 x 30 mm; $2.7 \mu\text{m}$) from Waters or a Kinetex EVO C18 trap column (2.1 x 20 mm; $2.6 \mu\text{m}$) from Phenomenex (Utrecht, The Netherlands). In contrast with the fully porous trap column used in Chapter 4, these columns were both packed with core-shell particles to reduce the backpressure during the dilution step. The non-polar pharmaceuticals were separated on a Cortecs phenyl (3.0 x 100 mm; $2.7 \mu\text{m}$) or an Acquity UPLC BEH C18 column (2.1 x 100 mm; $1.7 \mu\text{m}$) from Waters.

All connections between pump, valves, columns and detector were made with nanoViper tubing (inner diameters: 50-150 μm) from Thermo Scientific (Germering, Germany) or stainless steel tubing (diameter: 170 μm) from Agilent Technologies (Waldbronn, Germany) with the shortest possible length. To trap the non-polar compounds after eluting from the HILIC column, Rheodyne sample loops with volumes of 100 μL and 50 μL and VICI Valco T-pieces with a bore size of 0.25 mm were purchased from Sigma-Aldrich.

5.2.3 Apparatus

All experiments were executed on an Agilent Infinity 1290 system from Agilent Technologies that consisted of a 1290 quaternary pump, a 1290 autosampler with a maximum injection volume of 20 μL and a 1290 DAD detector with a 1.0 μL (V_{c}) flow cell and a path length of 10 mm. The system was further equipped with two Agilent 9-port/8-position ultra-high pressure valves (valves 1 and 2, max. pressure of 1200 bar) and a 1200 column heating compartment with an additional 9-port/8-position ultra-high pressure valve (valve 3) from Agilent Technologies. Chemstation software (Agilent Technologies) was used to operate the system, to control the valves and to acquire and analyze data.

Table 5.1: Pharmaceuticals used in this study with their drug class, stock solvents and concentrations in the stock and working solution. The log D values at pH 3.0 are predicted by Chemaxon Marvin software (www.chemaxon.com). The numbers and letters in the first column refer to the peak annotation in the Figures.

| # | Pharmaceutical | Drug Class | Sample stock solvent | Stock solution (mg/mL) | Working solution (µg/mL) | Log D (pH= 3.0) |
|---|-----------------------|--------------------------------|----------------------|------------------------|--------------------------|-----------------|
| 1 | Vidarabine | Anti-viral | 0.5 M HCl | 10 | 33.3 | -3.78 |
| 2 | Trimethoprim | Antibiotic | EtOH | 2.5 | 16.7 | 0.19 |
| 3 | Propranolol | Anti-hypertensive | H ₂ O | 10 | 33.3 | -0.66 |
| 4 | Metoprolol | Anti-hypertensive | H ₂ O | 20 | 133.3 | -1.48 |
| 5 | Codeine | Anti-tussive | H ₂ O | 10 | 33.3 | -2.16 |
| 6 | Metformin | Anti-diabetic | H ₂ O | 20 | 66.7 | -5.75 |
| 7 | Atenolol | Anti-hypertensive | EtOH | 10 | 133.3 | -2.82 |
| A | Caffeine | CNS stimulant | H ₂ O | 10 | 33.3 | -0.55 |
| B | Pentoxifylline | Phosphodiesterase inhibitor | H ₂ O | 10 | 50 | 0.23 |
| C | Sulfamethoxazole | Antibacterial | EtOH | 5 | 33.3 | 0.75 |
| D | Carbamazepine | Anti-convulsant | ACN | 5 | 16.7 | 2.77 |
| E | Oxazepam | Anti-anxiety | MeOH | 2 | 33.3 | 2.92 |
| F | Lorazepam | Anti-anxiety | ACN | 5 | 33.3 | 3.53 |
| G | β-estradiol | Hormone | EtOH | 5 | 83.3 | 3.75 |
| H | Testosterone* | Hormone | EtOH | 10 | 166.7 | 3.32 |
| I | 17α-ethinylestradiol* | Hormone | EtOH | 5 | 41.7 | 3.67 |
| J | Estrone* | Hormone | EtOH | 5 | 41.7 | 3.13 |
| K | Ibuprofen | Nonsteroidal anti-inflammatory | ACN | 10 | 33.3 | 3.84 |
| L | Diclofenac | Nonsteroidal anti-inflammatory | EtOH | 5 | 16.7 | 4.22 |
| M | Progesterone | Hormone | EtOH | 10 | 166.7 | 4.15 |

*Pharmaceuticals that were not included in the sample in Chapter 4.

5.2.4 Stock and working solutions

Sample stocks of all compounds were prepared in aqueous or organic solvents in concentrations ranging between 2 and 20 mg/mL (Table 5.1). A working solution was made by mixing appropriate volumes of the different pharmaceuticals and adding ACN to obtain a total sample volume of 1.5 mL with compound concentrations of 17-167 µg/mL in 95% organic solvent (see Table 5.1). These concentrations were selected to acquire compound peaks with comparable heights at a wavelength of 210 nm.

5.2.5 General methodology

Equilibration, separation and mobile phase dilution was performed using four mobile phases: **A)** 10 mM ammonium formate in water, pH 3.0 (buffer); **B)** ACN; **C)** 0.02% formic acid in H₂O; **D)** 0.02% formic acid in ACN. All mobile phases were degassed with helium prior to use.

The working solution was injected on the HILIC column in the setup shown in Figure 5.1, step A. The injection volume was scaled to the I.D. of the first dimension column, i.e. 0.5 µL for a 1.0 mm I.D. column and 2.2 µL for a 2.1 mm I.D. column. The non-polar pharmaceuticals eluting in the void of the HILIC column were directed to a sample loop by switching valve 2 (V2) just before the non-polar compounds eluted from the HILIC column (Figure 5.1, step B-C).

Once all non-polar compounds were eluted from the HILIC column, valve 2 was switched back to its original position and the polar compounds were separated on an Acquity BEH HILIC column using an isocratic mobile phase composition of 5:95 (v/v%) A:B (Figure 5.1, step D). After analysis of the polar compounds, the configuration of all valves was changed to dilute the ACN-plug with 0.02% FA in H₂O and direct the non-polar pharmaceuticals to the RP trap column (Figure 5.1, step E). For this purpose, a new mixing unit based on restriction capillaries was used (see § 5.2.6). After dilution, valves 1 and 2 were altered to direct the non-polar pharmaceuticals from the trap column in backflush mode towards the RP analytical column (Figure 5.1, step F). To separate the non-polar compounds, the mobile phase was varied from 100% C to 20:80 (v/v%) C:D in 8 min. For both HILIC and RP separation, the detection wavelength was set at 210 nm.

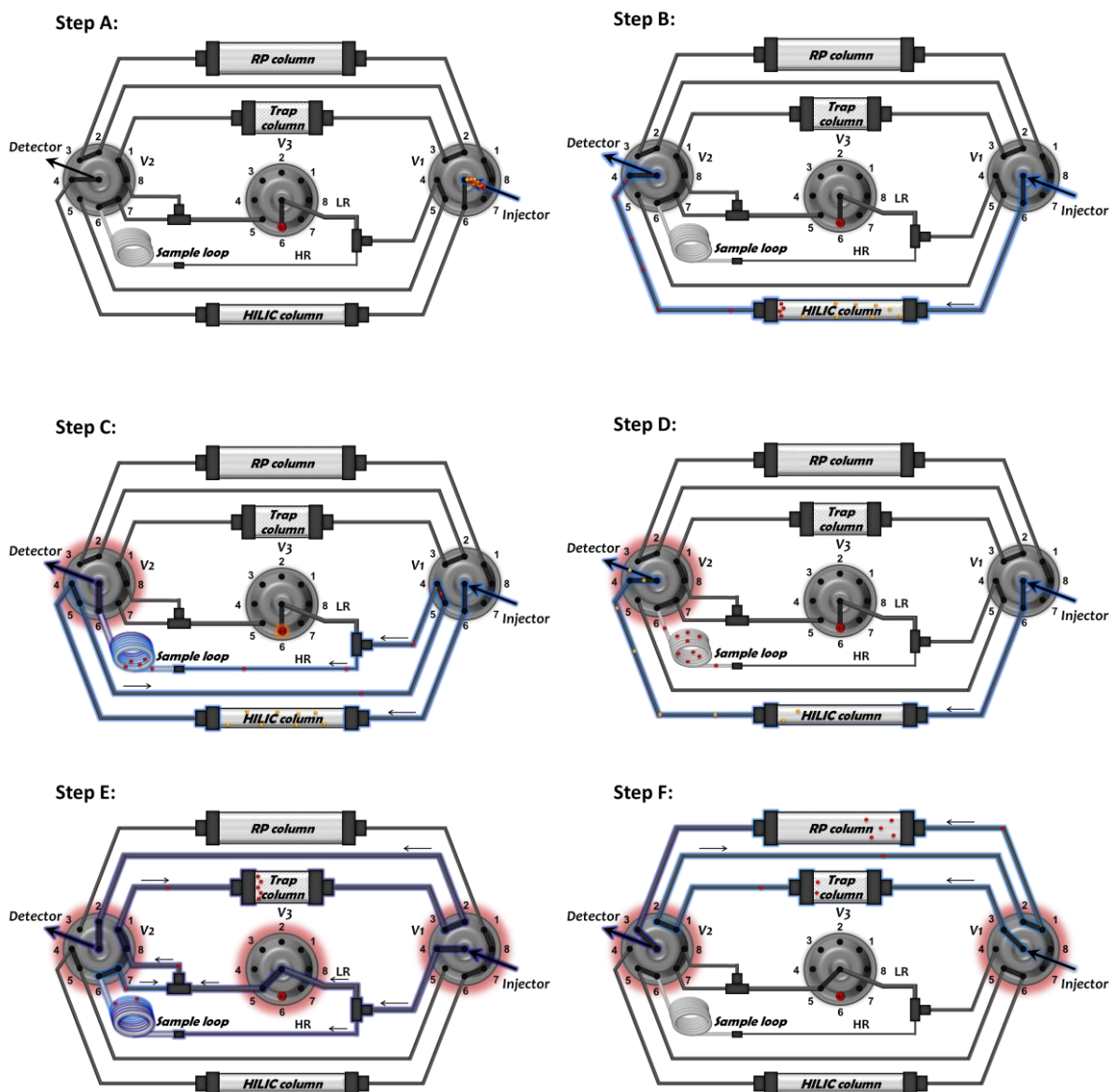


Figure 5.1: Step A: Scheme of the setup wherein the entire sample containing polar (●) and non-polar (●) compounds is injected on the HILIC column in a mobile phase composition of 5:95 (v/v%) 10 mM ammonium formate (pH 3):ACN. **Step B:** The polar compounds are retained on the HILIC column while the non-polar pharmaceuticals elute near the void volume. **Step C:** The configuration of valve 2 (V2) is changed to guide the non-polar compounds towards the sample loop through the HR restriction capillary by blocking the LR path. **Step D:** The non-polar pharmaceuticals are trapped in the sample loop. V2 is returned to its original position and the polar compounds are analyzed on the HILIC column. **Step E:** All valves (1, 2 and 3) are switched to open both restriction capillaries and to direct the non-polar compounds towards the trap column. The ACN plug wherein the non-polar compounds are dissolved is diluted when both paths converge due to the higher flow of 0.02% FA in H₂O through the LR restriction capillary in comparison with the HR restriction capillary. **Step F:** Valves 1 and 2 are altered to elute the non-polar pharmaceuticals in backflush from the trap column in order to analyze them on the RP column by changing the mobile phase composition from 100% 0.02% FA in H₂O to 20:80 (v/v%) 0.02% FA in H₂O: 0.02% FA in ACN.

5.2.6 Mixing unit consisting of restriction capillaries

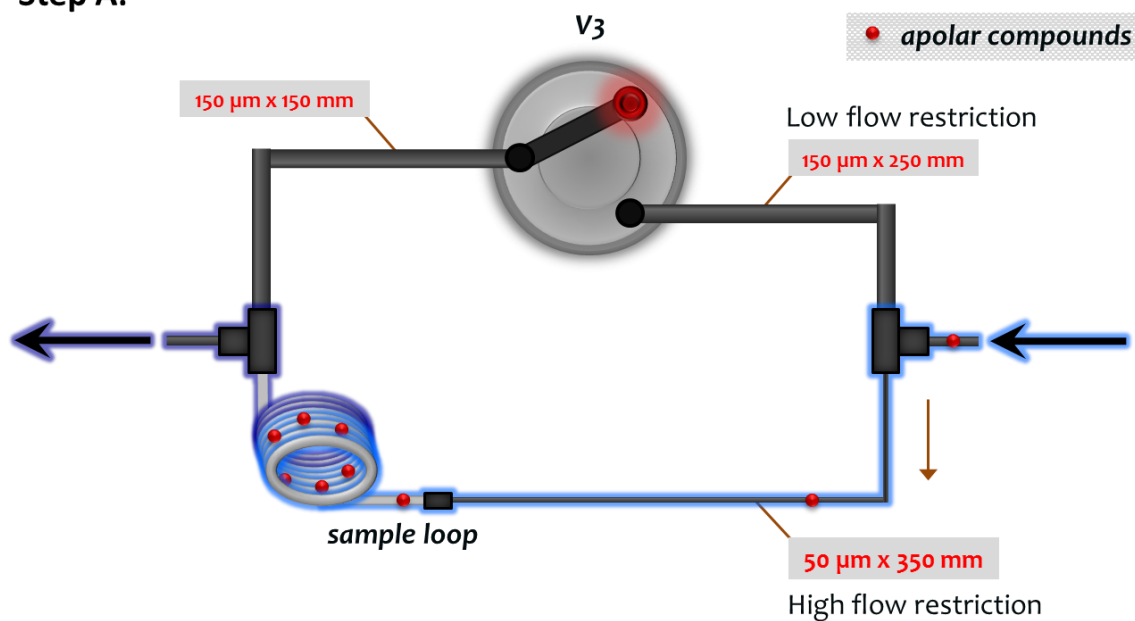
Using two restriction capillaries with different flow resistances (high flow resistance (HR) and low flow resistance (LR)) and two T-pieces, two flow paths were created to dilute the ACN-plug containing the non-polar pharmaceuticals. A simplified scheme of the restriction capillaries can be found in Figure 5.2. To obtain a uniform dilution and to minimize thermodynamic variations such as volume contraction and viscosity alterations that could influence the dilution ratio, the sample loop was positioned behind the HR capillary. To ensure sufficiently large differences in flow resistance, the inner diameter of the LR capillary was considerably larger than that of the HR capillary. When redirecting the non-polar pharmaceuticals to the sample loop, valve 3 (V3) (Figure 5.2, step A) was blocked to assure that the entire ACN-plug was directed towards the sample loop. Once all non-polar pharmaceuticals were collected in the sample loop (and after completion of the HILIC separation), the LR path was opened by switching valve 3 (Figure 5.2, step B). Subsequently, a high flow rate of aqueous mobile phase (0.02% FA in H₂O) was pumped over both restriction capillaries. Due to the large differences in flow resistance between the HR and LR capillary, a much higher flow of 0.02% FA in H₂O flowed through the LR capillary in comparison with the HR capillary and resulted in the dilution of the ACN-plug when both paths converged at the second T-piece. The capillary dimensions required to obtain a sufficiently high dilution ratio were calculated using the law of Hagen-Poiseuille [30]. The exact dilution ratio was subsequently verified experimentally by disconnecting both restriction capillaries from the second T-piece and by measuring the flow volumes eluting from the restriction capillaries individually at a fixed flow rate. This was done by prefilling the sample loop with 95:5 ACN:buffer (reflecting the actual situation) and with 0.02% FA in H₂O.

5.2.7 Recovery

For the non-polar pharmaceuticals, the recovery was determined by comparing the areas under the curve of the chromatographic peaks obtained on the coupled system ($AUC_{\text{coupled system}}$) with the areas under the curve when the working solution was injected directly on the RP column ($AUC_{\text{RP column}}$), using the same gradient conditions as for the RP column in the coupled system, as shown in eq. 5.1:

$$\text{Recovery (\%)} = \frac{AUC_{\text{coupled system}}}{AUC_{\text{RP column}}} \cdot 100\% \quad (5.1)$$

Step A:



Step B:

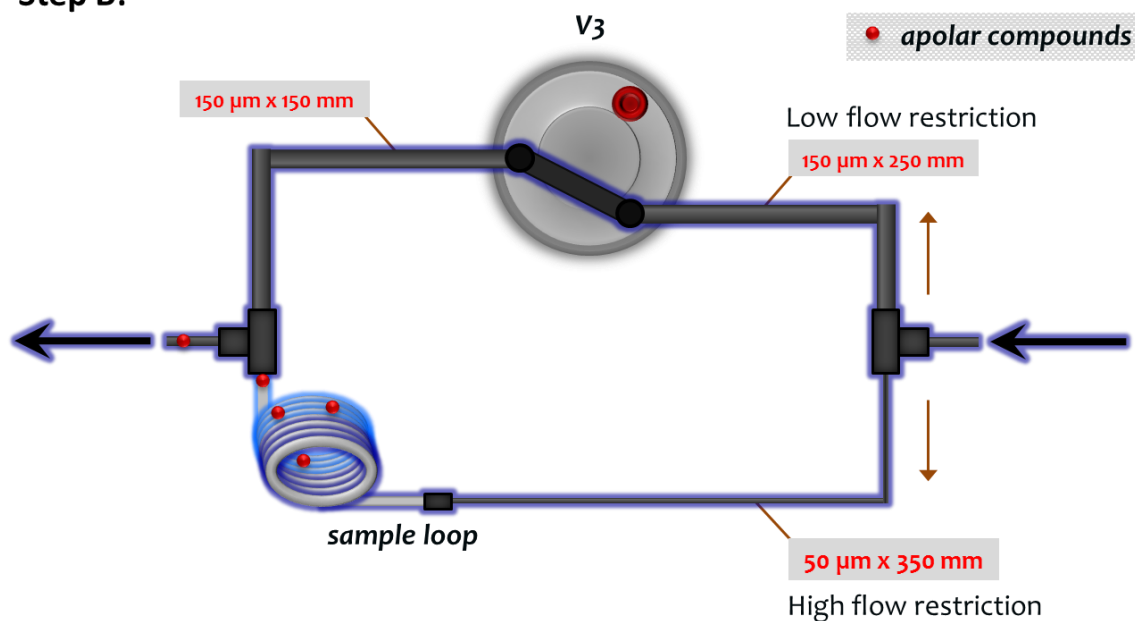


Figure 5.2: Simplified representation of the restriction capillaries. **Step A:** The ACN plug with non-polar pharmaceuticals (●) is directed to the sample loop through the HR restriction capillary by blocking the other path with switching valve 3 (V3). **Step B:** Both paths are opened by changing the configuration of valve 3. Due to the higher flow of water through the LR restriction capillary in comparison with the HR restriction capillary, the ACN plug is efficiently diluted when both paths converge again.

5.3 Results

In Chapter 4 a generic setup was equipped with commercially available mixers, however, with the available mixers in the lab, a maximum dilution factor of 1:50 was attainable. This allowed reducing the ACN content in the plug eluting from the HILIC column to 2.0% ACN after solvent exchange with 0.02% FA in H₂O [28,29]. It was observed that this dilution was not sufficient to efficiently trap semi-polar compounds such as caffeine on the reversed-phase column, resulting in broadened peak shapes. Increasing the dilution ratio was only possible by adding additional mixers to the setup, which decreased the flexibility of the setup and increased its cost and bulkiness. It was moreover observed that an abrupt change of the mobile phase composition during the dilution step, resulted in precipitation of non-polar pharmaceuticals within the microfluidic channels of the mixers, resulting in decreased recoveries. Although repeatable analyses were possible, acceptable recovery rates (80% - 91%) were only obtained when the entire mixing unit was flushed with sufficiently large volumes of pure water (\pm 10 mL), resulting in a total analysis time of 21.5 min (Figure 5.3).

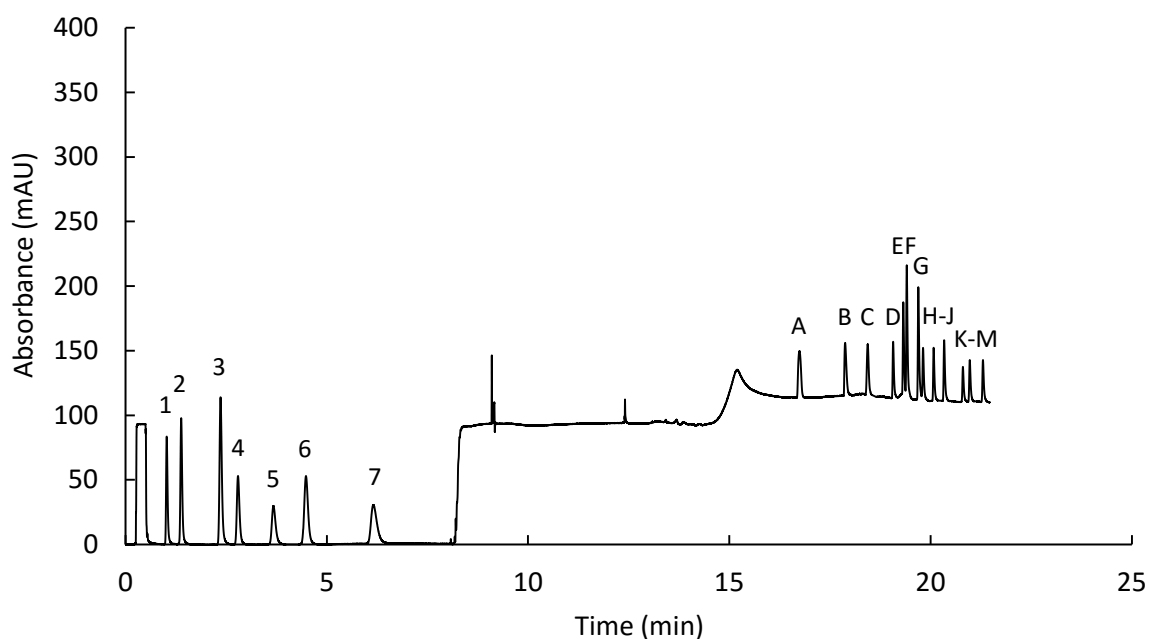


Figure 5.3: Chromatogram obtained using the setup described in Chapter 4 to connect the HILIC and RPLC columns in series. First dimension: Acquity BEH HILIC column (1.0 × 100 mm; 1.7 μ m); isocratic conditions: 95:5 (v/v%) ACN:10 mM ammonium formate (pH 3.0) at 0.25 mL/min. The non-polar compounds were directed to the sample loop by switching valve 2 at time points 0.23 min and 0.47 min. Second dimension: Zorbax Eclipse phenyl-hexyl (3.0 × 100 mm; 1.8 μ m); gradient conditions: from 100% 0.02% FA in H₂O to 20:80 (v/v%) 0.02% FA in H₂O:0.02% FA in ACN in 8 min at 0.5 mL/min. Dilution was done at 3.0 mL/min using four jet weaver mixers coupled in series leading to a total dilution volume of 3 mL. Trapping was done on a Cortecs phenyl (3.0 × 30 mm; 2.7 μ m). The injection volume was 0.5 μ L and detection wavelength was 210 nm. Peak annotation as in Table 5.1 with the exception of peak B: ticlopidine.

5.3.1 Restriction capillaries

5.3.1.1 Proof-of-concept

Since a dilution ratio of 1:50 was insufficient to adequately dilute the ACN-plug, a higher dilution factor of 1:75 was envisaged using a novel setup with restriction capillaries. Practically, this should be realizable by guiding 74:75 of the total flow through the LR capillary and 1:75 of the total flow through the HR capillary, implementing a split ratio of 1:75 in this way. To obtain this split ratio, the capillary dimensions and hence flow resistances of the restriction capillaries were carefully optimized. For an initial estimate of the required dimensions of the restriction capillaries, the law of Hagen-Poiseuille was used (eq. 5.2) [30]. This law applies to laminar flow in cylindrical tubing and describes the relation between the pressure drop over the tubing Δp and the viscosity of the solvent η , the diameter d and length L of the tubing and the flow rate F resulting in the following expression:

$$\Delta p = \frac{128 \cdot \eta \cdot L \cdot F}{\pi \cdot d^4} \quad (5.2)$$

Since the restriction capillaries in the proposed setup form a closed circuit, the pressure drop over both capillaries should be the same, allowing the equalization of the Hagen-Poiseuille expressions for the HR and LR capillaries. The resulting equation can be simplified by eliminating the constant parameters and the solvent viscosity, since the solvent entering both restriction capillaries during the dilution step will be the same. It is moreover demonstrated below that the ACN plug in the sample loop has no large influence on the viscosity of the solvent in the HR capillary, since the sample loop is positioned behind the HR capillary. The flow through each capillary (F_{HR} and F_{LR}) can be rewritten as a function of the total flow (F_{total}) and the (envisaged) dilution factor δ :

$$F_{HR} = \frac{1}{\delta} \cdot F_{total} \quad (5.3)$$

$$F_{LR} = \frac{\delta - 1}{\delta} \cdot F_{total} \quad (5.4)$$

Re-writing the law of Hagen-Poiseuille (eq. 5.2) for the HR and LR capillaries and replacing the respective flow rates F_{HR} and F_{LR} by the expressions in eqs. 5.3 and 5.4, an expression for the dilution factor δ for a specific set of tubing dimensions can subsequently be derived (eq. 5.5):

$$\frac{L_{HR} \cdot d_{LR}^4}{L_{LR} \cdot d_{HR}^4} + 1 = \delta \quad (5.5)$$

Different combinations of commercially available tubing dimensions were applied to eq. 5.5 to find capillary dimensions that would satisfy the envisaged dilution factor of 75 to obtain a good peak shape of caffeine in the second dimension. A good approximation was obtained with tubing dimensions of 50 μm x 350 mm for the HR capillary and 150 μm x 400 mm for the LR capillary, which resulted in a dilution factor of 72 (or a dilution ratio of 1:72).

For the practical implementation of these capillaries, nanoviper tubing was used. These capillaries were implemented in the setup as shown in Figure 5.2 to replace the commercially available mixers used in [23,24]. The dilution ratio was experimentally determined by disconnecting the LR and HR capillaries at their convergence point at the second T-piece (Figure 5.2) and sending a high flow ($F= 3.0$ mL/min, i.e. the maximum flow that could be used in combination with the trap column) of 0.02% FA in H_2O over both capillaries. This was done with the sample loop prefilled with either 95:5 (v/v%) ACN:buffer (reflecting the actual situation during the coupled experiment) or 0.02% FA in H_2O . As can be inferred from Table 5.2, the sample loop content only had a minor influence on the experimentally obtained dilution ratio, hence supporting the theory that the viscosity of the solvent in both restriction capillaries can in good approximation be assumed equal. The obtained Reynolds number of $Re= 17$ and $Re= 418$ in respectively the HR and LR capillary, moreover confirm that the flow was laminar in both capillaries. These observations and the experimentally obtained dilution ratio of $\sim 1:74$ hence indicate that the law of Hagen-Poiseuille can in good approximation be used to determine the dimensions required to obtain a particular dilution ratio.

Possible causes for the observed deviation between the experimentally measured and theoretically calculated dilution ratio, could be the experimental error of the procedure used to measure the flow volumes eluting from the restriction capillaries or the fact that nominal capillary diameters were used to calculate the theoretical dilution ratio. It can for example be calculated that a 2% variation in I.D. of the HR capillary leads to an 8% variation in the theoretically calculated dilution ratio.

Table 5.2: Experimentally obtained dilution factor for the restriction capillaries setup determined for different loop sizes (100 μL and 150 μL) and by prefilling the sample loop with different solvent compositions (aqueous and highly organic solvent content). Capillary dimensions were 150 μm x 400 mm (LR) and 50 μm x 350 mm (HR). The theoretical dilution factor was 72.

| Loop size | Dilution factor/relative standard deviation | Loop prefilled with 0.02% FA in H ₂ O | Loop prefilled with 95:5 ACN:buffer |
|-------------------|---|--|-------------------------------------|
| 100 μL | Dilution factor | 72.9 | 74.6 |
| | RSD (% , n= 5) | 0.8 | 1.2 |
| 150 μL | Dilution factor | 72.6 | 74.5 |
| | RSD (% , n= 5) | 0.3 | 0.6 |

5.3.1.2 Changing the dilution factor

To decrease or enhance the dilution factor, the dimensions of the restriction capillaries can be altered based on eq. 5.5. For practical reasons, the LR capillary dimensions preferable remain unaltered. Thus, different dilution factors can be obtained by changing the dimensions of the HR capillary.

It can moreover be derived that when two HR capillaries (HR₁ and HR₂) with different dimensions (different I.D. and different lengths) are coupled in series, the total obtained dilution factor δ_{tot} :

$$\delta_{\text{tot}} = \delta_1 + \delta_2 - 1 \quad (5.6)$$

With δ_1 the dilution factor that would be obtained by coupling only HR₁ in parallel with LR and δ_2 the dilution factor that would be obtained by coupling only HR₂ in parallel with LR. In extension, this expression can be rewritten as:

$$\delta_{\text{tot}} = \delta_1 + \delta_2 + \delta_3 + \dots + \delta_n - (n - 1) \quad (5.7)$$

for n pieces of tubing coupled in series to change the HR path.

The applicability of eq. 5.6 and 5.7 was verified experimentally by coupling one or two additional pieces of tubing with dimensions of 75 μm x 550 mm and 75 μm x 650 mm in series with the original HR path using zero-dead volume connections. Experimental dilution ratios of 1:97 and 1:127, respectively, were found (see Table 5.3). This is in good agreement with the theoretically calculated dilution factors of 1:94 and 1:120, respectively. Although smaller dilution factors were not relevant for the separation under consideration, Table 5.4 also

includes theoretically calculated and experimentally verified values for smaller dilution factors (ranging between $\delta= 5$ and $\delta= 50$) to demonstrate the flexibility of the mixing unit and the ease with which the dilution ratio can be altered. The Reynolds numbers obtained in the HR and LR capillaries at a maximum flow rate of 3.0 mL/min are also indicated and demonstrate that the flow was laminar under all circumstances.

5.3.2 HILIC x RP (1.0 x 3.0 mm)

To evaluate the newly proposed mixing unit, the commercial mixers used in Chapter 4 were replaced by restriction capillaries resulting in an experimentally determined dilution ratio of 1:74 (see § 5.3.1.1) as shown schematically in Figures 5.1 and 5.2. An injection volume of 0.5 μL was employed to inject the working solution on the HILIC column (Figure 5.1, step A).

Separation of the polar compounds was obtained on an Acquity BEH HILIC column (1.0 x 100 mm) using an isocratic mobile phase composition of 5:95 (v/v%) A:B at a flow rate of 0.25 mL/min. The non-polar pharmaceuticals eluting in the void of the HILIC column (Figure 5.1, step B) were directed to the sample loop by switching valve 2 at time points 0.23 min (Figure 5.1, step C) and 0.47 min (Figure 5.1, step D). This resulted in an ACN-rich plug containing the non-polar compounds with a volume of 60 μL ((0.47 min – 0.23 min) x 0.25 mL/min). To accommodate this ACN-rich plug, a sample loop with a volume of 100 μL was employed in the setup. After analysis of the polar compounds, the configuration of valves 1 and 2 was changed to dilute the ACN-plug with 0.02% FA in H₂O and direct the non-polar pharmaceuticals to the RP trap column (Figure 5.1, step E). For this purpose, a Cortec phenyl 3.0 x 30 mm trap column with 2.7 μm core-shell particles was employed. Due to the low backpressure of the core-shell particles, a flow rate of 3.0 mL/min could be used during the dilution of the ACN-rich plug, hence minimizing the dilution time and hence the dwell time of the analysis. After dilution, the switching valves were altered to direct the non-polar pharmaceuticals from the trap column in backflush mode towards the Cortecs phenyl analytical column (3.0 x 100 mm) (Figure 5.1, step F). To separate the non-polar compounds, the mobile phase was varied from 100% C to 20:80 (v/v%) C:D in 8 min at a flow rate of 0.5 mL/min. As shown in Figure 5.4, a baseline separation was obtained for almost all pharmaceuticals in a total analysis time of 19.5 minutes. The higher dilution factor obtained with the restriction capillaries moreover had a positive influence on the peak shape of caffeine (comparing peak A in Figures 5.4 and 5.3).

Table 5.3: Experimental dilution ratios obtained with restriction capillaries in combination with a 100 μL sample loop prefilled with different solvent compositions (aqueous and highly organic solvent content). The LR capillary dimensions are 150 μm x 400 mm. The HR capillary dimensions are given in the Table. Note that the theoretical dilution factor for one piece of tubing with dimensions 75 μm x 550 mm is 23, while that of one piece of tubing with dimensions 75 μm x 650 mm is 27. The Reynolds numbers obtained in the HR and LR capillaries, at a total flow rate of 3.0 mL/min are also shown.

| HR capillary dimensions | Dilution factor/relative standard deviation | Loop prefilled with 0.02% FA in H ₂ O | Loop prefilled with 95:5 ACN:buffer | Re (HR) | Re (LR) |
|--------------------------------|---|--|-------------------------------------|---------|---------|
| 50 μm x 350 mm + | Dilution factor | 96.4 | 96.9 | 13 | 419 |
| 75 μm x 550 mm | RSD (% , n= 5) | 0.2 | 0.6 | | |
| 50 μm x 350 mm + | Dilution factor | 126.2 | 127.6 | 10 | 420 |
| 75 μm x 550 mm + | RSD (% , n= 5) | 1.2 | 1.0 | | |
| 75 μm x 650 mm | | | | | |

Table 5.4: Theoretical and experimental dilution ratios obtained with restriction capillaries in combination with a 100 μL sample loop prefilled with aqueous solvent. The LR capillary dimensions are 150 μm x 400 mm. The HR capillary dimensions are given in the Table. The Reynolds numbers obtained in the HR and LR capillaries, at a total flow rate of 3.0 mL/min are shown.

| HR capillary dimensions | Theoretical dilution factor | Experimental dilution factor | RSD (n= 4) (%) | Re (HR) | Re (LR) |
|---------------------------------------|-----------------------------|------------------------------|----------------|---------|---------|
| 100 μm x 350 mm | 5.4 | 5.9 | 1.0 | 216 | 352 |
| 2 x (100 μm x 350 mm) | 9.9 | 11.0 | 1.5 | 116 | 385 |
| 3 x (100 μm x 350 mm) + | 24.3 | 26.4 | 1.1 | 48 | 408 |
| 75 μm x 250 mm | | | | | |
| 2 x (100 μm x 350 mm) + | 50.2 | 52.5 | 0.3 | 24 | 416 |
| 75 μm x 250 mm | | | | | |
| 50 μm x 150 mm | | | | | |

To ensure that all non-polar compounds were adequately transferred from the sample loop to the trap column, the effect of increasing dilution volumes (7.4 mL, 9.0 mL, 10.0, 11.0 mL, 12.0 mL, 14.8 mL and 22.5 mL) on the obtained recoveries for the non-polar analytes was investigated (see Table 5.5). Smaller dilution volumes of e.g. 5 mL resulted in poor recoveries since the sample was not completely transferred from the loop to the trap column. The minimal volume required to rinse the sample loop once was 7.4 mL. This can be understood as follows: when a total flow of 3.0 mL/min is applied to the restriction capillaries, the effective flow through the HR capillary will be $1/74 \times 3.0 \text{ mL/min} = 40.5 \text{ }\mu\text{L/min}$. Considering the sample loop has a volume of 100 μL , a total dilution time of 2.47 min is required to flush the sample loop once. This corresponds with a total dilution volume (over the entire mixing unit) of $3.0 \text{ mL/min} \times 2.47 \text{ min} = 7.4 \text{ mL}$. In the same way, it can be calculated that dilution volumes of 9.0 mL, 10.0, 11.0 mL, 12.0 mL, 14.8 mL and 22.5 mL, correspond with one sample loop volume times 1.2, 1.4, 1.5, 1.6, 2.0 and 3.0, respectively. It was observed that optimum recoveries (between 91% and 95%) were obtained for dilution volumes of 11.0 mL, however, a dilution volume of 9.0 mL was considered a good compromise between minimum trapping time and optimal recovery (88% - 93%) (Figure 5.4).

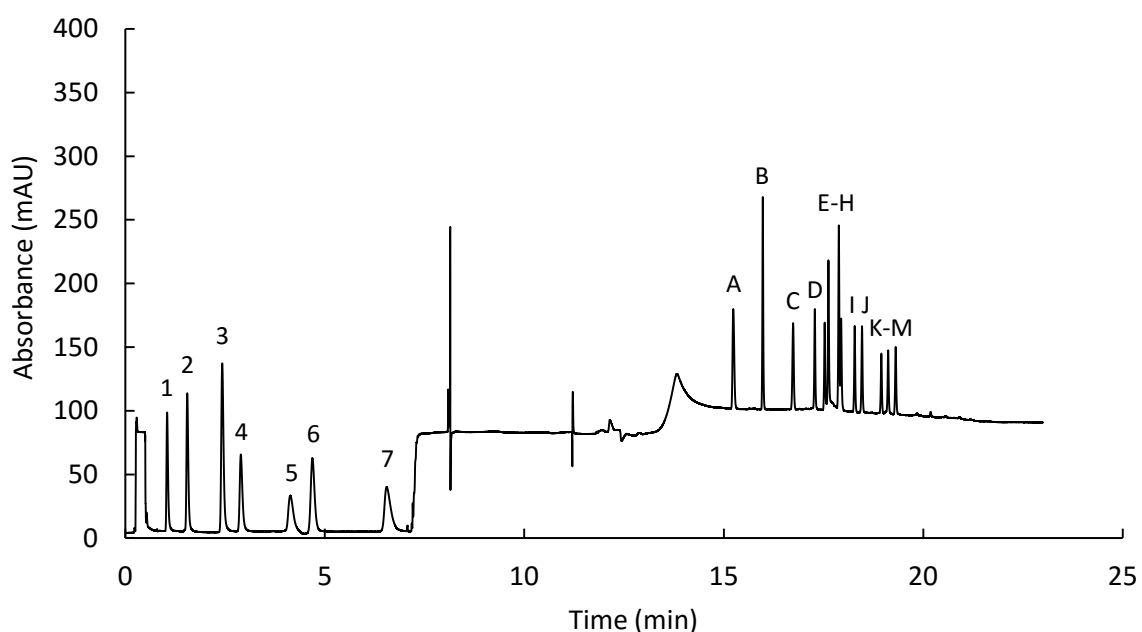


Figure 5.4: Chromatogram obtained on the 1.0 x 3.0 setup as shown in Figure 5.1. First dimension: Acquity BEH HILIC column (1.0 x 100 mm; 1.7 μm); isocratic conditions: 95:5 (v/v%) ACN:10 mM ammonium formate (pH 3.0) at 0.25 mL/min. The non-polar compounds were directed to the sample loop by switching valve 2 at time points 0.23 min and 0.47 min. Second dimension: Cortecs phenyl (3.0 x 100 mm; 2.7 μm); gradient conditions: from 100% 0.02% FA in H_2O to 20:80 (v/v%) 0.02% FA in H_2O :0.02% FA in ACN in 8 min at 0.5 mL/min. Dilution and trapping was done at 3.0 mL/min on a Cortecs phenyl (3.0 x 30 mm; 2.7 μm). Dilution ratio was 1:74 and dilution volume 9.0 mL. The injection volume was 0.5 μL and detection wavelength was 210 nm. Peak annotation as in Table 5.1.

This indicates that the sample loop should be rinsed at least 1.2 times to obtain adequate recoveries. At higher dilution volumes (> 14.8 mL), recoveries for semi-polar compounds such as caffeine decreased considerably, indicating that these compounds were flushed out of the trap column when trapping continued for too long. All analyses showed excellent repeatabilities (for apolar compounds: RSD retention times < 0.2% and RSD peak areas generally < 1.0%), despite the frequent switching of the valves.

Table 5.5: Recoveries for the non-polar compounds on the setup wherein a 1.0 mm I.D. HILIC column was coupled in series with a 3.0 mm I.D. phenyl column. The peak area ratios were determined by injecting the working solution on the coupled system and directly on the RP column (n= 3). Trap column dimensions were: 3.0 x 30 mm Cortex phenyl column. A dilution ratio of 1:74 was evaluated for dilution volumes ranging between 7.4 mL and 23.1 mL.

| # | Pharmaceutical | Recovery (%) | | | | | | |
|---|----------------------|--------------|------------|------------|------------|------------|------------|------------|
| | | 7.4 mL | 9.0 mL | 10.0 mL | 11.0 mL | 12.0 mL | 15.4 mL | 23.1 mL |
| A | Caffeine | 83.9 ± 0.4 | 90.5 ± 0.3 | 91.9 ± 0.2 | 92.4 ± 0.4 | 92.1 ± 0.2 | 79.2 ± 1.5 | 3.1 ± 3.2 |
| B | Pentoxifylline | 82.7 ± 0.4 | 90.3 ± 0.2 | 91.9 ± 0.2 | 92.6 ± 0.2 | 92.7 ± 0.1 | 92.5 ± 0.5 | 92.1 ± 1.1 |
| C | Sulfamethoxazole | 91.2 ± 0.4 | 91.7 ± 0.1 | 92.3 ± 0.3 | 92.8 ± 0.5 | 94.0 ± 0.4 | 92.7 ± 0.2 | 93.3 ± 1.0 |
| D | Carbamazepine | 90.9 ± 0.3 | 91.8 ± 0.3 | 92.8 ± 0.1 | 93.8 ± 0.3 | 94.0 ± 0.1 | 94.3 ± 0.4 | 93.1 ± 0.8 |
| E | Oxazepam | 88.8 ± 0.7 | 89.2 ± 0.2 | 90.7 ± 0.6 | 90.7 ± 0.4 | 91.1 ± 0.2 | 91.8 ± 0.3 | 90.8 ± 0.9 |
| F | Lorazepam | 91.4 ± 1.0 | 92.7 ± 0.4 | 93.5 ± 0.3 | 93.1 ± 0.1 | 94.7 ± 0.2 | 94.4 ± 0.5 | 95.1 ± 1.0 |
| G | β-estradiol | 89.7 ± 0.5 | 90.7 ± 0.2 | 92.1 ± 0.3 | 91.7 ± 0.6 | 93.5 ± 0.7 | 92.0 ± 0.8 | 91.4 ± 1.2 |
| H | Testosterone | 89.7 ± 0.9 | 90.8 ± 0.3 | 91.7 ± 0.7 | 91.3 ± 0.4 | 88.1 ± 0.3 | 90.6 ± 0.5 | 89.4 ± 1.0 |
| I | 17α-ethinylestradiol | 90.2 ± 0.6 | 90.3 ± 0.1 | 91.5 ± 0.7 | 91.8 ± 0.6 | 92.3 ± 0.6 | 92.7 ± 0.6 | 92.5 ± 1.6 |
| J | Estrone | 90.6 ± 0.5 | 90.4 ± 0.3 | 92.6 ± 0.4 | 93.1 ± 0.5 | 92.2 ± 0.3 | 94.3 ± 0.6 | 91.5 ± 1.2 |
| K | Ibuprofen | 86.6 ± 0.3 | 90.7 ± 0.4 | 91.4 ± 0.5 | 93.7 ± 0.2 | 93.3 ± 0.7 | 95.0 ± 0.6 | 87.0 ± 1.1 |
| L | Diclofenac | 81.7 ± 0.5 | 88.2 ± 0.8 | 88.3 ± 0.1 | 91.5 ± 0.3 | 91.0 ± 0.7 | 97.5 ± 0.4 | 87.5 ± 1.0 |
| M | Progesterone | 88.8 ± 0.7 | 92.1 ± 0.5 | 93.2 ± 0.5 | 94.6 ± 0.4 | 93.7 ± 0.1 | 89.3 ± 0.2 | 85.1 ± 1.1 |

5.3.3 HILIC x RP (1.0 x 2.1 mm)

To improve the sensitivity of the analysis and investigate the flexibility of the setup, additional modifications to the basic setup were evaluated. A first adaptation was the replacement of the 3.0 mm I.D. column in the second dimension by a 2.1 mm I.D. column to decrease sample dilution on the second dimension column and obtain sharper/higher peaks. For this purpose, the phenyl analytical column (3.0 x 100 mm; 2.7 μm) in the second dimension and correspondingly the phenyl trap column (3.0 x 30 mm; 2.7 μm) were replaced by a C18 analytical column (2.1 x 100 mm; 1.7 μm) and a C18 trap column (2.1 x 20 mm; 2.6 μm). A C18 stationary phase was selected as a viable alternative for the phenyl column since there were no 2.1 x 20 mm phenyl columns commercially available that would allow the use of the same flow rate (3.0 mL/min) to trap the non-polar compounds. The HILIC separation conditions and valve switching times remained unchanged, while the RP separation conditions were scaled to the smaller column dimension. The mobile phase composition was hence changed from 100% C to 20:80 (v/v%) C:D in 8 min at a flow rate of 0.3 mL/min.

In comparison with the basic HILIC x RP (1.0 x 3.0 mm) setup in Figure 5.4, higher sensitivities were obtained for the non-polar pharmaceuticals due to the smaller internal diameter of the trap and analytical column in the second dimension (Figure 5.5), while the total analysis time was 21 min, due to the slightly different selectivity of the C18 column. However, the use of a smaller C18 trap column resulted in an inferior recovery (~54%) for caffeine and sulfamethoxazole (~57%) when using a dilution volume of 9.0 mL (Table 5.6). For all other components, recoveries were between 87% and 97%. Since the recoveries for caffeine and sulfamethoxazole further decreased when using a higher dilution volume of 11.0 mL (Table 5.6), it was presumed that these compounds could not be efficiently trapped on the trap column under consideration. Compared to the 1.0 x 3.0 mm analysis, where a 3.0 x 30 mm phenyl trap column was used, the C18 trap column seemed less suitable to retain the semi-polar pharmaceuticals caffeine and sulfamethoxazole, while yielding high recovery rates for all other, non-polar analytes. This could be due to differences in retention capacity of the stationary phase or the smaller bed volume of the 2.1 x 20 mm C18 trap column.

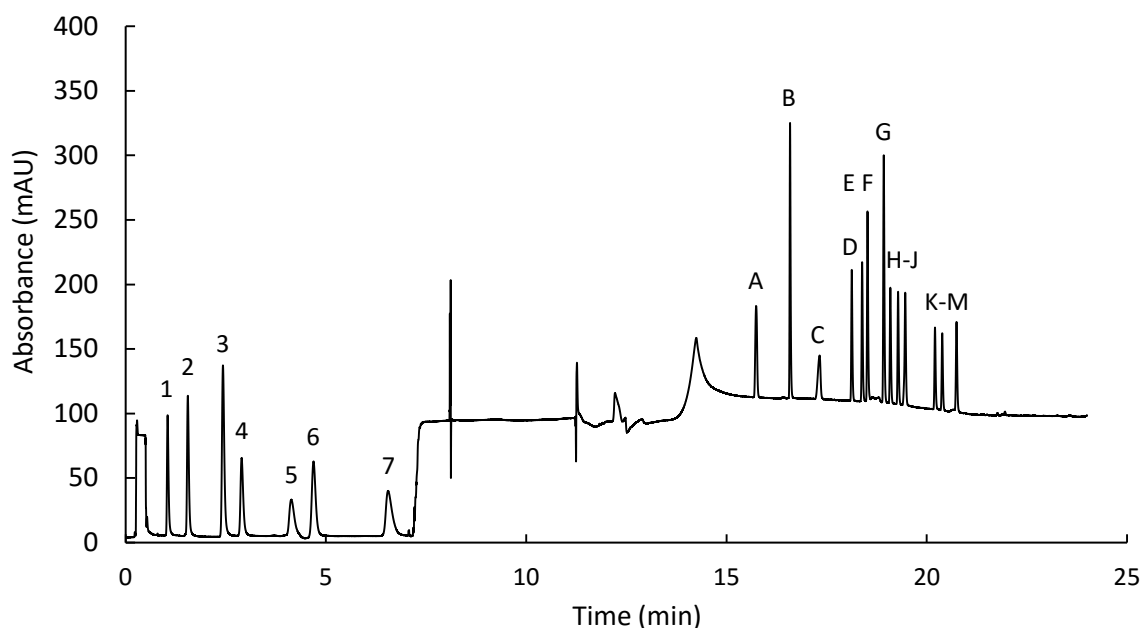


Figure 5.5: Chromatogram obtained on the 1.0 x 2.1 setup as shown in Figure 5.1. First dimension: Acquity BEH HILIC column (1.0 × 100 mm; 1.7 μm); isocratic conditions: 95:5 (v/v%) ACN:10 mM ammonium formate (pH 3.0) at 0.25 mL/min. The non-polar compounds were directed to the sample loop by switching valve 2 at time points 0.23 min and 0.47 min. Second dimension: Acquity C18 column (2.1 x 100 mm; 1.7 μm); gradient conditions: from 100% 0.02% FA in H₂O to 20:80 (v/v%) 0.02% FA in H₂O:0.02% FA in ACN in 8 min at 0.3 mL/min. Dilution and trapping was done at 3.0 mL/min on a Kinetex C18 trap column (2.1 x 20 mm; 2.6 μm). Dilution ratio was 1:74 and dilution volume 9.0 mL. The injection volume was 0.5 μL and detection wavelength was 210 nm. Peak annotation as in Table 5.1.

Using a 2.1 x 30 mm phenyl trap column, the recovery rates of caffeine and sulfamethoxazole were enhanced considerably (Table 5.6), while the peak shapes of the early eluting compounds remained relatively sharp. Optimum recoveries were obtained for a dilution volume of 9.0 mL and decreased when the dilution volume was increased to 11.0 mL (Table 5.6). Since the phenyl trap column was longer than the C18 trap column, it generated a higher backpressure in comparison with the C18 trap column, restricting the maximum flow rate at which dilution could be performed to 2.5 mL/min. However, with this 1.0 x 2.1 setup, all compounds could still be separated within 21.5 min when a dilution volume of 9.0 mL was employed (Figure 5.6 (a)), with recoveries ranging between 82% and 96%. Since the C18 column in the second dimension had a slightly different selectivity than the phenyl column, an increased resolution resulting in a complete baseline separation was obtained.

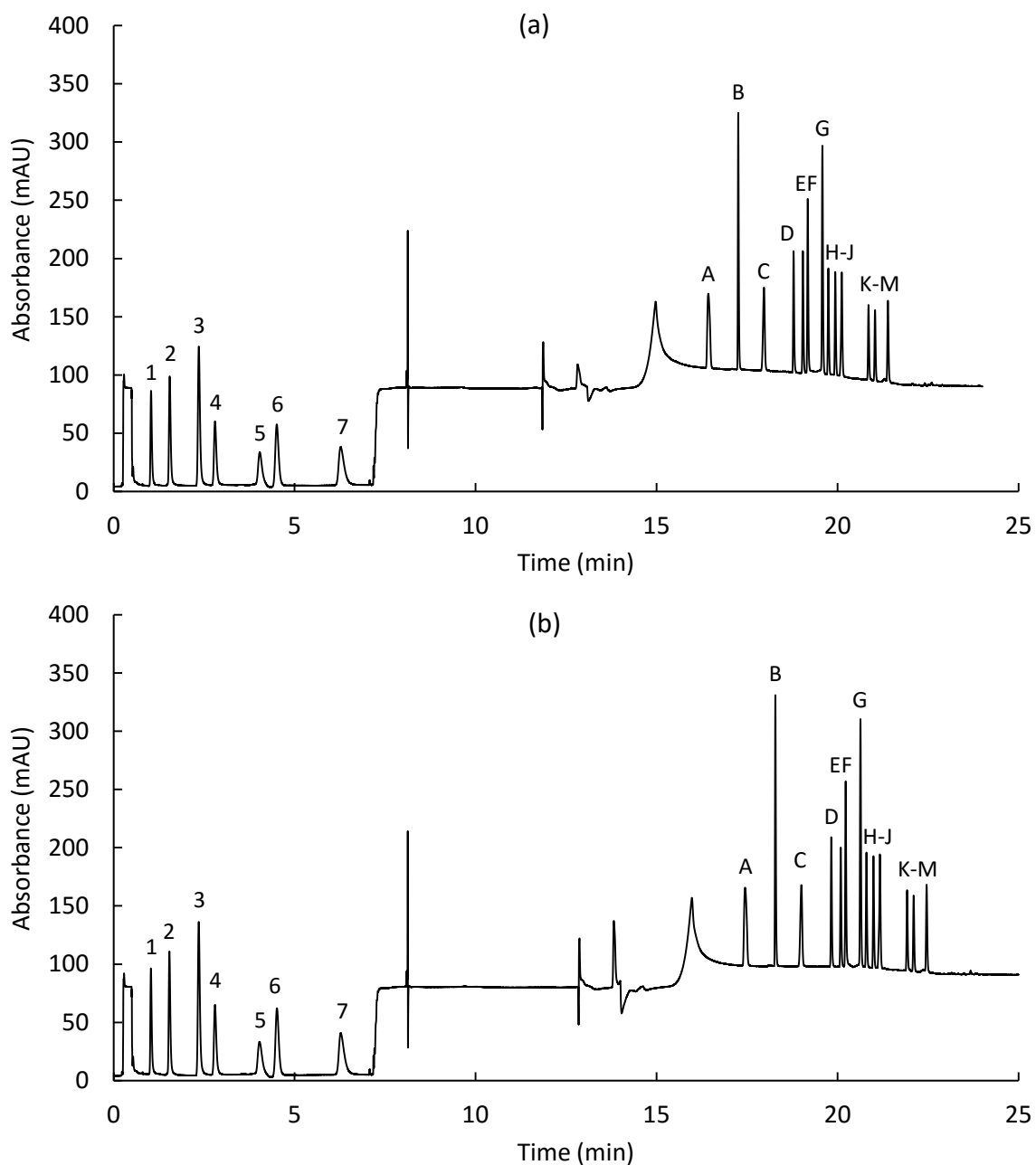


Figure 5.6: Chromatograms obtained with the 1.0 x 2.1 setup as shown in Figure 5.1. First dimension: Acquity BEH HILIC column (1.0 × 100 mm; 1.7 μm); isocratic conditions: 95:5 (v/v%) ACN:10 mM ammonium formate (pH 3.0) at 0.25 mL/min. The non-polar compounds were directed to the sample loop by switching valve 2 at time points 0.23 min and 0.47 min. Second dimension: Acquity BEH C18 column (2.1 x 100 mm; 1.7 μm); gradient conditions: from 100% 0.02% FA in H₂O to 20:80 (v/v%) 0.02% FA in H₂O:0.02% FA in ACN in 8 min at 0.3 mL/min. Dilution and trapping was done at 2.5 mL/min on a Cortecs phenyl (2.1 x 30 mm; 2.7 μm). In **(a)** the dilution ratio was 1:74 and dilution volume 9.0 mL. In **(b)** the dilution ratio was 1:97 and dilution volume 11.6 mL. The injection volume was 0.5 μL and detection wavelength was 210 nm. Peak annotation as in Table 5.1.

Additionally, it was tested whether a higher dilution ratio could increase the recovery of these semi-polar analytes. For this purpose, a dilution ratio of 1:97 was applied and the dilution volume of 9.0 mL was accordingly scaled to 11.6 mL to ensure the sample loop would be rinsed 1.2 times. Since a lower flow rate was applied to the HR capillary when the dilution factor was increased, a larger total volume was required to rinse the sample loop at least 1.2 times. The more favorable trapping conditions created by increasing the dilution ratio, resulted in slightly improved recoveries for caffeine (85%) in a total analysis time of 22.5 min (Figure 5.6 (b)), while peak shapes remained similar to when applying a dilution ratio of 1:74. However, when the dilution volume was increased to 14.6 mL (1.5 x loop volume), partial elution of caffeine from the trap column appeared, resulting in a recovery of 53% (Table 5.6). Therefore, to further enhance the recovery for caffeine with this setup, alternative stationary phases to trap the non-polar components should be explored. For all other compounds, the increased dilution ratio did not have a noticeable effect on the obtained recoveries.

Table 5.6: Recoveries for the non-polar compounds on different setups. The peak area ratios were determined by injecting the working solution on the coupled system and directly on the RP column ($n=3$). Trap column dimensions and selectivities were: 2.1 x 30 mm Cortex phenyl column or 2.1 x 20 mm Kinetex Evo C18. Dilution ratios of 1:74 and 1:97 were evaluated for dilution volumes of 9.0 mL and 11.0 mL (dilution ratio 1:74) and 11.6 mL and 14.6 mL (dilution ratio 1:97), corresponding with 1.2 and 1.5 x the sample loop volume, respectively.

| # | Pharmaceutical | Recovery (%) | | | | | |
|---|----------------------|---------------------------------|------------|---------------------------------|------------|---------------------------------|------------|
| | | 1.0 x 2.1 (2.1 x 20 mm trap) | | 1.0 x 2.1 (2.1 x 30 mm trap) | | 1.0 x 2.1 (2.1 x 30 mm trap) | |
| | | dilution ratio: 1:74 | | dilution ratio: 1:74 | | dilution ratio: 1:97 | |
| | | 9.0 mL | 11.0 mL | 9.0 mL | 11.0 mL | 11.6 mL | 14.6 mL |
| A | Caffeine | 54.0 ± 0.6 | 28.4 ± 3.2 | 81.6 ± 1.4 | 47.1 ± 6.1 | 85.1 ± 1.2 | 52.9 ± 2.9 |
| B | Pentoxifylline | 91.9 ± 0.6 | 97.0 ± 0.8 | 93.1 ± 0.4 | 93.6 ± 0.2 | 92.9 ± 0.8 | 94.0 ± 0.4 |
| C | Sulfamethoxazole | 56.8 ± 0.9 | 28.7 ± 2.7 | 95.9 ± 0.6 | 94.9 ± 0.3 | 96.3 ± 0.9 | 95.5 ± 0.3 |
| D | Carbamazepine | 93.6 ± 0.5 | 98.1 ± 0.7 | 94.5 ± 0.2 | 93.2 ± 0.3 | 95.1 ± 0.7 | 93.7 ± 0.6 |
| E | Oxazepam | 93.8 ± 0.4 | 97.8 ± 0.8 | 94.8 ± 0.2 | 93.9 ± 0.4 | 94.6 ± 0.7 | 94.2 ± 0.5 |
| F | Lorazepam | 93.1 ± 0.3 | 97.7 ± 1.0 | 94.7 ± 0.3 | 92.4 ± 0.4 | 94.2 ± 0.7 | 94.0 ± 0.5 |
| G | β-estradiol | 92.4 ± 0.3 | 97.0 ± 1.3 | 93.6 ± 0.2 | 91.3 ± 0.5 | 93.8 ± 0.5 | 93.1 ± 0.4 |
| H | Testosterone | 91.6 ± 0.6 | 98.0 ± 0.7 | 93.9 ± 0.2 | 93.1 ± 0.5 | 93.4 ± 0.6 | 94.3 ± 0.5 |
| I | 17α-ethinylestradiol | 90.5 ± 0.6 | 97.0 ± 1.6 | 92.7 ± 0.6 | 89.2 ± 0.2 | 93.3 ± 0.7 | 91.2 ± 0.5 |
| J | Estrone | 93.2 ± 0.4 | 97.6 ± 1.2 | 94.4 ± 0.3 | 92.5 ± 0.5 | 94.3 ± 0.6 | 93.5 ± 0.4 |
| K | Ibuprofen | 93.9 ± 0.5 | 98.5 ± 0.4 | 94.9 ± 0.5 | 94.7 ± 0.4 | 94.6 ± 0.8 | 94.1 ± 0.4 |
| L | Diclofenac | 87.2 ± 0.4 | 97.6 ± 0.8 | 94.1 ± 0.6 | 93.5 ± 0.3 | 89.8 ± 0.5 | 91.5 ± 0.5 |
| M | Progesterone | 97.3 ± 0.4 | 98.2 ± 1.2 | 95.5 ± 1.2 | 96.8 ± 0.5 | 86.7 ± 0.6 | 86.6 ± 0.1 |

5.3.4 HILIC x RP (2.1 x 3.0 mm)

As an alternative approach to enhance the detection signal of the basic HILIC x RP (1.0 x 3.0 mm) setup, a HILIC column with an internal diameter of 2.1 mm (2.1 x 100 mm; 1.7 μm) was implemented in the first dimension. This allowed scaling up the injection volume on the HILIC column to 2.2 μL , enhancing the total amount of sample introduced into the system. The flow rate in the first dimension was scaled to 1.1 mL/min (in accordance with the larger column I.D.), while the valve switching times to redirect the non-polar compounds to the sample loop were set at $t = 0.23$ min and $t = 0.36$ min. This resulted in an ACN-plug containing the non-polar compounds with a volume of 143 μL . To accommodate this larger ACN plug, the volume of the sample loop was increased to 150 μL .

To ensure sufficient flushing of this larger sample loop, dilution volumes were scaled to 13.3 mL (1.2 x loop volume) and 16.7 mL (1.5 x loop volume). The flow rate for trapping remained 3.0 mL/min, since the trap column dimensions used in this setup were 3.0 x 30 mm (phenyl trap column).

Since a concentration dependent UV-detector was used in this study and both the injection volume and flow rate on the HILIC column were scaled proportionally to their inner diameters, no differences in sensitivity were expected for the 1.0 mm I.D. (Figure 5.4) and the 2.1 mm I.D. separation (Figure 5.7). Indeed, the peak areas for the polar components were similar in Figure 5.4 and Figure 5.7, however, a small difference in peak height could be observed. The higher and sharper peaks obtained with the 2.1 mm I.D. column were attributed to the relatively smaller extra-column contribution obtained for the 2.1 mm I.D. column and a better column efficiency. In contrast, the gain in sensitivity obtained for the non-polar pharmaceuticals by applying a higher initial injection volume was considerable, while recoveries were maintained between 88% and 98% (Table 5.7) and peak shapes for the early eluting compounds were excellent. When using a dilution volume of 13.3 mL, the entire analysis was done in 21 min (Figure 5.7). In accordance with the 1.0 x 3.0 setup, the recovery of caffeine could be increased to 94% when using an increased dilution volume of 16.7 (1.5 x sample loop) resulting in a total analysis time of 22 min.

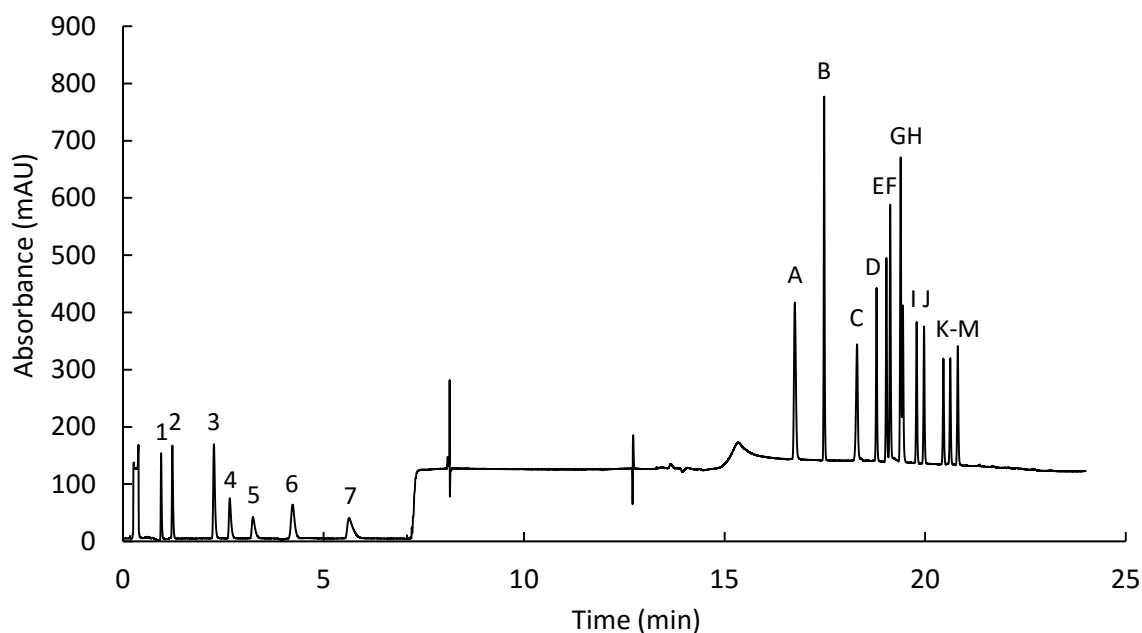


Figure 5.7: Chromatogram obtained with the 2.1 x 3.0 setup as shown in Figure 5.1. First dimension: Acquity BEH HILIC column (2.1 × 100 mm; 1.7 μm); isocratic conditions: 95:5 (v/v%) ACN:10 mM ammonium formate (pH 3.0) at 1.1 mL/min. The non-polar compounds were directed to the sample loop by switching valve 2 at time points 0.23 min and 0.36 min. Second dimension: Cortecs phenyl (3.0 × 100 mm; 2.7 μm); gradient conditions: from 100% 0.02% FA in H₂O to 20:80 (v/v%) 0.02% FA in H₂O:0.02% FA in ACN in 8 min at 0.5 mL/min. Dilution and trapping was done at 3.0 mL/min on a Cortecs phenyl (3.0 × 30 mm; 2.7 μm). Dilution ratio was 1:74 and dilution volume 13.3 mL. The injection volume was 0.5 μL and detection wavelength was 210 nm. Peak annotation as in Table 5.1.

5.3.5 HILIC x RP (2.1 x 2.1 mm)

To obtain a more flexible setup wherein both column diameters are equal and potentially interchangeable, the HILIC and RP columns in the first and second dimension of the basic setup were substituted by 2.1 mm I.D. columns. Again, an injection volume of 2.2 μL was applied in the first dimension, switching times of valve 2 were maintained at 0.23 min and 0.36 min and the ACN plug (143 μL) containing the non-polar pharmaceuticals was directed to a 150 μL loop. Dilution and trapping on a Cortecs phenyl trap (2.1 × 30 mm; 2.7 μm) was done with a volume of 13.3 mL (1.2 x loop volume) or 16.7 mL (1.5 x loop volume) at a flow rate of 2.5 mL/min. The RP separation was performed as previously discussed (§ 5.3.3) on the Acquity BEH C18 column (2.1 × 100 mm; 1.7 μm). Using this setup all compounds could be analyzed with high efficiency, good peak shapes and optimum sensitivity within 23.5 min when applying a dilution volume of 13.3 mL (Figure 5.8). Furthermore, acceptable recovery rates ranging between 83% and 97% were obtained (Table 5.7). Despite the acceptable recoveries obtained for caffeine

and sulfamethoxazole, their peak shapes were slightly less sharp compared to setups wherein a 3.0 mm I.D. column was used in the second dimension. At higher dilution volumes (16.7 mL) the recovery for caffeine decreased again (Table 5.7). Although the recovery of caffeine could be slightly increased to 84% by applying a higher dilution ratio of 1:97 (Table 5.7), this was at the cost of an extra dilution time of 1.7 min (for a dilution volume of 17.5 mL). A higher dilution ratio moreover did not have an influence on the obtained peak shapes of the early eluting compounds. Peak broadening due to injection is proportional with the injected volume (V_{inj}^2) and inversely proportional with the compression factor (CF) [31]. Since both injected volume and CF will increase with increasing dilution ratio, the resulting peak shape is expected to strongly depend on the variation of CF with the dilution ratio. This implies that –although an increased dilution ratio can have a positive effect on the obtained recoveries– the dilution ratio should not be overdimensioned to avoid a negative impact on the resulting peak shapes.

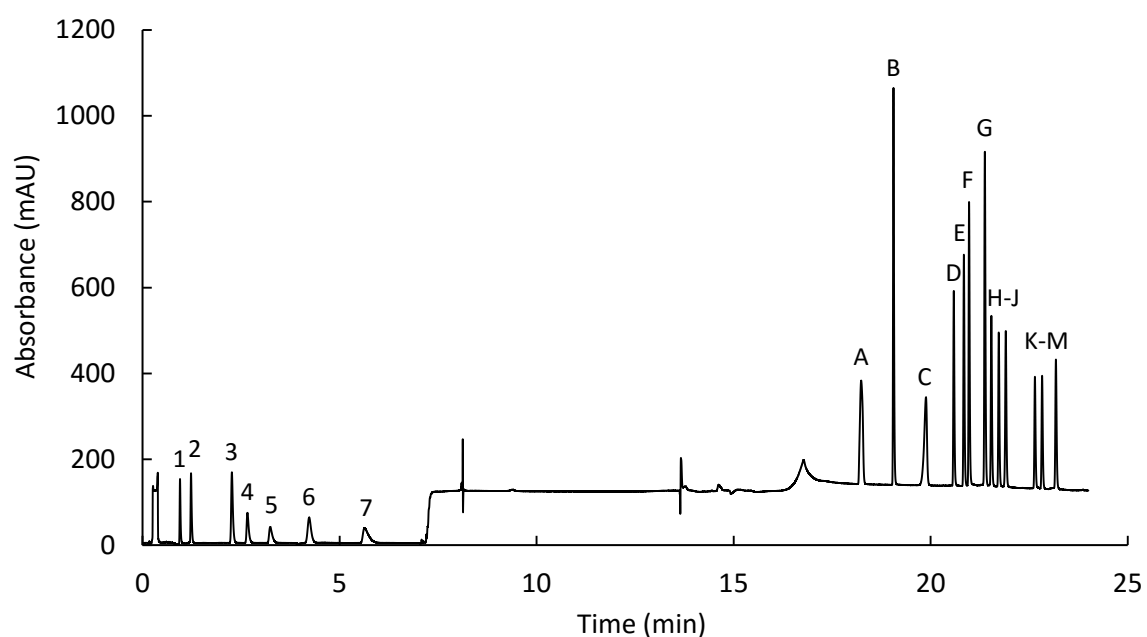


Figure 5.8: Chromatogram obtained with the 2.1 x 2.1 setup as shown in Figure 5.1. First dimension: Acquity BEH HILIC column (2.1 × 100 mm; 1.7 μm); isocratic conditions: 95:5 (v/v%) ACN:10 mM ammonium formate (pH 3.0) at 1.1 mL/min. The non-polar compounds were directed to the sample loop by switching valve 2 at time points 0.23 min and 0.36 min. Second dimension: Acquity UPLC BEH C18 column (2.1 x 100 mm; 1.7 μm); gradient conditions: from 100% 0.02% FA in H₂O to 20:80 (v/v%) 0.02% FA in H₂O:0.02% FA in ACN in 8 min at 0.3 mL/min. Dilution and trapping was done at 2.5 mL/min on a Cortecs phenyl (2.1 x 30 mm; 2.7 μm). Dilution ratio was 1:74 and dilution volume 13.3 mL. The injection volume was 2.2 μL and detection wavelength was 210 nm. Peak annotation as in Table 5.1.

Table 5.7: Recoveries of the non-polar compounds on different setups. The peak area ratios were determined by injecting the working solution on the coupled system and directly on the RP column (n=3). The trap columns were: 3.0 x 30 mm and 2.1 x 30 mm Cortex phenyl. Dilution ratios of 1:74 and 1:97 were evaluated for dilution volumes of 13.3 mL and 16.7 mL (dilution ratio 1:74) and 17.5 mL and 21.8 mL (dilution ratio 1:97), corresponding with 1.2 and 1.5 x the sample loop volume, respectively.

| # | Pharmaceutical | Recovery (%) | | | | | |
|---|----------------------|--------------------------------------|------------|--------------------------------------|------------|--------------------------------------|------------|
| | | 2.1 x 3.0 (3.0 x 30 mm trap) 1:74 | | 2.1 x 2.1 (2.1 x 30 mm trap) 1:74 | | 2.1 x 2.1 (2.1 x 30 mm trap) 1:97 | |
| | | 13.3 mL | 16.7 mL | 13.3 mL | 16.7 mL | 17.5 mL | 21.8 mL |
| A | Caffeine | 88.0 ± 0.2 | 93.8 ± 0.2 | 82.9 ± 1.4 | 46.4 ± 6.7 | 84.0 ± 0.2 | 37.8 ± 7.6 |
| B | Pentoxifylline | 89.0 ± 0.1 | 94.9 ± 0.3 | 89.7 ± 0.5 | 94.8 ± 0.2 | 89.4 ± 0.5 | 94.8 ± 0.4 |
| C | Sulfamethoxazole | 94.6 ± 0.2 | 95.4 ± 0.1 | 95.8 ± 0.3 | 89.5 ± 2.6 | 91.2 ± 2.7 | 49.0 ± 7.4 |
| D | Carbamazepine | 95.9 ± 0.3 | 96.7 ± 0.2 | 96.6 ± 0.3 | 96.0 ± 0.2 | 96.8 ± 0.3 | 96.4 ± 0.3 |
| E | Oxazepam | 93.3 ± 0.3 | 94.3 ± 0.2 | 95.4 ± 0.3 | 95.8 ± 0.2 | 95.4 ± 0.2 | 95.6 ± 0.3 |
| F | Lorazepam | 96.2 ± 0.3 | 97.6 ± 0.2 | 95.5 ± 0.4 | 95.9 ± 0.2 | 95.7 ± 0.2 | 95.9 ± 0.3 |
| G | β-estradiol | 96.0 ± 0.3 | 96.2 ± 0.4 | 96.7 ± 0.5 | 97.0 ± 0.1 | 96.1 ± 0.2 | 96.4 ± 0.3 |
| H | Testosterone | 95.3 ± 0.3 | 98.2 ± 0.6 | 95.6 ± 0.4 | 96.8 ± 0.1 | 95.9 ± 0.2 | 96.5 ± 0.3 |
| I | 17α-ethinylestradiol | 94.2 ± 0.4 | 94.8 ± 0.2 | 94.4 ± 0.5 | 94.6 ± 0.1 | 95.0 ± 0.3 | 95.3 ± 0.3 |
| J | Estrone | 94.6 ± 0.5 | 95.3 ± 0.2 | 94.2 ± 0.3 | 94.4 ± 0.2 | 95.2 ± 0.3 | 95.4 ± 0.3 |
| K | Ibuprofen | 98.4 ± 0.3 | 98.6 ± 0.2 | 96.3 ± 0.4 | 96.6 ± 0.1 | 96.4 ± 0.3 | 96.3 ± 0.3 |
| L | Diclofenac | 88.6 ± 0.3 | 93.4 ± 0.2 | 89.5 ± 0.3 | 93.3 ± 0.3 | 90.9 ± 0.2 | 94.5 ± 0.4 |
| M | Progesterone | 95.6 ± 0.3 | 94.7 ± 0.2 | 93.1 ± 0.5 | 94.7 ± 0.3 | 94.4 ± 0.2 | 96.1 ± 0.1 |

5.4 Conclusion

With the objective of attaining a generic UHPLC setup that has the ability to analyze both polar and non-polar compounds in a single chromatographic run, a new mixing unit allowing the coupling of orthogonal HILIC and RP columns in series has been developed. The proposed mixing unit is based on the use of two restriction capillaries with sufficiently large flow resistances to alter the mobile phase composition in between separations. Orthogonal columns are coupled in series to a commercially available UHPLC system using two high-pressure switching valves. This allows to direct unretained non-polar compounds from a HILIC column in first dimension to a sample loop with a sufficiently large volume to trap these non-

polar compounds. This sample loop is coupled in series with a restriction capillary with a high backpressure, which is in turn coupled in parallel with a restriction capillary with a much lower backpressure. By sending a highly aqueous mobile phase over both restriction capillaries, the highly organic mobile phase in the sample loop wherein the non-polar compounds are dissolved can be diluted to a mobile phase composition suitable for reversed-phase analyses. It is demonstrated that the extent of this dilution (the dilution ratio or dilution factor) can easily be tweaked by adjusting the dimensions of the high restriction capillary.

The presented setup has proven successful for the separation of a set of pharmaceuticals using a combination of HILIC and RPLC. Other column combinations (for different applications) will be evaluated in follow-up studies.

It is moreover demonstrated that the I.D. of the columns used in first and second dimension can be altered to increase the injected mass on the setup and/or decrease the dilution on the second dimension column. Both measures allow increasing the sensitivity of the analysis. Under optimum dilution conditions, the proposed setups can be used to perform repeatable analyses that provide good recoveries ranging between 82% and 99% within a total analysis time of maximum 23.5 min. Since a higher dilution factor only has a limited influence on the recovery of early eluting compounds in the second dimension, the use of trap columns with alternative selectivities will be investigated in follow-up studies to further improve trapping of semi-polar components. The use of commercially available equipment for fast and efficient solvent mixing presents a promising approach to use the serial coupling of orthogonal columns in routine applications.

5.5 References

- [1] J. De Vos, K. Broeckhoven, S. Eeltink, *Anal. Chem.* **88**, 262–278 (2016).
- [2] C.E.D. Nazario, M.R. Silva, M.S. Franco, F.M. Lanças, *J. Chromatogr. A.* **1421**, 18–37 (2015).
- [3] S. Buckenmaier, C.A. Miller, T. van de Goor, M.M. Dittmann, *J. Chromatogr. A.* **1377**, 64–74 (2015).
- [4] L. Havlíková, H. Vlčková, P. Solich, L. Nováková, *Bioanalysis.* **5**, 2345–2357 (2013).
- [5] A. Vass, J. Robles-Molina, P. Pérez-Ortega, B. Gilbert-López, M. Dernovics, A. Molina-Díaz, et al., *Anal. Bioanal. Chem.* **408**, 4857–4869 (2016).
- [6] C. Arnaudguilhem, K. Bierla, L. Ouerdane, H. Preud'homme, A. Yiannikouris, R. Lobinski, *Anal. Chim. Acta.* **757**, 26–38 (2012).
- [7] E.L. Schymanski, H.P. Singer, J. Slobodnik, I.M. Ipolyi, P. Oswald, M. Krauss, et al., *Anal. Bioanal. Chem.* **407**, 6237–6255 (2015).
- [8] N. Fontanals, R.M. Marcé, F. Borrull, *J. Chromatogr. A.* **1218**, 5975–5980 (2011).
- [9] E. Cífková, M. Holapek, M. Lísa, M. Ovcacíková, A. Lycka, F. Lynen, et al., *Anal. Chem.* **84**, 10064–10070 (2012).
- [10] C.M. Willemse, M.A. Stander, A. De Villiers, *J. Chromatogr. A.* **1319**, 127–140 (2013).
- [11] A. Periat, S. Fekete, A. Cusumano, J. Veuthey, A. Beck, M. Lauber, et al., *J. Chromatogr. A.* **1448**, 81–92 (2016).
- [12] C. Díez, D. Guillarme, A. Staub, E. Cognard, D. Ortelli, P. Edder, et al., *Anal. Chim. Acta.* **882**, 127–139 (2015).
- [13] J. Ruta, J. Boccard, D. Cabooter, S. Rudaz, G. Desmet, J.L. Veuthey, et al., *J. Pharm. Biomed. Anal.* **63**, 95–105 (2012).
- [14] J.C. Heaton, D. V McCalley, *J. Chromatogr. A.* **1427**, 37–44 (2016).
- [15] A. Kumar, J.P. Hart, D. V. McCalley, *J. Chromatogr. A.* **1218**, 3854–3861 (2011).
- [16] C.M. Willemse, M.A. Stander, J. Vestner, A.G.J. Tredoux, A. De Villiers, *Anal. Chem.* **87**, 12006–12015 (2015).
- [17] K. Zhang, Y. Li, M. Tsang, N.P. Chetwyn, *J. Sep. Sci.* **36**, 2986–2992 (2013).
- [18] W. Sun, L. Tong, J. Miao, J. Huang, D. Li, Y. Li, et al., *J. Chromatogr. A.* **1431**, 79–88 (2016).
- [19] A.F.G. Gargano, M. Duffin, P. Navarro, P.J. Schoenmakers, *Anal. Chem.* **88**, 1785–1793 (2016).
- [20] G. Vanhoenacker, I. Vandenheede, F. David, P. Sandra, K. Sandra, *Anal. Bioanal. Chem.* **407** 355–366 (2015).
- [21] P.G. Stevenson, D.N. Bassanese, X.A. Conlan, N.W. Barnett, *J. Chromatogr. A.* **1337**, 147–154 (2014).
- [22] M. Holcapek, M. Ovcacíková, M. Lísa, E. Cífková, T. Hájek, *Anal. Bioanal. Chem.* **407**, 5033–5043 (2015).
- [23] D.R. Stoll, E.S. Talus, D.C. Harmes, K. Zhang, *Anal. Bioanal. Chem.* **407**, 265–277 (2015).
- [24] G. Vivó-Truyols, S. van der Wal, P.J. Schoenmakers, *Anal. Chem.* **82**, 8525–8536 (2010).

- [25] S. Louw, A.S. Pereira, F. Lynen, M. Hanna-brown, P. Sandra, **1208**, 90–94 (2008).
- [26] G. Greco, S. Grosse, T. Letzel, *J. Sep. Sci.* **37**, 630–634 (2014).
- [27] J. Haggarty, M. Oppermann, K. Cook, S. Weidt, K.E. V Burgess, *Metabolomics*. 1465–1470 (2015).
- [28] D. Cabooter, K. Choikhet, F. Lestremau, M. Dittmann, G. Desmet, *J. Chromatogr. A.* **1372**, 174–186 (2014).
- [29] D. Cabooter, G. Loos, K. Shoykhet, M. Dittmann, G. Desmet, (2016).
- [30] J. Pfitzner, *Anaesthesia*. **31**, 273–275 (1976).
- [31] R.E. Wilson, S.R. Groskreutz, S.G. Weber, *Anal. Chem.* **88**, 5112–5121 (2016).

CHAPTER 6

Development of a generic SPE methodology for the simultaneous analysis of polar and non-polar pharmaceuticals in environmental water samples

6.1 Introduction

The increased drug consumption of the past decades has been accompanied by an increased discharge of pharmaceuticals and hence a higher amount of pharmaceuticals entering our waste, surface and/or ground water. Although the concentrations of these micro-pollutants are generally very low, it has been demonstrated that they can have a negative impact on the aqueous environment [1,2]. The presence of pharmaceuticals in water can lead to organ failure, a disturbed growth or even drastically decline animal populations [3]. The uncertainty about the long-term exposure effects has moreover raised the interest to monitor drug concentrations in waste, surface and drinking water. Due to the very low concentrations wherein these molecules are present, highly sensitive assays are required to evaluate the occurrence of pharmaceuticals, drug metabolites and transformation products. Since these trace compounds are hard to detect using standard liquid chromatography (LC) or gas chromatography (GC) methodologies hyphenated with mass spectrometry (MS), an additional sample preparation is often applied to further purify and pre-concentrate the target analytes.

For quantitative analysis, liquid-liquid extraction (LLE) wherein the analytes are extracted based on the partitioning between an aqueous and an organic solvent, used to be the standard [4]. To increase the extraction efficiency, multiple improvements such as working at elevated temperatures and pressures have been made [5]. Nevertheless, for environmental water analysis LLE procedures have gradually been displaced by alternative techniques such as stir-bar sorptive extraction (SBSE) [6,7] and in particular solid-phase extraction (SPE) [8]. In general, SPE is more efficient than LLE and comprises higher selectivities and extraction capacities resulting in enhanced sensitivities. The retention mechanisms in SPE are based on the same principles as in LC. Depending on the physico-chemical characteristics of the analytes, an appropriate stationary sorbent is chosen to retain the compounds by ion-exchange and/or partitioning between the solid stationary phase and a liquid mobile phase. After conditioning the stationary sorbent with a solvent similar to the sample matrix, samples up to 1000 mL are loaded on the cartridge [9,10]. Consequently, the sorbent is washed to remove salts and interfering substances prior to elution. Before injection onto an LC or GC column, the eluate can optionally be evaporated and reconstituted in an appropriate solvent to further concentrate the analytes and to make the sample matrix compatible with LC or GC analysis [11].

In environmental analysis, the main purpose is to pre-concentrate the compounds of interest, however, SPE can also be used to reduce matrix effects. Due to the availability of large sample volumes, higher sensitivities are obtained by extracting more water. However, studies have shown a decrease in absolute recovery when sample volumes are too high [12,13]. Therefore, optimum sample volumes are to be determined to obtain the best compromise between sensitivity, extraction speed and recovery. Alternatively, the bed volume can be adjusted based on the sample volume, since the total binding capacity of the sorbent is estimated to be 5% of the bed weight for silica based sorbents and 10% - 15% for polymeric sorbents [11]. However, it is important to assure sufficient binding capacity based on the sample complexity and compound concentrations. The flexibility of SPE can moreover be extended by combining different sorbent selectivities when the analysis of a broad range of analytes is envisaged [14,15]. Moreover, by performing multiple extractions simultaneously, high throughput analyses are feasible.

The analysis of pharmaceutical components in environmental water samples is highly challenging due to the wide range of polarity wherein different drugs, metabolites and degradation products appear. Therefore, a generic, single injection UHPLC methodology for the simultaneous analysis of polar and non-polar compounds was previously developed in Chapters 4 and 5. The proof-of-concept of this approach was demonstrated for a number of pharmaceutical compounds with a large variety in polarity, spiked in ultrapure water.

To ensure an adequate pre-concentration of the pharmaceuticals envisaged in Chapters 4 and 5, an SPE procedure capable of retaining compounds with a wide variety in polarity is required. Therefore, the purpose of this Chapter was to investigate whether a similar principle of combining stationary phase materials for SPE could be applied to develop a generic SPE procedure for pharmaceuticals in environmental water. Simulated wastewater (SWW) was chosen as the aqueous matrix, since the matrix composition of environmental water samples can be very different depending on the sampling location. Since the large total organic content of wastewater effluent and in particular influent may cause serious interferences when analyzing environmental samples, the complexity of the water composition may have an impact on the extraction efficiency of the targeted analytes. Besides inducing clogging, these matrix substances can compete with compounds of interest to interact with the stationary phase reducing the binding capacity of the bed. Therefore, method development in the field

of water research is commonly done using SWW, which is independent of the sample origin [16,17]. Moreover, the use of a uniform and representative SWW simplifies method validation due to the availability of analyte-free blank matrices.

6.2 Experimental

6.2.1 Chemicals and solvents

The pharmaceuticals used in this study are listed together with their drug class, supplier and predicted log D values (at pH 3.0 using Marvin Sketch software) in Table 6.1. To allow for UV detection during method development, working samples were prepared by spiking ultrapure water or SWW with individual stock solutions at 17-167 mg/L. When extraction was performed under acidic conditions, 0.1% FA was added to the SWW. The SWW matrix consisted of 96 mg/L NaHCO₃, 7 mg/L NaCl (Fisher Scientific, Loughborough, UK), 60 mg/L CaSO₄·2H₂O, 1.2 mg/L NH₄H₂PO₄ (Merck, Darmstadt, Germany), 6 mg/L urea (S.C. Federa S.V., Brussels Belgium), 4 mg/L KCl (ChemLab, Zedelgem, Belgium), 3 mg/L CaCl₂, 22 mg/L meat extract (Sigma Aldrich, Steinheim, Germany), 32 mg/L peptone (BD Biosciences, Le Pont-de-Claix, France) and 125 mg/L MgSO₄·7H₂O (Acros Organics, Geel, Belgium) resulting in a chemical oxygen demand of 53.2 mg/L and a pH of 7.5.

The solvents used to elute SPE cartridges or to prepare stock solutions, SWW samples or mobile phases were acetonitrile (ACN, HPLC grade), ethanol (EtOH, absolute, analytical reagent grade), isopropanol (IPA, analytical reagent grade) and HCl solution (37.5 w/w%), purchased from Fisher Chemical (Loughborough, UK). Acetic acid (AA) (ACS reagent grade) was obtained from VWR (Fontenay-sous-Bois, France). Methanol (MeOH, HPLC grade), 7M NH₄OH in MeOH and formic acid (FA, 99%) were from Acros Organics (Geel, Belgium) and ammonium formate (AF, ≥ 99.995%) was from Sigma-Aldrich. Ultrapure water (H₂O, conductivity = 0.1 μS/cm, pH 6.00) was produced in the laboratory using a Milli-Q gradient purification system from Millipore (Bedford, MA, USA).

Table 6.1: List of pharmaceuticals used to develop a generic sample preparation methodology.

| Pharmaceutical | Drug Class | Supplier | Log D (pH= 3.0) | Pharmaceutical | Drug Class | Supplier | Log D (pH= 3.0) |
|-----------------------------|--------------------------------|----------------------------------|-----------------|----------------------------|------------------------------------|----------------------------------|-----------------|
| β-estradiol | Hormone | Sigma Aldrich (Italy) | 3.75 | Diclofenac | Nonsteroidal anti-inflammatory | Sigma Aldrich (Italy) | 4.22 |
| 17α-ethinylestradiol | Hormone | Sigma Aldrich (China) | 3.90 | Dipyridole | Thrombus formation inhibitor | Sigma Aldrich (Italy) | 1.17 |
| Amitriptyline | Antidepressive | NODCAR (Egypte) | 1.31 | Escitalopram | Antidepressive | NODCAR (Egypt) | 0.26 |
| Atenolol | Anti-hypertensive | Sigma Aldrich (India) | -2.82 | Estrone | Hormone | Sigma Aldrich (Italy) | 4.31 |
| Bezafibrate | Anti-cholesterol | Sigma Aldrich (China) | 3.93 | Fluoxetine | Antidepressive | TCL (Belgium) | 0.93 |
| Caffeine | CNS stimulant | Available in the lab as standard | -0.55 | Guanylurea | Transformation product metformin | Acros Organics (Belgium) | -4.61 |
| Carbamazepine | Anti-convulsant | Alpha Pharma (Belgium) | 2.77 | Hydrochlorothiazide | Diuretic | Sigma Aldrich (Italy) | -0.58 |
| Cilostazole | Platelet-aggregation inhibitor | NODCAR (Egypte) | 3.31 | Ibuprofen | Nonsteroidal anti-inflammatory | Available in the lab as standard | 3.84 |
| Ciprofloxacin | Antibiotic | Acros Organics (Belgium) | -1.68 | Imipramine | Antidepressive | Available in the lab as standard | 0.78 |
| Clindamycin | Antibiotic | Alpha Pharma (Belgium) | -2.43 | Iopromide | Contrast agent | USP reference standard | 0.48 |
| Clozapine | Antipsychotic | TCL (Belgium) | -0.96 | Irbesartan | Angiotensin II receptor antagonist | Sigma Aldrich (USA) | 3.80 |
| Codeine | Anti-tussive | Available in the lab as standard | -2.16 | Ketoprofen | Nonsteroidal anti-inflammatory | Sigma Aldrich (China) | 3.56 |
| Diazepam | Anti-anxiety | s.a. Pharminnova n.v. (Belgium) | 2.81 | Lidocaine | Antiarrhythmic | s.a. Certa n.v. (Belgium) | -0.63 |

Table 6.1: Continued

| Pharmaceutical | Drug Class | Supplier | Log D (pH= 3.0) | Pharmaceutical | Drug Class | Supplier | Log D (pH= 3.0) |
|----------------|--------------------------------|----------------------------------|-----------------|------------------|------------------------------------|----------------------------------|-----------------|
| Lorazepam | Anti-anxiety | Fagron (Belgium) | 3.53 | Progesterone | Hormone | Sigma Aldrich (China) | 4.15 |
| Metformin | Anti-diabetic | Sigma Aldrich (USA) | -5.75 | Propranolol | Anti-hypertensive | Alpha Pharma (Belgium) | -0.66 |
| Metoprolol | Anti-hypertensive | Available in the lab as standard | -1.48 | Sertraline | Antidepressive | NODCAR (Egypt) | 1.91 |
| Naproxen | Nonsteroidal anti-inflammatory | Acros Organics (Belgium) | 2.96 | Sulfamethoxazole | Antibacterial | Sigma Aldrich (Italy) | 0.75 |
| Olanzapine | Antipsychotic | Lake Chemicals (China) | -1.02 | Theophylline | Anti-astma | NODCAR (Egypt) | -0.77 |
| Oxazepam | Anti-anxiety | Available in the lab as standard | 2.92 | Testosterone | Hormone | Sigma Aldrich (Germany) | 3.37 |
| Paracetamol | Analgesic | Alpha Pharma (Belgium) | 0.91 | Ticlopidine | Antiplatelet | Sanofi Chimie (Belgium) | 0.76 |
| Paroxetine | Antidepressive | NODCAR (Egypt) | -0.09 | Trimethoprim | Antibiotic | Available in the lab as standard | -0.19 |
| Pentoxifylline | Phosphodiesterase inhibitor | European Pharmacopoeia (France) | 0.23 | Valsartan | Angiotensin II receptor antagonist | Sigma Aldrich (USA) | 4.55 |
| Phenazone | Nonsteroidal anti-inflammatory | TCL (Belgium) | 1.22 | Venlafaxine | Antidepressive | NODCAR (Egypt) | -0.76 |
| Pipamperone | Antipsychotic | Sigma Aldrich (Italy) | -4.60 | Vidarabine | Anti-viral | Available in the lab as standard | -3.78 |

6.2.2 Solid-phase extraction

Since the retention of both polar and non-polar substances was required, universal hydrophilic lipophilic balanced (HLB) sorbents from Waters (Oasis HLB; 200 mg, 6 mL) and Sigma Aldrich (Supel-Select HLB; 200 mg, 6 mL) were initially compared by spiking ultrapure water. For the compounds that were not retained on HLB sorbents, Supel-Select SCX (200 mg, 6 mL) and Oasis MCX (150 mg, 6 mL) strong cation exchange, Discovery DSC-WCX (500 mg, 6 mL) weak cation exchange and SupelClean ENVI-carb (500 mg, 6 mL) activated carbon cartridges were evaluated. To obtain optimum recovery rates for all pharmaceuticals, the best performing SPE tubes were combined in series and the optimum elution order was tested.

All extractions were performed using a Biotage VacMaster-10 vacuum manifold from Sopachem NV (Eke, Belgium) coupled to a 840.3 FT18 KNF Neuberger vacuum pump (Freiburg, Germany). Flow rates were kept below 5 mL/min. The SPE cartridges were first conditioned with 5 mL methanol and equilibrated with 10 mL ultrapure water (with 0.1% FA when working at pH 3.0). Subsequently, 100 mL of (spiked) ultrapure water or SWW was extracted on the cartridges, while the sample recipients were rinsed 3 times with 5 mL ultrapure water (with 0.1% FA when working at pH 3.0) to assure a complete transfer of the analytes. The sorbents were then dried under vacuum for 30 min prior to elution with 4 times 1 mL MeOH, 2% FA in H₂O, 2.5% AA in MeOH and 7M NH₄OH in MeOH or 5 times 1 mL 7M NH₄OH in MeOH. After elution, the samples/eluates were evaporated until dryness using a Shel-Lab 1410 vacuum oven (Cornelius, OR, USA) at room temperature and finally, the samples were reconstituted with 1 mL 40/60 H₂O:ACN (v/v%). Chromafil Xtra PTFE (polytetrafluoroethylene/teflon) filters (0.45 µm) from Macherey Nagel (Düren, Germany) were positioned under the SPE tubes during the entire extraction process.

6.2.3 Instrumentation and analytical conditions

All experiments were performed on an Infinity 1290 UHPLC system with a DAD detector from Agilent Technologies (Waldbronn, Germany). Recovery values were determined using an Acquity BEH HILIC column (1.0 x 100 mm; 1.7 µm) and a Waters Acquity UPLC BEH C18 analytical column (2.1 x 100 mm; 1.8 µm) both from Waters (Wexford, Ireland). Chemstation software (Agilent Technologies) was used to operate the system and to acquire and analyze the data.

6.2.4 Recovery

The recovery of the different SPE cartridges was evaluated by comparing the areas under de curve of the chromatographic peak (AUC) from a spiked ultrapure water or SWW sample at 17 - 167 mg/L after extraction with a reference sample at the same concentration (eq. 6.1).

$$\text{Recovery (\%)} = \frac{\text{AUC}_{\text{sample}}}{\text{AUC}_{\text{reference}}} \cdot 100\% \quad (6.1)$$

6.3 Results and discussion

6.3.1 Optimization of SPE procedure

In this study, polymeric Supel-Select HLB and Oasis HLB SPE cartridges were evaluated for a selection of 48 pharmaceuticals with a large range in polarities (Table 6.1) spiked in ultrapure water. As can be derived from Table 6.2, both HLB tubes displayed a poor recovery for the most hydrophilic components. However, overall Oasis HLB resulted in superior recoveries, therefore it was decided to continue further experiments with the Oasis HLB cartridges.

Since the methodology should be applicable for real water samples, simulated wastewater (SWW) was subsequently used to mimic environmental matrices. The organic content of this SWW could reduce the binding capacity of the stationary bed and have an influence on the extraction efficiency of the targeted compounds. To investigate the effect of the pH on the extraction efficiency, both acidic (pH 3.0) and neutral (pH 7.5) conditions were tested and the results in Table 6.2 demonstrate that similar results were obtained under both pH conditions. Besides for 9 and 6 hydrophilic pharmaceuticals at pH 3.0 and 7.5, respectively, acceptable recoveries between 71% and 109% were obtained.

Since most compounds with low recovery values on the Oasis HLB cartridge were positively charged at pH 3.0, the SWW samples were finally brought to pH= 3.0 with formic acid prior to extraction to test weak cation-exchange (WCX), strong cation-exchange (SCX or MCX) and activated carbon sorbents (ENVI-carb). As can be seen in Table 6.3, the ENVI-carb cartridges were completely inadequate for the extraction of these highly polar molecules. The WCX sorbents were eluted with two types of acids to neutralize the anionic functional groups and promote elution of the cationic analytes. Although similar recoveries were obtained for both eluents, insufficient retention was obtained for most compounds. For the extractions

performed with the strong-cation exchange cartridges, elution was performed by neutralizing the molecules with ammonia in MeOH. As can be deduced from Table 6.3, most compounds that were not or insufficiently retained on the HLB cartridge at pH 3.0, could be retained relatively well (recovery > 85%) on either SCX, MCX or both cartridges. Exceptions were metformin, paracetamol and ticlopidine. Metformin that has a pK_{a1} value of 10.3 could not be neutralized with ammonia and hence remained on the cartridge during elution. Ticlopidine has a pK_a of 6.9 and should be positively charged at pH 3 and therefore retained on SCX/MCX. Since it becomes neutral in ammonia, a good recovery was expected. However, a recovery of around 31% - 32% was obtained on both strong cation-exchange cartridges. Considering paracetamol was too polar to be efficiently retained on HLB and neutrally charged at pH 3.0, only little retention was achieved due to the reversed-phase character of both sorbents. Furthermore, atenolol ($pK_{a1}= 9.7$) was only partly eluted from the SCX cartridge while a good recovery was obtained with MCX. Since overall, better recoveries were obtained on the MCX cartridge in comparison with the SCX cartridge, the combination of an Oasis MCX and an Oasis HLB cartridge was subsequently tested for the entire sample. The samples were first loaded on the HLB sorbent and the flow through was immediately subjected to MCX. When the cartridges were eluted simultaneously in this order, reduced recoveries were obtained for ciprofloxacin (15%), which is partly zwitterionic during elution and lorazepam (31%) that showed some sort of affinity for the MCX sorbent presumably by an electron dislocation due to a mesomeric effect. In the final methodology, the HLB and MCX cartridge were therefore exchanged during the drying step prior to elution. In this way, the compounds that were retained on HLB would never be subjected to the MCX sorbent. Using the final proposed HLB/MCX combination wherein the cartridges are switched prior to elution, a most versatile recovery was obtained. Except for metformin that could not be eluted from the sorbent and ticlopidine which had a recovery of only 25%, good recovery rates between 75% and 106% were obtained for all pharmaceuticals (Table 6.4). Although recoveries between 80% and 120% are considered acceptable according to the ICH guidelines [18,19], lower recovery rates can be considered satisfactory provided that they are repeatable when performing multi-residue analysis in complex sample matrices [20].

Table 6.2: Individual recovery values for the pharmaceuticals spiked in ultrapure water or simulated wastewater. Elution was done with 4 x 1 mL of MeOH (HLB). The eluate was evaporated under vacuum and reconstituted in 1 mL of 40/60 H₂O:ACN. All pharmaceuticals are ordered according to ascending log D.

| Pharmaceutical | Ultra-pure water | | Simulated wastewater | |
|---------------------|------------------|------------------|----------------------|--------------------|
| | Oasis HLB | Supel-Select HLB | Oasis HLB (pH 3.0) | Oasis HLB (pH 7.5) |
| Metformin | 0.0 | 0.0 | 0.0 | 0.0 |
| Guanylurea | 0.0 | 0.0 | 0.0 | 0.0 |
| Pipamperone | 100.8 | 3.8 | 109.4 | 99.4 |
| Vidarabine | 0.0 | 0.0 | 0.0 | 2.2 |
| Atenolol | 5.2 | 0.0 | 0.0 | 92.7 |
| Clindamycine | 98.3 | 17.5 | 97.6 | 107.2 |
| Codeine | 90.8 | 0.6 | 23.1 | 97.3 |
| Ciprofloxacin | 74.1 | 37.6 | 108.6 | 93.0 |
| Metoprolol | 97.1 | 21.4 | 95.4 | 95.6 |
| Olanzapine | 55.3 | 0.0 | 23.1 | 101.8 |
| Clozapine | 94.6 | 53.5 | 96.6 | 93.5 |
| Theophylline | 130.1 | 71.2 | 99.0 | 48.7 |
| Venlafaxine | 93.2 | 27.2 | 98.8 | 98.6 |
| Propranolol | 93.8 | 113.6 | 100.5 | 92.6 |
| Lidocaine | 94.5 | 2.7 | 33.4 | 97.1 |
| Hydrochlorothiazide | 102.4 | 95.0 | 102.1 | 97.3 |
| Caffeine | 97.2 | 96.5 | 96.8 | 94.4 |
| Trimethoprim | 98.3 | 5.7 | 99.7 | 101.4 |
| Paroxetine | 102.0 | 92.6 | 95.0 | 71.5 |
| Pentoxifylline | 102.7 | 91.8 | 105.3 | 102.1 |
| Escitalopram | 96.9 | 109.9 | 98.3 | 95.5 |
| Iopromide | 97.9 | 8.8 | 93.9 | 93.4 |
| Sulfamethoxazole | 101.1 | 92.0 | 99.0 | 92.4 |
| Ticlopidine | 33.3 | 82.0 | 71.1 | 34.3 |
| Imipramine | 94.4 | 113.4 | 96.6 | 88.7 |
| Paracetamol | 103.2 | 78.2 | 43.3 | 39.6 |
| Fluoxetine | 94.3 | 92.1 | 95.9 | 85.4 |
| Dipyridole | 91.6 | 171.2 | 94.6 | 91.4 |
| Phenazone | 103.1 | 97.8 | 101.0 | 99.5 |
| Amitriptyline | 102.3 | 91.4 | 99.3 | 100.0 |
| Sertraline | 95.8 | 112.5 | 96.6 | 76.3 |
| Carbamazepine | 94.1 | 113.9 | 99.3 | 99.4 |

Table 6.2: *Continued*

| Pharmaceutical | Ultra-pure water | | Simulated wastewater | |
|-------------------------------|------------------|------------------|----------------------|--------------------|
| | Oasis HLB | Supel-Select HLB | Oasis HLB (pH 3.0) | Oasis HLB (pH 7.5) |
| Diazepam | 119.7 | 108.2 | 96.8 | 95.1 |
| Oxazepam | 102.2 | 101.5 | 104.2 | 108.0 |
| Naproxen | 94.0 | 112.0 | 97.0 | 98.8 |
| Cilostazole | 94.8 | 112.3 | 97.2 | 99.0 |
| Testosterone | 96.0 | 112.5 | 58.4 | 98.9 |
| Lorazepam | 95.6 | 106.8 | 98.7 | 99.3 |
| Ketoprofen | 99.6 | 91.6 | 97.7 | 97.0 |
| β -estradiol | 102.0 | 91.0 | 98.0 | 96.0 |
| Irbesartan | 104.4 | 189.6 | 98.0 | 87.7 |
| Ibuprofen | 96.3 | 94.5 | 97.8 | 97.7 |
| 17 α -ethinylestradiol | 98.3 | 106.7 | 99.2 | 97.4 |
| Bezafibrate | 96.5 | 113.9 | 97.3 | 99.5 |
| Progesterone | 101.3 | 84.8 | 97.2 | 94.8 |
| Diclofenac | 101.9 | 97.3 | 95.4 | 96.0 |
| Estrone | 103.2 | 88.4 | 91.7 | 92.5 |
| Valsartan | 95.5 | 179.6 | 97.9 | 99.8 |

Table 6.3: *Recovery of the compounds that were not retained on Oasis HLB spiked in ultrapure water and extracted with weak cation exchange (WCX) and activated carbon (ENVI-carb) sorbents. The compounds that were not retained on Oasis HLB when spiked in SWW at pH 3.0 were extracted with strong cation exchange (MCX and SCX), Elution was done with 4 x 1 mL of NH₄OH in MeOH (MCX and SCX), 2% FA in H₂O or 2.5% AA in MeOH (WCX) or ACN (ENVI-carb). The eluate was evaporated under vacuum and reconstituted in 1 mL of 40/60 H₂O:ACN.*

| Pharmaceutical | WCX (2% FA) | WCX (2.5% AA) | ENVI-carb | MCX | SCX |
|----------------|-------------|---------------|-----------|------|------|
| Metformin | 48.8 | 44.8 | 0.0 | 0.0 | 17.1 |
| Guanylyurea | 26.8 | 23.6 | 0.0 | 88.3 | 0.0 |
| Vidarabine | 0.0 | 0.0 | 0.0 | 91.9 | 0.0 |
| Atenolol | 52.9 | 54.7 | 120.1 | 98.8 | 35.2 |
| Codeine | n.a. | n.a. | n.a. | 91.3 | 85.7 |
| Olanzapine | 57.3 | 60.1 | 1.0 | 96.8 | 95.7 |
| Lidocaine | n.a. | n.a. | n.a. | 84.5 | 76.4 |
| Ticlopidine | n.a. | n.a. | n.a. | 31.0 | 32.2 |
| Paracetamol | n.a. | n.a. | n.a. | 26.0 | 7.3 |

Table 6.4: Recovery values for the pharmaceuticals spiked in simulated wastewater. Elution was done with 5 x 1 mL of NH₄OH in MeOH. The eluate was evaporated under vacuum and reconstituted in 1 mL of 40/60 H₂O:ACN.

| Pharmaceutical | HLB/MCX (pH 3.0) | Pharmaceutical | HLB/MCX (pH 3.0) |
|----------------------|------------------|------------------|------------------|
| β-estradiol | 99.1 | Ketoprofen | 98.1 |
| 17α-ethinylestradiol | 99.6 | Lidocaine | 90.8 |
| Amitriptyline | 98.6 | Lorazepam | 94.6 |
| Atenolol | 98.0 | Metformin | 0.0 |
| Bezafibrate | 98.8 | Metoprolol | 101.4 |
| Caffeine | 97.4 | Naproxen | 98.4 |
| Carbamazepine | 98.7 | Olanzapine | 103.6 |
| Cilostazole | 97.5 | Oxazepam | 94.4 |
| Ciprofloxacin | 87.8 | Paracetamol | 84.0 |
| Clindamycin | 99.5 | Paroxetine | 89.9 |
| Clozapine | 91.3 | Pentoxifylline | 98.0 |
| Codeine | 92.5 | Phenazone | 95.5 |
| Diazepam | 93.5 | Pipamperone | 106.4 |
| Diclofenac | 100.3 | Progesterone | 95.1 |
| Dipyridole | 94.5 | Propranolol | 99.5 |
| Escitalopram | 98.6 | Sertraline | 75.4 |
| Estrone | 98.6 | Sulfamethoxazole | 76.5 |
| Fluoxetine | 93.4 | Theophylline | 97.0 |
| Guanyurea | 82.4 | Testosterone | 76.0 |
| Hydrochlorothiazide | 104.1 | Ticlopidine | 25.4 |
| Ibuprofen | 98.0 | Trimethoprim | 92.7 |
| Imipramine | 88.7 | Valsartan | 98.7 |
| Iopromide | 100.5 | Venlafaxine | 98.5 |
| Irbesartan | 85.5 | Vidarabine | 86.4 |

With the presented solid-phase extraction methodology the total analysis sensitivity could theoretically be enhanced with a factor 100 since a total volume of 100 mL water was extracted and finally reconstituted in 1 mL. Considering the observed recovery rates in this study, an increase in sensitivity with a factor 75 or 106 should be achieved for most pharmaceuticals. Moreover, higher sensitivities are feasible when larger water volumes (e.g. 200 or 500 mL) are extracted.

6.4 Conclusion

Due to the ease of use, solid phase extraction can be considered as a fast sample preparation technique which can easily be employed to selectively extract, concentrate or purify target analytes from environmental water samples. By combining HLB and MCX sorbents, good recoveries between 75% and 106% were achieved for most pharmaceuticals evaluated in this study. Only metformin (0%), that remained retained on the SPE cartridge, and ticlopidine (25%) could not adequately be extracted. However, the developed HLB/MCX SPE methodology can be considered as a viable technique to extract pharmaceuticals with a large range in polarities from aqueous samples. Except for two compounds the sensitivity was increased with a minimum factor of 75. Although LC-UV studies were very promising, further research is necessary to validate the presented offline SPE methodology in a routine setup wherein also mass spectrometry is evaluated to further lower detection limits. To assure a reliable quantitative analysis of real water samples repeatable recoveries and LOQ-values in the sub ng/L range are required.

6.5 References

- [1] R. Triebkorn, H. Casper, V. Scheil, J. Schwaiger, *Anal. Bioanal. Chem.* **387**, 1405–1416 (2007).
- [2] W. Sanchez, W. Sremski, B. Piccini, O. Palluel, E. Maillot-Maréchal, S. Betoulle, et al., *Environ. Int.* **37**, 1342–1348 (2011).
- [3] K.E. Arnold, A.R. Brown, G.T. Ankley, J.P. Sumpter, K.E. Arnold, *Philos. Trans. R. Soc. B.* **369**, (2014).
- [4] T.A. Bellar, W.L. Budde, *Anal. Chem.* **60**, 2076–2083 (1988).
- [5] G. Loos, A. Van Schepdael, D. Cabooter, *Philos. Trans. R. Soc. A.* **374**, (2016).
- [6] E. Baltussen, P. Sandra, F. David, C. Cramers, *J. Microcolumn Sep.* **11**, 737–747 (1999).
- [7] F. David, P. Sandra, *J. Chromatogr. A.* **1152**, 54–69 (2007).
- [8] L. Vergeynst, H. Van Langenhove, K. Demeestere, *TrAC - Trends Anal. Chem.* **67**, 192–208 (2015).
- [9] C. Nannou, C. Kosma, T. Albanis, *Int. J. Environ. Anal. Chem.* **95**, 1242–1262 (2015).
- [10] J. Kumirska, A. Plenis, P. Łukaszewicz, M. Caban, N. Migowska, A. Białk-Bielińska, et al., *J. Chromatogr. A.* **1296**, 164–178 (2013).
- [11] D.W. Watson, D.E. Raynie, *LCGC North Am.* **32**, 908–915 (2014).
- [12] N. Migowska, M. Caban, P. Stepnowski, J. Kumirska, *Sci. Total Environ.* **441**, 77–88 (2012).
- [13] M. Boisvert, P.B. Fayad, S. Sauvé, *Anal. Chim. Acta.* **754**, 75–82 (2012).
- [14] E.L. Schymanski, H.P. Singer, J. Slobodnik, I.M. Ipolyi, P. Oswald, M. Krauss, et al., *Anal. Bioanal. Chem.* **407**, 6237–6255 (2015).
- [15] S. Huntscha, H.P. Singer, C.S. McArdell, C.E. Frank, J. Hollender, *J. Chromatogr. A.* **1268**, 74–83 (2012).
- [16] N. Miranda-garcía, S. Suárez, B. Sánchez, J.M. Coronado, S. Malato, M.I. Maldonado, *Appl. Catal. B Environ.* **103**, 294–301 (2011).
- [17] J. Marugán, R. van Grieken, C. Pablos, *Environ. Technol.* **31**, 1435–1440 (2010).
- [18] US Food and Drug Administration, Text on Validation of Analytical Procedures, 1995.
- [19] US Food and Drug Administration, Guidance for industry: Q2B validation of analytical procedures: methodology, 1996.
- [20] A.L.N. van Nuijs, I. Tarcomnicu, L. Bervoets, R. Blust, P.G. Jorens, H. Neels, et al., *Anal. Bioanal. Chem.* **395**, 819–828 (2009).

CHAPTER 7

General discussion and conclusions

7.1 Improving wastewater treatment strategies

The increasing production of drugs and the consequently cumulative occurrence of pharmaceuticals, metabolites and degradation products in the environment has increased the interest to remove these micro-pollutants from environmental water. Since these drugs may have a harmful effect on the aquatic environment and in extension human health, guidelines are introduced by the European Union to restrict their emission levels. Furthermore, wastewater treatment plants are more frequently being equipped with additional tertiary treatment strategies to reduce the amount of excreted medicines in sewage water. The removal of pharmaceuticals, however, can be very challenging due to the general high stability and persistence of drugs. Therefore, in an extensive search to develop new and efficient treatment mechanisms, different advanced oxidation processes are being investigated.

In Chapter 3, the degradation of iopromide (IOP), sulfamethoxazole (SMX), 17 α -ethinylestradiol (EE₂) and diclofenac (DCF) by electrochemical oxidation using a boron-doped diamond (BDD) electrode was studied. To optimize the elimination efficiency in simulated wastewater (SWW) and real hospital effluent (RWW), the influence of different parameters such as the electrical current applied to the electrode, the initial compound concentration, the working temperature and the flow rate through the electrochemical cell was examined. Although fairly good degradation rates were obtained for all four components in SWW and RWW, the elimination of IOP was considerably slower due to the strong electron dispersion over the entire molecule caused by the strong electronegative iodine groups. Therefore, IOP had a low reactivity towards oxidizing agents such as OH^{*} [1]. Moreover, complete mineralization of all four pharmaceuticals was very time-consuming and therefore not practical. To further enhance the removal process of the parent pharmaceuticals and their degradation products, more experiments are required to obtain optimum settings. Alternatively, a combination of BDD and other advanced oxidation processes such as ozonolysis and UV irradiation or adsorption/nanofiltration techniques could improve wastewater treatment strategies. Photocatalytic degradation kinetic studies by Doll et al. for example demonstrated to be very promising for the treatment of iodinated contrast media such as IOP [2]. Alternatively, electron beam irradiation can effectively be employed to reduce IOP concentrations [3].

7.2 Development of a generic UHPLC methodology

The formation of multiple transformation products during different degradation processes, that are generally more hydrophilic than their parent compounds, in combination with the large amount of other pharmaceuticals present in real water samples, requires a generic analytical methodology to simplify the screening of (eco)toxic substances. Due to the high complexity of environmental water samples, there are no standardized protocols to evaluate the presence, degradation and removal of drugs. Therefore, a novel approach wherein orthogonal HILIC and RPLC columns were coupled in series using two external switching valves was explored in Chapters 4 and 5. Non-polar compounds that were not retained on the HILIC column were redirected and temporarily stored in a sample loop. After analysis of the hydrophilic components on the HILIC column, the valves were switched to separate the non-polar pharmaceuticals on an RPLC column. To modify the sample matrix from a large percentage of organic solvent to highly aqueous, an innovative mixing unit was developed to dilute the mobile phase in between the HILIC and RPLC dimension. It was demonstrated that the use of two parallel restriction capillaries with different flow resistances to alter the mobile phase composition, was more flexible and economical in comparison with commercially available mixers. The dilution ratio or dilution factor could easily be adjusted by changing the dimensions of the high resistance restriction capillary. In this way, columns with altered internal diameters could be used to enhance the sensitivity by increasing the injection volume or minimizing the dilution on the second dimension column. To reduce the delay time caused by the dwell volume of the mixing unit, a trap column was installed between the mixing unit and the RPLC column allowing the use of high flow rates during the mobile phase dilution. The proposed setup was proven successful to perform repeatable analyses that provided good recoveries under optimum dilution conditions.

This novel setup opens the way for the simultaneous analysis of complex samples comprising both hydrophobic and hydrophilic components within acceptable total analysis times and can therefore be used for routine applications.

7.3 Strive for highest possible flexibility

Major advantages of serially coupled orthogonal columns are the extended peak capacities intermediate to one- and two-dimensional separations, the independent method

development for the first and second dimension analysis and the easy to interpret chromatograms. Due to the optimized and selective separation of polar compounds in HILIC and non-polar compounds in RPLC, matrix substances will be spread out more over the corresponding elution windows resulting in reduced matrix interferences. Therefore, multi-residue analysis of the entire sample will be feasible with a single injection. Although the proposed setup has proven successful for the analysis of multiple pharmaceuticals with strongly different physico-chemical characteristics, complete baseline separation of all compounds was not achieved in all instances. In follow-up studies alternative selectivities can be investigated both to improve the trapping of semi-polar components and to obtain various elution strategies for specific molecules. Besides environmental water analysis, the setup can also be applied in numerous other fields that deal with complex samples, such as for example food analysis, bioanalysis or impurity screening of active pharmaceutical ingredients.

Furthermore, depending on the research objectives, alternative column combinations can be employed. Consequently, a flexible mixing unit wherein the dilution volume can easily be adjusted is desirable. When e.g. strong cation exchange or chiral columns are coupled in series with a reversed-phase column, a less drastic mobile phase conversion will be required in comparison with the serial coupling of HILIC and RPLC. Therefore, the current setup can be extended with two additional switching valves to connect multiple high resistance restriction capillaries in series to change the resistance of the HR restriction capillary in a dynamic way (Figure 7.1). The implementation of two extra valves, however, makes the setup more complicated and requires extremely comprehensive methods to ensure a smooth run.

A second solvent delivery system could also be envisaged to increase the flexibility of the setup. To avoid prolonging the total analysis time excessively, a maximum dilution factor of 100 is recommended. When two new generation UHPLC pumps are used, all dilution ratios between 1:1 and 1:100 can accurately be applied since a stable minimum flow rate of 30 $\mu\text{L}/\text{min}$ and maximum flow rate of 3000 $\mu\text{L}/\text{min}$ are feasible. Controlling the different pumps can easily be done using one software program with a simple firmware update. However, in this study the use of a single solvent delivery pump was targeted to make the setup more economical.

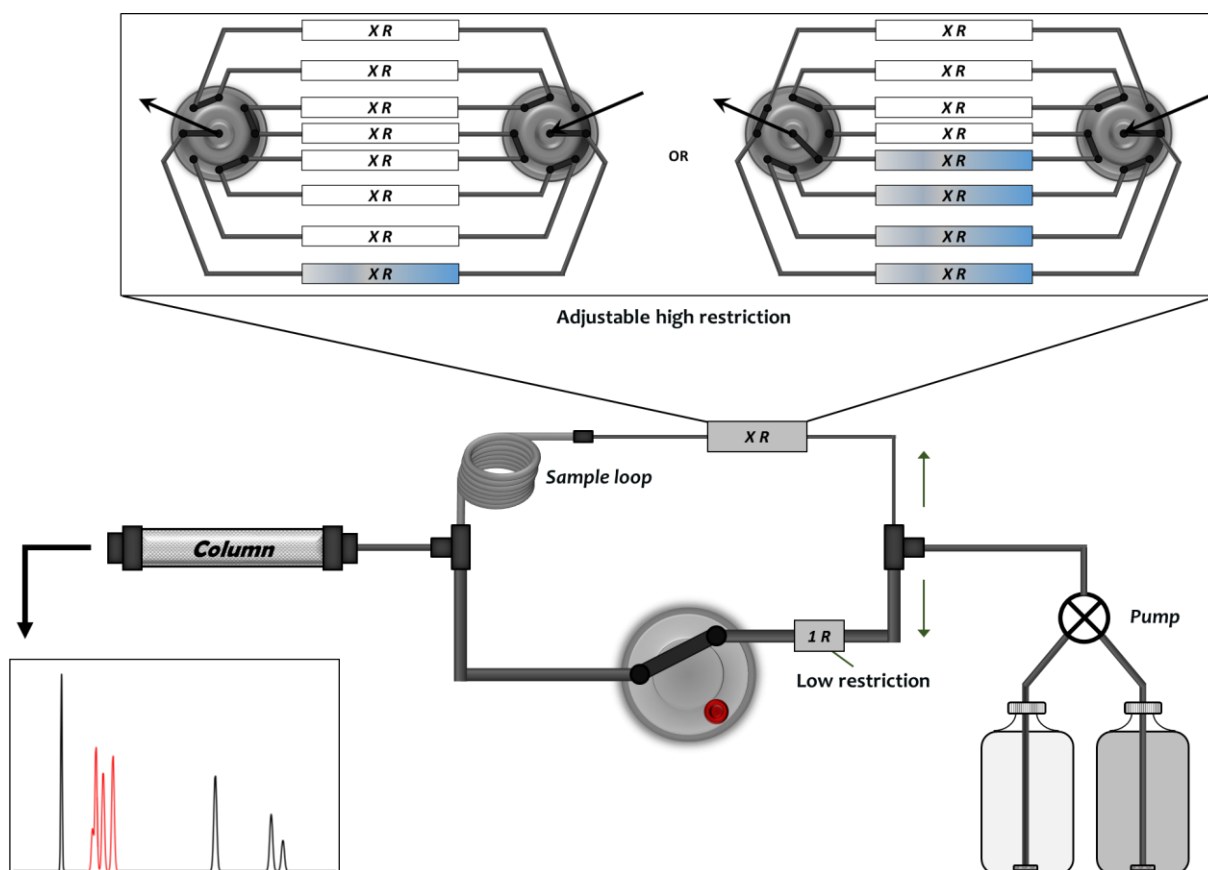


Figure 7.1: Scheme of the restriction capillaries wherein the high resistance restriction capillary can be substituted by two additional switching valves that connect multiple tubing (possibly with different dimensions). By changing the configuration of the valves one specific or a set of different capillaries can be coupled in series to adjust the flow resistance through the high resistance restriction capillary.

When the analysis of multiple analogous compounds is required, the combination of two orthogonal columns is not always sufficient to obtain a baseline separation. For this purpose, the setup can be accommodated with multiple sample loops and an additional set of columns with different selectivities. Using a similar format as for the adjustable restriction capillaries in Figure 7.1, multiple sample loops can be connected between two additional switching valves. With the availability of extra sample loops, (partly) co-eluting peaks can be sequentially fractionated by redirecting them to different reservoirs where they are temporarily trapped prior to analysis. Subsequent to the first dimension separation, the different fractions can consecutively be analyzed on a second dimension column of choice. Depending on the analyte characteristics, the different fractions can be sent to and analyzed onto different trap and analytical columns that are positioned in parallel in the second dimension according to the same principle using additional valves. Furthermore, the sample loops can be used in series to adjust the sample loop volume when a smaller or larger first dimension cut is required. To

avoid complex combinations of numerous valves with a multitude of columns, tubing and sample loops, miniaturization wherein the different valve patterns, columns and paths lengths are etched on microchips could be envisioned to obtain ultimate flexibility. Besides the gain in simplicity to practically manipulate a chip, miniaturization is accompanied by a higher sensitivity and transferability to other instruments.

7.4 Optimization of the sample preparation procedure

Since the occurrence of pharmaceuticals in European waters is typically in the $\mu\text{g/L}$ to ng/L range, an additional sample preparation methodology was developed in Chapter 6 to pre-concentrate the analytes. Using the generic SPE procedure developed in this thesis, a simultaneous extraction of polar and non-polar pharmaceuticals from simulated wastewater was achieved. Although high recoveries were obtained for most components, further research is required to assure retention of the most hydrophilic substances and elution of strongly retained components.

Although offline solid-phase extraction (SPE) is often used to extract environmental water samples, online sample preparation can be considered to develop fully automated methodologies which reduce the total analysis time and solvent consumption. In comparison with conventional offline SPE methodologies, online SPE is easy to use, cost-efficient and more robust due to its automation. In addition, by injecting the entire sample onto the analytical column, high sensitivities can be obtained using small sample amounts e.g. 1-5 mL [4–6]. Although high-throughput analyses are feasible with online SPE, precautions are to be taken to prevent clogging of precipitates on the column or declining recoveries caused by offline filtration due to adsorption of substances on e.g. sediments or floating particles.

Alternatively, to reduce the total analysis time or in particular when the setup is used to perform bioanalysis, microextraction by packed sorbent (MEPS) can be employed. In fact, this technique is a miniaturized form of SPE wherein sample volume and solvent consumption are minimized by packing the sorbents in a syringe [7]. MEPS is a simple, inexpensive and quick technique that can easily be automated, ideally when only small sample volumes are available. However, the limited number of available sorbents and more complicated combination of multiple sorbents result to date in a minor genericity to perform a simultaneous extraction of compounds with a large range in polarities [8].

7.5 Method validation for real water samples

To demonstrate the applicability of the entire methodology for the analysis of real water samples, the previously developed SPE method and UHPLC setup should be hyphenated to a state-of-the-art triple quadrupole mass spectrometer. The entire offline SPE-LC-MS/MS methodology can then be validated to ensure it can be used in routine analysis. Separation of the sample will be done according to the procedure described in Chapter 5. However, switching valve 3 as described in Chapter 5 needs to be substituted by a 2-position, 6-port valve to divert the high aqueous flow rate during the dilution step to the waste (Figure 7.2). This valve is necessary to avoid exposing the ESI source to the high flow rate of water during the dilution of the ACN plug. With this adjustment, the MS/MS analysis will be possible in a dynamic multiple reaction monitoring (dMRM). In this mode, small retention time windows are specified for each compound to reduce the number of transitions that will be measured simultaneously. This will result in longer cycle times and consequently higher peak intensities. The gain in sensitivity by minimizing the number of compounds for which the mass spectrometer needs to scan simultaneously moreover emphasizes the major importance of a good chromatographic separation prior to MS detection.

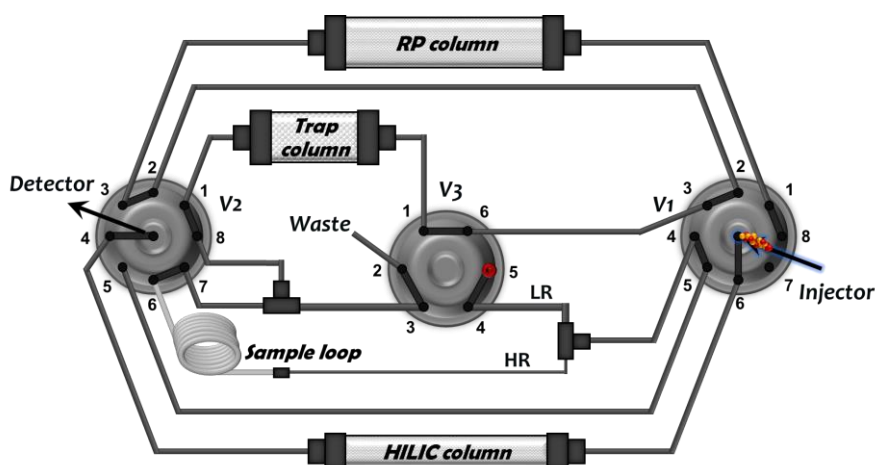


Figure 7.2: Scheme of the setup wherein the entire sample containing polar (●) and non-polar (●) compounds will be injected onto the HILIC column. The polar compounds will be retained on the HILIC column while the non-polar pharmaceuticals will elute near the void volume. The configuration of valve 2 (V2) will be changed to guide the non-polar compounds towards the sample loop through the HR restriction capillary by blocking the LR path with valve 3 (V3). When the non-polar pharmaceuticals will be trapped in the sample loop, V2 will be returned to its original position and the polar compounds will be analyzed on the HILIC column by changing the mobile phase composition. Subsequently, all valves (1, 2 and 3) will be switched to open both restriction capillaries. The ACN plug wherein the non-polar compounds are dissolved will be diluted with water and the non-polar components will be trapped on the trap column. Finally, valves 1 and 2 will be altered to elute the non-polar pharmaceuticals in backflush from the trap column in order to analyze them on the RP column by changing the mobile phase composition.

Limits of detection (LODs) and limits of quantification (LOQs) can be determined by spiking extracted SWW with different concentrations to obtain a signal-to-noise ratio of 3:1 and 10:1, respectively. Subsequently, calibration curves can be created for each component using linear regression analysis. The analysis of SWW extracts spiked with three different concentration levels (low, mid, high) can be performed to define the matrix effect according to the strategy of Matuszewski et al. [20] and following equation eq. 7.1.

$$\text{Matrix effects (\%)} = 1 - \frac{\text{AUC}_{\text{spiked SWW extract}}}{\text{AUC}_{\text{spiked solvent}}} \cdot 100\% \quad (7.1)$$

Furthermore, the recovery of the optimized HLB/MCX SPE method can also be evaluated by spiking a SWW sample with a low, middle and high concentration prior to extraction. Precision or repeatability can be examined by measuring the RSD on the recovery and retention time for these different concentrations in triplicate.

Since matrix conditions are constant when SWW is used, analyte-free blanks are readily available in contrast with real water samples. Matrix effects (ME) can thus be evaluated by comparing the analyte concentrations in SWW and ultrapure water both spiked with three known concentration levels. When real water samples are to be analyzed, it is however recommended to investigate matrix suppression and/or enhancement for each new set of samples to determine the absolute concentration of a component, since ME can be highly dependent on the origin of the sample. One option is the addition of structural analogues, that are not already present in the matrix, to the sample [9]. Because structural analogues differ in functional group(s) and/or backbone structure from the analytes of interest, the retention time and/or the ionization of the molecule can be different. For this reason, the internal standard can be more or less prone to matrix effects resulting in theoretical recoveries that may differ from the actual value. Alternatively, when the sample matrix already contains trace elements of the analyte of interest prior to spiking, the principle of standard addition can be used to determine the analyte concentration [10]. A more expensive but simpler and more accurate alternative is the use of isotopically labelled standards (SIL-IS) added to the sample prior to analysis. SIL-IS behave exactly the same as their non-labelled variants from a physico-chemical point of view. This results in a similar retention time and ionization simplifying the quantitation of the targeted substance. Moreover, in this way the recovery of the sample preparation and matrix interference during ionization can be taken into account [11,12]. When not all SIL-IS are available or when the cost in e.g. multi-residue analysis is too

high, the recovery and interference during ionization can be determined by an alternative approach proposed by González et al. [13]. The matrix effect of multiple compounds can be compensated by a post-column infusion (PCI) of eight different SIL-IS similar to the analytes of interest. Based on the ME for every drug/PCI-SIL-IS response, the most suitable internal standard was determined and subsequently used to reconstruct the chromatograms for each analyte [13].

7.6 Mapping of pharmaceutically relevant contaminants

In order to obtain more information about emerging contaminants such as pharmaceuticals, metabolites and their degradation products, the advanced analytical techniques proposed in this study can be used to analyze real water samples. This will allow mapping the occurrence of pharmaceuticals in e.g. Belgian and/or European watercourses. Since very little is known about the toxicity levels of transformation products, it is important to understand the degradation pathways of different wastewater treatment strategies. Therefore, extensive research is needed to identify harmful degradation products and evaluate the removal of parent compounds. For this purpose, samples will ideally be screened with high resolution mass spectrometry (HRMS) and/or in MS^n mode. In monitoring programs, HRMS would also be the most recommended technique to perform a qualitative untargeted screening of water samples prior to quantitative analysis. To perform a reliable quantification it is moreover of great importance that all molecules are ionized. An inferior ionization of certain substances can result in a reduced sensitivity and/or unreliable results. Therefore, the combination of various ionization techniques is suggested. Ideally, an APCI and/or APPI interface is used alternately with an ESI source both in positive and negative ionization mode to cover as much molecules as possible. Such dual ionization sources can be used to analyze polar and non-polar volatile compounds simultaneously.

7.7 References

- [1] H. Mohan, K.-D. Asmus, *J. Chem. Soc. Perkin Trans. 2.* **3**, 1795–1800 (1987).
- [2] T.E. Doll, F.H. Frimmel, *Water Res.* **38**, 955–964 (2004).
- [3] M. Kwon, Y. Yoon, E. Cho, Y. Jung, B.-C. Lee, K.-J. Paeng, et al., *J. Hazard. Mater.* **227-228**, 126–134 (2012).
- [4] S. Idder, L. Ley, P. Mazellier, H. Budzinski, *Anal. Chim. Acta.* **805**, 107–115 (2013).
- [5] J. Camilleri, R. Baudot, L. Wiest, E. Vulliet, C. Cren-Olivé, G. Daniele, *Int. J. Environ. Anal. Chem.* **95**, 67–81 (2014).
- [6] N. V. Heuett, C.E. Ramirez, A. Fernandez, P.R. Gardinali, *Sci. Total Environ.* **511**, 319–330 (2015).
- [7] M. Abdel-Rehim, Z. Altun, L. Blomberg, *J. Mass Spectrom.* **39**, 1488–1493 (2004).
- [8] M.M. Moein, A. Abdel-Rehim, M. Abdel-Rehim, *Trends Anal. Chem.* **67**, 34–44 (2015).
- [9] N. Dorival-García, A. Zafra-Gómez, F.J. Camino-Sánchez, A. Navalón, J.L. Vilchez, *Talanta.* **106**, 104–118 (2013).
- [10] S. Kowal, P. Balsaa, F. Werres, T.C. Schmidt, *Anal. Bioanal. Chem.* **405**, 6337–6351 (2013).
- [11] T. Anumol, S.A. Snyder, *Talanta.* **132**, 77–86 (2015).
- [12] T.L. Jones-Lepp, R.L. Taniguchi-Fu, J. Morgan, T. Nance, M. Ward, D.A. Alvarez, et al., *Anal. Bioanal. Chem.* **407**, 6481–6492 (2015).
- [13] O. González, M. Van Vliet, C.W.N. Damen, F.M. Van Der Kloet, R.J. Vreeken, T. Hankemeier, *Anal. Chem.* **87**, 5921–5929 (2015).

CHAPTER 8

Summary – samenvatting

8.1 Summary

In this thesis the degradation by electrochemical oxidation via boron doped diamond (BDD) was assessed for the selected pharmaceutical compounds iopromide (IOP), sulfamethoxazole (SMX), 17 α -ethinylestradiol (EE₂) and diclofenac (DCF) in simulated wastewater (SWW) and real hospital effluent wastewater (RWW). The influence of the applied current, the flow rate through the electrochemical cell, the initial compound concentration and the wastewater matrix (SWW versus RWW) was evaluated. This study confirmed that the degradation has pseudo first-order reaction kinetics for all experimental conditions tested. It was shown that SMX, EE₂ and DCF degraded readily in SWW and RWW, however, the degradation of IOP was considerably slower, which is in agreement with previously reported slow degradation kinetics using typical advanced oxidation processes. Activation energies for the degradation reactions were calculated and it was shown that the flow rate in the electrochemical cell only had a moderate effect on the degradation rate of EE₂ and DCF. In contrast, the applied current had a major effect. The BDD electrochemical oxidation was shown to be an effective technique for removing pharmaceutical components from the effluent of a biological hospital wastewater treatment plant. However, the slower degradation of generally more hydrophilic transformation products should be taken into account when a full mineralization and a toxicity screening of the pharmaceuticals is pursued.

This study sparked the interest for the analysis of samples with increasing complexity. Appropriate analytical methods to evaluate the presence, metabolism, degradation and removal efficiency of specific compounds were necessary for this purpose. Therefore, a generic methodology was developed to overcome the need for multiple analyses on complementary columns to cover the separation of all compounds due to large differences in polarity. A commercially available ultra-high performance liquid chromatography (UHPLC) system was equipped with two external switching valves to connect hydrophilic interaction liquid chromatography (HILIC) and reversed-phase liquid chromatography (RPLC) columns in series for the sequential analysis of polar and non-polar compounds. The principle relies on the isolation of unretained peaks eluting from a first dimension column in a sample loop, before directing them to a second column for separation. The setup was successfully applied for the separation of 32 pharmaceutical compounds with a wide range of polarities. Since the mobile phases employed in highly orthogonal separations were not directly compatible, a

mixing unit was required to alter the mobile phase composition before executing the second dimension separation. To deal with the incompatibility of the HILIC eluate and the ensuing RPLC separation, in first instance commercially available mixers were included in the setup. Later, a novel mixing unit was proposed, based on the use of two restriction capillaries with different flow resistances to dilute the mobile phase eluting from the first dimension with a solvent appropriate for the second dimension separation.

The restriction capillaries were implemented using three high-pressure switching valves and two T-pieces. It was demonstrated that the dilution ratio can be adequately predicted using the law of Hagen-Poiseuille and can be adjusted easily by changing the dimensions of the restriction capillaries. The dilution volume required to obtain acceptable recoveries was investigated and the use of different column diameters in the first and second dimension was proposed to increase the sensitivity of the analysis. Under optimum dilution conditions, recoveries ranging between 82% and 99% were always obtained, while repeatability values were excellent. The proof-of-concept of the different setups was demonstrated for the separation of 20 pharmaceuticals with log D-values ranging between -5.75 and 4.22 .

Since information about the occurrence of pharmaceuticals in water is scarce and pharmaceuticals are typically only present in the $\mu\text{g/L}$ to ng/L range in European waterways, a solid-phase extraction (SPE) procedure combining hydrophilic lipophilic balanced and strong cation exchange sorbents allowing the simultaneous extraction of polar and non-polar pharmaceuticals from simulated wastewater was evaluated. Besides for metformin that could not be eluted from the SPE cartridge and ticlopidine that could not adequately be extracted, good recovery rates between 75% and 106% were obtained for all studied compounds. To demonstrate the applicability of the presented setup in routine water analysis, further research is required to validate the entire methodology.

8.2 Samenvatting

In deze thesis werd de afbraak van de geneesmiddelen iopromide (IOP), sulfamethoxazole (SMX), 17 α -ethinylestradiol (EE₂) en diclofenac (DCF) bestudeerd. Deze componenten werden gespiked in gesimuleerd afvalwater (SWW) en reëel ziekenhuis afvalwater (RWW) en vervolgens onderworpen aan elektrochemische oxidatie door middel van een met boor gedoteerde diamant electrode (BDD). Om de afbraak te optimaliseren, werd de invloed van de stroomsterkte, het debiet doorheen de elektrochemische cel, de initiële concentratie aan medicijnen en de afvalwatermatrix (SWW versus RWW) geëvalueerd. Deze studie bevestigde dat de afbraak steeds een pseudo eerste-orde reactiekinetiek volgt voor alle experimenteel geteste parameters. Ondanks het feit dat SMX, EE₂ en DCF eenvoudig werden afgebroken in zowel SWW als RWW, was de afbraak van IOP beduidend trager. Deze lagere eliminatiesnelheid was in overeenstemming met eerder gerapporteerde waarden die een trage afbraakkinetiek aantoonde voor IOP in typische geavanceerde oxidatieprocessen. Verder werden de activeringsenergieën voor de afbraakreacties berekend en bleek het debiet doorheen de elektrochemische cel slechts een klein effect te hebben op de afbraaksnelheid van EE₂ en DCF. De stroomsterkte daarentegen was van groot belang. Voor het verwijderen van geneesmiddelen uit het effluent van een biologische ziekenhuis waterzuiveringsinstallatie bleek de BDD elektrochemische oxidatie een efficiënte techniek te zijn. Wanneer echter een volledige mineralisatie van deze afvalstoffen en een positieve toxiciteitscreening nagestreefd wordt, moet rekening gehouden worden met het feit dat de verwijdering van afbraakproducten welke meestal hydrofieler zijn, veel trager is.

Dit onderzoek leidde tot de interesse om stalen met toenemende complexiteit te kunnen analyseren. Om de aanwezigheid, het metabolisme en de afbraak van specifieke verbindingen te kunnen evalueren, zijn geschikte analytische methoden noodzakelijk. Daarom werd in deze thesis een generische methodologie ontwikkeld om alle componenten in één run te kunnen scheiden, waardoor geen meerdere analyses op orthogonale kolommen vereist zijn om de grote verschillen in polariteit aan te kunnen. Hiervoor werd een commercieel beschikbaar ultra-hoog performant vloeistof chromatografie (UHPLC) toestel uitgerust met twee externe schakelkranen om hydrofiële interactie vloeistofchromatografie (HILIC) en omgekeerde fase vloeistof chromatografie (RPLC) kolommen serieel met elkaar te verbinden waardoor polaire en niet-polaire moleculen sequentieel geanalyseerd konden worden. Het principe berustte op de tijdelijke isolatie van componenten die niet weerhouden werden op de eerste dimensie

kolom in een apart reservoir. Nadat de scheiding in eerste dimensie afgelopen was, werden de weggeleide componenten naar de tweede kolom gestuurd om de analyse verder te zetten. De opstelling werd succesvol toegepast voor de scheiding van 32 farmaceutische verbindingen met een sterke variabiliteit in polariteit. Aangezien de mobiele fasen gebruikt in deze zeer orthogonale scheidingen sterk verschillend waren van elkaar, was een menging nodig om de samenstelling na de eerste dimensie te wijzigen vooraleer de tweede dimensie gestart kon worden. Om het HILIC-eluent geschikt te maken voor de daaropvolgende RPLC-scheiding werden in eerste instantie commercieel beschikbare mixers ingepast in de opstelling. Later werd een nieuwe menging ontwikkeld op basis van restrictiecapillairen met verschillende stromingsweerstand. Op deze manier kon de mobiele fase uit de eerste dimensie eenvoudig verdund worden met een oplossing die geschikt was om de scheiding in de tweede dimensie aan te vatten.

De restrictiecapillairen werden geïmplementeerd door middel van drie schakelkranen en twee T-stukken. Er werd aangetoond dat de verdunningsverhouding bij goede benadering voorspeld kon worden volgens de wet van Hagen-Poiseuille en gemakkelijk kon worden aangepast door de afmetingen van de restrictiecapillairen te wijzigen. Het verdunningsvolume dat nodig was om aanvaardbare recovery's te bekomen werd onderzocht en het gebruik van verschillende kolomdiameters in de eerste en tweede dimensie werd voorgesteld om de gevoeligheid van de analyse te verhogen. Voor elke combinatie werden onder optimale verdunningsomstandigheden steeds recovery's tussen 82% en 99% bekomen, terwijl de herhaalbaarheden uitstekend waren. Het concept werd succesvol toegepast om 20 geneesmiddelen met log D-waarden tussen -5,75 en 4,22 te scheiden.

Aangezien er slechts weinig informatie beschikbaar is over de aanwezigheid van geneesmiddelen in water en farmaceutische producten gewoonlijk slechts in de $\mu\text{g/L}$ tot ng/L range aanwezig zijn in Europese waterlopen, werd een extra vaste fase extractie (SPE) methode getest om de gevoeligheid van de analyse te verhogen. Hierbij werden hydrofiel lipofiel gebalanceerde (HLB) en sterke kation uitwisseling (MCX) adsorbentia gecombineerd om gelijktijdig polaire en niet-polaire geneesmiddelen uit gesimuleerd afvalwater te kunnen extraheren. Behalve voor metformine, wat niet van de SPE-cartridge geëluëerd kon worden en ticlopidine dat onvoldoende geëxtraheerd kon worden, werden goede recovery's tussen 75% en 106% bekomen voor alle bestudeerde verbindingen. Om de toepasbaarheid van de voorgestelde setup voor routine analyses aan te tonen, is echter meer onderzoek vereist om de hele methodologie te valideren.

Scientific acknowledgements and conflict of interest statement

Funding agency

The authors gratefully acknowledge the Flanders Innovation and Entrepreneurship (IWT/130227), the Research Foundation Flanders (1509114N) and the Industrial Research Fund of KU Leuven (KP/10/006 and C24/16/038) for their financial support. Furthermore, Glenn Loos acknowledges the Ysebaert Devos Fund (Faculty of Pharmacy, KU Leuven) for financial support.

Contributions

The BDD electrolysis cell was kindly made available by Advanced Waste Water Solutions (Hulst, The Netherlands) and Agilent Technologies is kindly thanked for providing the Agilent Infinity UHPLC system through a University Relations Grant (3114). Raf Dewil (Department of Chemical Engineering, Process and Environmental Technology Lab, KU Leuven) and Thomas Scheers (Faculty of Management and Technology, University College Leuven-Limburg) are acknowledged for their active participation in setting up the experiments, the critical discussions and their help with drafting Chapter 3. My promoter Deirdre Cabooter and all other authors are thanked for critically correcting the above manuscripts and their approval to publish the final versions.

Competing interests

All the authors involved declare no conflicts of interest.